In vitro effects of rooibos herbal tea (*Aspalathus linearis)* against methamphetamine on the mouse blood brain barrier

by

Tarryn Kay Prinsloo

(2813088)

Submitted in fulfilment for the degree

Magister Scientiae

Department of Medical Biosciences

University of the Western Cape

Bellville

Supervisor: Prof D Fisher

Co-supervisor: Dr K Gamieldien

November 2014

DECLARATION

I, Tarryn Kay Prinsloo (2813088), declare that the " ***In vitro*** **effects of rooibos herbal tea (*Aspalathus linearis)* against methamphetamine on the mouse blood brain barrier** " is my own work, that has not been submitted before for any degree or assessment at any other university, and that all the sources I have used or quoted have been indicated and acknowledged by means of complete references.

Student name	:	Tarryn Kay Prinsloo
Signature	:	
Date Signed	:	25 February 2015

PUBLICATIONS ARISING FROM THIS THESIS

Prinsloo, T. K., Gamieldien, K. and Fisher, D. (2011) *In vitro* cytotoxic analysis of methamphetamine on mouse brain endothelial (bEnd5) cells. *Sci Res Essays* **7**, 9.

Prinsloo, T. K., Gamieldien, K. and Fisher, D (2015) Herbal tea extract (*Aspalathis linearis*) decreases the permeability of *in vitro* blood-brain barrier (bEnd5) model. *Manuscript in preparation.*

Prinsloo, T. K., Gamieldien, K. and Fisher, D (2015) Fermented rooibos protects the *in vitro* blood-brain barrier (bEnd5) model against methamphetamine: Implications on cell numbers and cell cycles. *Manuscript in preparation.*

ACKNOWLEDGEMENTS

"Vision without execution is just hallucination."
- Henry Ford

Firstly, I would like to thank The Almighty for allowing me to further my academic career and granting me the strength to see it through.

Thank you to my mother for all her sacrifices and being a pillar of strength throughout the years and to my father who was not able to witness the conquering of this milestone in the flesh.

To my supervisor Prof. David Fisher, for the firm belief in me, allowing me the opportunity to further my studies and teaching me the patience to do so.

My sincere gratitude goes to Dr. Kareemah Gamieldien whose presence was constant throughout any event both personally and professionally. Thank you for being a pillar of strength, a role model to a young scientist and for your ability to motivate in the darkest of times.

To the Neurobiology group *viz.* Miss Linda Sissing, Miss Shireen Mentor, Mr. Siya Mafunda and Miss Kelly Thomas for the academic support and creating the necessary working atmosphere.

The Medical Bioscience Department for the infrastructure, creating a true academic family and the academic assistance needed for this study to be successful.

The National Research Foundation (NRF) for the financial support.

Thank you to Mr. Fanie Rautenbach at the Oxidative Stress Research Centre in Cape Peninsula University of Technology for the rooibos chemical analysis and Miss

Rozanne Adams at the Cell Imaging Unit (fluorescence live cell imaging and flow cytometry) at Stellenbosch University for the flow cytometry analysis.

Last, but most certainly not least, to my family and dearest friends for keeping me sane and motivated, my utmost appreciation.

ABSTRACT

Methamphetamine (MA), also known as 'Tik', has detrimental short- and long-term psychological and morphological effects on the central nervous system (CNS). The lipophilic nature of MA allows it to cross the blood-brain barrier (BBB) which normally plays a protective role in limiting solute exchange (including narcotics) into the neuronal tissue. Numerous studies have indicated that MA not only crosses the BBB but is implicated in distorting its crucial role in that it increases the permeability of the endothelial cells and thereby compromises its core homeostatic function. The speculated mechanism by which MA elicits its effects involves elevated ROS production which may be reversed by antioxidant treatment. Rooibos herbal tea (*Aspalathus linearis*) which is well documented for its antioxidative properties and ROS scavenging abilities may therefore be the ideal candidate to reverse the harmful ROS-induced effects of MA.

The aim of the study was to investigate the *in vitro* ameliorating potential of fermented rooibos (R_f) against the MA-induced effects on mouse brain endothelial (bEnd5) cells by utilizing various assays (trypan blue exclusion and XTT viability assays) and physiological parameters (cell numbers, viability, monolayer permeability and cell cycle phases) over a period of 96 hrs. Statistical analysis was performed using the Wilcoxon rank sum test with $P<0.05$ denoted as significant.

Once-off exposure to physiological MA concentrations and R_f resulted in % viability similar to controls by 96 hrs with suppression observed only when the cells were exposed to daily MA (0.1-1000 µM) ($P\leq0.0063$). Exposure to supraphysiological concentrations (≥100 µM) of MA greatly suppressed viability ($P\leq0.0463$). Both daily and once-off treatment to the combinations initially resulted in increased viability however by 96 hrs was similar to- or exceeding the controls ($P\leq0.0180$). MA exposure also resulted in decreased live cell numbers ($P\leq0.0339$) with no effect when exposed to R_f by 96 hrs. The combinations resulted in cell numbers comparable to controls. Dose-dependent increases in electrical resistance were observed in response to singular MA and R_f treatment with lower MA concentrations displaying significant decreases

(P≤0.0064). Similar trends were observed with combinations however greater resistance was observed. Increased G1-phase populations (P≤0.0495) in response to singular MA and R_f exposure was noted followed by decreased S-phase fractions (P≤0.0356). While MA decreased G2-M phase cells (P≤0.0498) it was unaffected by R_f. In contrast, the combination of MA and R_f decreased events in the G1-phase (P≤0.0483), with an increased S-phase population (P≤0.0415).

In conclusion, the single compounds displayed mirroring effects, decreasing the cells' permeability and causing G1-phase arrest. The modulatory effects of R_f in combination with MA was illustrated with the restoration of viability and live cell numbers comparable to that of controls, and a more restrictive monolayer as well as reversal of the G1-phase arrest. Findings suggest that R_f may reverse the adverse effects of MA on the BBB.

Keywords: methamphetamine, rooibos, viability, permeability, cell cycles, cell numbers

LIST OF ABBREVIATIONS

A549	:	adrenocarcinomic human alveolar basal epithelial cells
A. linearis	:	*Aspalathus linearis*
AAE	:	ascorbic acid equivalents
AAPH	:	2-methylpropionamidine dihydrochloride
ABTS	:	2,2'-azino-bis(3-ethylbenzothiazoline-6-sulfonic acid
AC	:	astrocyte
AMPH	:	amphetamine
ARPE-9	:	retinal pigment epithelial cells
ATP	:	adenosine triphosphate
AWA	:	acetone/water/acetic acid
BBB	:	blood-brain barrier
bEnd5	:	mouse brain endothelial cells
BMVEC	:	brain microvascular endothelial cells
$C_{20}H_{10}Na_2O_5$	:	fluorescein sodium salt
cdc2	:	cyclin-dependent 1 gene
CE	:	catechin equivalents
CNS	:	central nervous system
CO_2	:	carbon dioxide
CPUT	:	Cape Peninsula University of Technology
CSF	:	cerebrospinal fluid
CVD	:	cardiovascular disease
DA	:	dopamine
ddH_2O	:	double distilled water
dH_2O	:	distilled water
DMACA	:	4-dimethylaminocinnamaldehyde
DMEM	:	Dulbecco's modified eagle medium
DNA	:	deoxyribose nucleic acid
DO	:	deferoxamine
DP	:	delphinidin

EA.hy926	:	human embryonic endothelial cells
EC	:	endothelial cell
e.g.	:	example
ERS	:	electrical resistance system
et al.	:	"and others"
EtOH	:	ethanol
FACS	:	fluorescence activated cell sorter
FBS	:	fetal bovine serum
Fe^{2+}	:	ferrous iron
Fe^{3+}	:	ferric iron
Fe^{3+}-TPTZ	:	ferric iron 2, 4, 6-tri [2-pyridyl]-s-triazine
$FeCl_3.H_2O$	:	iron (III) chloride hexahydrate
FL2	:	fluorescent channel 2
FL2A	:	fluorescent channel 2 area
FL2W	:	fluorescent channel 2 width
FRAP	:	ferric reducing antioxidant power assay
FSC	:	forward scatter
G_1/G1-phase	:	gap phase
G_2/G2-phase	:	second gap phase
GAE	:	gallic acid equivalents
GPNT	:	rat brain vascular endothelial cells
GSH/GSSG	:	glutathione/glutathione disulfide
H295R	:	human adrenocortical carcinoma cells
hBMVEC	:	human brain microvascular endothelial cells
HCl	:	hydrogen chloride/hydrochloric acid
In situ	:	"on site/in position"
In vitro	:	"in glass"
In vivo	:	"within the living"
ISF	:	interstitial fluid
JNK	:	Jun-N-terminal kinase
M_1/M1-phase	:	mitotic phase

MA	:	methamphetamine
MDH	:	mitochondrial dehydrogenase activity
MeOH	:	methanol
MMP	:	matrix metalloproteinase
MN9D	:	dopaminergic cells
MOA	:	monoaminergic
MRC	:	Medical Research Council
MTT	:	3-(4, 5-dimethylthiazol-2-YI)-2, 5 diphenyltetrazolium bromide
n	:	sample number
Na_2CO_3	:	sodium carbonate
$Na_2HPO_4.2H_2O$	:	di-sodium hydrogen orthophosphate dehydrate
NAC	:	N-acetylcysteine
$NaH_2PO_4.H_2O$	:	di-hydrogen orthophosphate-1-hydrate
NEAA	:	non essential amino acids
NHF	:	normal human embryonic fibroblasts
NO	:	nitric oxide
nNOS	:	neuronal nitric oxide synthase
NVU	:	neurovascular unit
OCM-1	:	human melanoma cells
$OONO^-$	:	peroxynitrate
ORAC	:	oxygen radical absorbance capacity
OS	:	oxidative stress
P53	:	tumour suppressor protein 53
P-gp	:	P-glycoprotein
PA	:	proanthocyanidin
PBS	:	phosphate buffered saline
PC	:	pericyte
PCA	:	perchloric acid
PI	:	propidium iodide
QE	:	quercetin equivalents

R1	:	gate one
R2	:	singlet cells
R2-cells	:	rat cerebellum neural cells
R_f	:	fermented rooibos
RNS	:	reactive nitrogen species
ROS	:	reactive oxygen species
rpm	:	revolutions per minutes
RT	:	room temperature
S-phase	:	DNA synthesis phase
SACENDU	:	South African Community Epidemiology Network on Drug Use
SEM	:	standard error of mean
SH-SY5Y	:	human neuroblastoma carcinoma cells
SK-N-SH	:	human neuroblastoma-dopaminergic cells
SSC	:	side scatter
TE	:	trolox equivalents
TEAC	:	trolox equivalent antioxidant capacity
TEER	:	transendothelial electrical resistance
TC	:	tissue culture
TH	:	*Thunbergia laurifolia*
TJ	:	tight junction
TPTZ	:	2, 4, 6-tri [2-pyridyl]-s-triazine
U-118	:	human glioblastoma cells
viz.	:	namely
XTT	:	2,3-bis-(2-methoxy-4-nitro-5-sulfophenyl)-2H-tetrazolium-5-carboxanilide

UNITS OF MEASUREMENT AND SYMBOLS

abs	:	absorbance
ca.	:	circa
g	:	grams
G	:	G-force
hr	:	hour
hrs	:	hours
M	:	molar
m^2	:	meters squared
mAU	:	milliabsorbance units
mg	:	milligrams
mg/l	:	milligrams per liter
mg/ml	:	milligrams per milliliter
mg/kg	:	milligrams per kilogram
min	:	minutes
ml	:	millilitres
mM	:	millimolar
nm	:	nanometer
nM or nmol	:	nanomolar
µl	:	microliters
µg/ml	:	micrograms per millilitre
µM or µmol	:	micromolar
$\Omega.cm^2$	:	ohms centimeters squared
β	:	beta
°C	:	degrees Celsius
%	:	percentage
±	:	plus minus
>	:	greater than
<	:	less than
≥	:	greater or equal to
≤	:	less or equal to
*	:	significant increase
#	:	significant decrease
~	:	approximately

TABLE OF CONTENTS

CHAPTER 3…….

LIST OF FIGURES

1 Introduction

2 Methodology

3 Results

LIST OF TABLES

1 Introduction

2 Methodology

3 Results

LIST OF APPENDICES

CHAPTER 1

1 Introduction

1.1 Methamphetamine Statistics

The use of methamphetamine (MA) has become a pandemic problem which continues to increase with devastating outcomes on socio-economic status, crime and violence rates, and general progression. Globally, the estimated number of users range between 13.7-56.5 million of which the percentage of the population, aged between 15-64 years old, range between 0.3-1.3%. The Asian region accounts for the highest annual users (±38.2 million) followed by the African (±6.2 million) and American regions, respectively. There is however only data on MA usage in the Southern African sub-region with none obtained from the remaining sub-regions. Therefore, the total is subject to change (United Nations Office on Drugs and Crime, 2011) and thus these numbers may be higher than reported. More recently, it has been reported that in Africa, the trends in MA drug use has increased between 2000 and 2011. There is a direct correlation between the elevated usage and the need for rapid manufacturing as seizures of amphetamine (AMPH)-type stimulants also increased globally by 66% in 2011 from 2010 (United Nations Office on Drugs and Crime, 2013).

In South Africa, MA (commonly referred to as 'tik') abuse has become an alarming problem in the communities of Cape Town, Western Cape. Its abuse is strongly noted in the youth sector as 7% of learners between grade 8 and 11 admitted to long term use of MA (Reddy *et al*., 2013). The highest user level is reported among those under 19 years old. Moreover, according to the Medical Research Council (MRC), 98% of "tik" addicts who seek help in South Africa are from the Western Cape. Treatment data from South African Community Epidemiology Network on Drug Use (SACENDU) indicated that compared to other Republic of South Africa provinces, use of MA as a primary drug of abuse is highest in the Western Cape (35%) followed by the Eastern Cape at 5%. In 2002, less than 1% of clients at one of the largest drug treatment centres in the Western Cape, Cape Town Drug Counseling Centre, used "tik". This amount increased to 52%

in 2008 (Modernization Programme, 2010). The demand for treatment for the use of MA and MA-related problems sharply increased from 2002 to 2008 as the majority (currently 70%) is in treatment for the first time (Plüdderman *et al*., 2009).

Treatment demand data collected by the MRC's SACENDU project from 25 specialist treatment centres indicate that between 2002 and 2008, the total number of patients admitted for various drugs increased from 1551 to 2537. The number of patients admitted for MA as a primary drug choice was 13 in the last 6 months of 2002 which rapidly rose to 944 in the first 6 months of 2008. The overall ages ranged between 13-61 years old with an alarming 30-50% accounting for patients between the ages of 13 and 15. Patients that utilized MA as their primary drug choice and attended Cape Town treatment centres in 2008 are from over 180 suburbs or towns. More than 20 patients seeking help emanated from Bellville, Eerste River, Kraaifontein, Manenberg and Mitchell's Plain. The sharp increase of patients seeking treatment could be an indication that MA and associated drugs popularity are also increasing amongst the community (Plüdderman *et al*., 2009). Treatment centers which attend to MA abuse and relapses largely employ psychosocial approaches as no accepted medical treatments have been established. Thus, there is a pivotal requirement for treatment development.

1.2 Current Trends in Methamphetamine Therapy

In the absence of accepted medical treatment for MA abuse, there is a desperate need to accelerate the very slow pace of clinical testing for new possible therapies in the treatment of MA addiction (Cretzmeyer *et al*., 2003). The proposed reason for the difficulty in treatment is thought to be that with MA abuse, the "memories" of addiction might be "hardwired" and involve actual structural changes to brain neurons (e.g. dendritic spine density) that make addiction resistant to therapeutic intervention (Kish, 2008). Preliminary data support the possibility that "drug substitution therapy" might be useful in the treatment of MA addiction. The mechanism explaining the transition from MA-liking to intense compulsive wanting could involve a "pathological learning" process in which dopamine (DA) facilitates (Kish, 2008). Based on the research

available on MA treatment abuse, promising interventions can be identified, but no clear treatment of choice could be found (Cretzmeyer *et al*., 2003).

According to the MRC, treatment strategies include introducing science-based models of substance abuse treatment into community settings, brief screening, monitoring and interventions (Plüdderman *et al*., 2009). Frawley and Smith (1992) investigated treatment using aversion therapy where patients were treated in different compartmentalized sections (educational groups, individual and family counseling, and aftercare planning) based on need. This form of treatment had no significant outcome. Huber *et al*. (1997) involved extensive data collection on outpatient matrix model program (which is designed to integrate several disparate interventions into a comprehensive, structural approach comprising of individual therapy, relapse therapy and family education groups, urine testing and 12-step program involvement) and results for process variables only were reported which concluded that the findings provide a benchmark for the effectiveness of psychosocial interventions allowing comparisons with other treatments. Research was also done on matrix treatment programs and desipramine (an anti-depressant) which evaluated the impact of psychosocial intervention rather than pharmacotherapy. The results indicated no significant differences with better rates observed when treatment was increased coupled with an extended duration (Shoptaw *et al*., 1994).

Other pharmacological approaches also deemed fruitless involved aripiprazol (Stoops *et al*., 2006), GABA agents such as gabapentin, baclofen (Heinzeling *et al*., 2006), vigabatrin (Fechtner *et al*., 2006), selective serotonin reuptake inhibitors (Piasecki *et al*., 2002), ondansetron (Johnson *et al*., 2008) and mirtazapine (Harper and Napler, 2005), and a PROMETA™ treatment programme used primarily for MA addiction consisting of flumazenil, gabapentin and hydroxyzine (Ling *et al*., 2011). Studies involving bupropion (Elkashef *et al*., 2008) and modafinil (McElhiney *et al*., 2009) have demonstrated potential as a treatment on the effects of MA. Anti-methamphetamine monoclonal antibodies have shown potential by reducing MA administration, locomotor effects and discriminative stimulus effect in rats and pigeons (Byrnes-Blake *et al*., 2005;

Daniels *et al*., 2006). The relatively unsuccessful remedial programs mentioned in the forgoing studies concentrated on addressing the physiological aspects without taking into account the psychological aspects of addiction.

1.3 Nomenclature and Chemical Properties of Methamphetamine

Methamphetamine (MA) is also chemically known as N, α-dimethylphenethylamine having a chemical formula of $C_{10}H_{15}N$ (Figure 1.1). It also referred to as desoxyephedrine, methylamphetamine, phenylisopropylmethylamine, and a variety of other similar systematic names. MA has a molecular weight of 149.9 g/mol and belongs to the family, phenethylamine and the class, AMPHs (Logan, 2002).

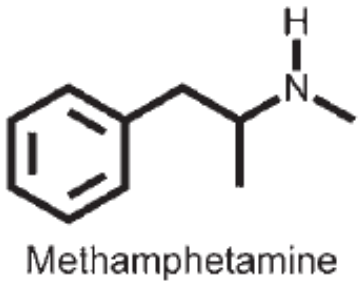

Figure 1.1 Chemical structure of MA (Hendrickson *et al.*, 2006).

1.4 Overview of Methamphetamine Synthesis and Its Effects

MA is a potent, addictive psychostimulant that affects many areas of the central nervous system (CNS) by causing neurotoxicity. It is commonly a white, odourless, bitter-tasting crystalline powder that readily dissolves in water or alcohol (Chen *et al.*, 2003; Thiriet *et al.*, 2005; Chen *et al*., 2012). MA is also found in three other forms: crystalline/powder, pill/tablet, rock and paste/base form (Figure 1.2) (Topp *et al*., 2002; Degendhart and Topp, 2003; Dore and Sweeting, 2006). Based on these forms, it can be snorted, orally ingested or injected intravenously. In South Africa, MA is predominantly smoked as the user experiences a rapid onset and intense "high" of the drug (Logan, 2002; Nordahl *et al*., 2003; Kish, 2008). The drug can easily be made in clandestine laboratories using the red-phosphorus and the lithium-ammonia reduction method (Logan, 2002). However, the active ingredient required, pseudoephedrine, must be present which can easily be obtained from relatively inexpensive over-the-counter

medications such as Advil Cold, Sudafed, Bromfed, etc. (Armellin *et al*., 2006; Barker and Antia, 2007). There are environmental and health dangers that accompany illicit production due to the exposure of a combination of corrosive gases or chemicals produced. The mild effects include: nausea, dizziness, headaches, anxiety, coughing, chest pain, shortness of breath and lethargy. More serious effects include: pulmonary edema, kidney failure, liver damage, irritation and severe chemical burns to the skin and to the mucous membranes of the nose, mouth and throat, frostbite, conjunctivitis, corneal injury, blindness, damage to the CNS, and death (Oregon Department of Human Resources, 1988).

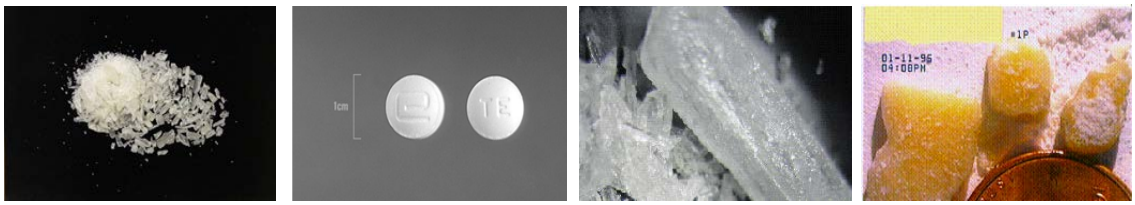

Fig A. Crystalline powder | Fig B. Pill/tablet | Fig C. Rock | Fig D. Paste/base

Figure 1.2 Forms of MA administered for recreational purposes: **A** Crystalline powder (most common) form (http://sshs.amaisd.org/index.php/alcohol-and-drug-prevention/meth/). **B** Pill/tablet form (http://www.methproject.org/answers/whats-meth-made-of.html#Whats-in-Meth). **C** Rock form (http://nurseandlawyer.com/page/2/). **D** Paste/base form (http://methdata.tripod.com/).

1.5 Metabolism and Bioavailability of Methamphetamine

Although MA ultimately affects various organs, it is of vital importance to establish the metabolic route of MA as well as the amount of MA the tissues get exposed to. When MA is administered, it is mainly metabolized in the liver through *p*-hydroxylation, β-hydroxylation, *N*-demethylation and deamination in rats (Dring *et al*., 1970; Caldwell *et al*., 1972a). This is similar with AMPH (Dring *et al*., 1970). In humans however, both aromatic hydroxylation and demethylation are significant reactions in MA metabolism (Caldwell *et al*., 1972a, Caldwell *et al*., 1972b; Kanamori *et al*., 2005). Initially, MA undergoes *N*-demethylation, aromatic hydroxylation and aliphatic hydroxylation metabolic reactions (Caldwell *et al*., 1972a). Demethylation accounts for 30% of all metabolites and ultimately produces benzoic acid (Caldwell *et al*., 1972a; Caldwell *et*

al., 1972b). Deamination has a low occurrence in humans, accounting for 6% of the dose (5% benzoic acid and 1% benzyl methyl ketone) (Caldwell *et al*., 1972a). Aromatic hydroxylation on the other hand accounts for approximately one third of ^{14}C excreted in 24 hours (Dring *et al*., 1970; Caldwell *et al*., 1972a). In addition, secondary reactions may involve β-hydroxylation (Caldwell *et al*., 1972a; Kanamori *et al*., 2005).

Dring *et al*. (1970) and Caldwell *et al*. (1972a) observed similar results when they performed AMPH metabolic studies on various species (human, guinea pig and rat) after administrating ^{14}C-labelled AMPH. After 3-4 days, 90% of AMPH and MA were present in human urine samples and approximately 54-65% in the first day. Moreover, up to 30% of the drug remained unchanged and 20% as total benzoic drug. Minor metabolites included hippuric acid, norepinephrine, an acid labile precursor of benzyl methyl ketone, 4-hydroxynorepinephrine, 4-hydroxymethamphetamine, and 4-hydroxyamphetamine (Dring *et al*., 1970; Caldwell *et al*., 1972a; Caldwell *et al*., 1972b). Moreover, Caldwell *et al.* (1972a) also investigated biliary excretion of AMPH and MA in rat and found the major metabolites in agreement with their previous mentioned findings. After 24 hours, 18% of MA metabolites were found in bile while 69% of AMPH metabolites were found in urine and 16% in bile. Moreover, MA and AMPH metabolites in bile are reabsorbed and excreted in the urine (Caldwell *et al*., 1972b). Renal clearance for both smoked and intravenous routes was equivalent with a significant amount of MA (37 - 45%) excreted in urine (Cook *et al.*, 1993). In addition, suspended hepatocyte cultures incubated with MA revealed the presence of the following metabolites in the culture supernatants: AMPH, p-hydroxymethamphetamine and p-hydroxyamphetamine which are consistent with the previous findings (Kanamori *et al*., 2005).

Once MA is reabsorbed into the blood stream, it has a circulating half-life of 5 hours (Kish, 2008) and similar results have illustrated the geometric half-life of MA to be 11.1 hours when smoked, 11.4-12.2 hours when intravenously injected, and 10.7 hours when administered via the intranasal route (Cook *et al.*, 1993; Harris *et al.*, 2003; Schifano *et al.*, 2007; Cruickshank and Dyer, 2009; Shabani *et al.*, 2012) with bioavailabilities of

79% for intranasal (Harris *et al.*, 2003), 90.3 ± 10.4% for smoked MA hydrochloride and 67.2 ± 3.1% for oral MA administration (Schifano *et al.*, 2007). A drug with a high bioavailability will have more pronounced psychoactive effect (Schifano *et al.*, 2007). This could explain the popularity of smokable MA as a high bioavailability can be achieved with this formulation (Cook *et al.*, 1993; Schifano *et al.*, 2007). Studies on the bioavailability of MA have been restricted to blood and urine analysis (Melega *et al*., 2007; Schifano *et al*., 2007), while reports investigating the bioavailability of MA to the CNS are limited to Martins and colleagues, 2011.

1.6 Effects of Acute Methamphetamine Exposure

After acute MA administration, the release of epinephrine, norepinephrine and dopamine in the sympathetic nervous system takes place which accounts for the common effects including euphoria, increased energy, performance and self-confidence (Cretzmeyer *et al*., 2003; Nordahl *et al*., 2003; Moszczynska *et al.*, 2004; Plüdderman *et al*., 2009). These initial effects make the drug more attractive however the drug on a regular basis causes insomnia, suppressed appetite, hyperthermia, restlessness, irritability, increased/heightened sexual behaviour and tremors (Cretzmeyer *et al*., 2003; Nordahl *et al*., 2003; Thiriet *et al.*, 2005; Barr *et al*., 2006; Plüdderman *et al*., 2009). Respiratory effects include increased respirations, hypertension and pulmonary edema, and a decreased lung capacity. Cardiovascular effects include increased heart rate and blood pressure, tachycardia and/or arrhythmias (Logan, 2002; Cretzmeyer *et al*., 2003; Barr *et al*., 2006; Plüdderman *et al*., 2009). Users run the risk of over dose characterised by dehydration, hyperthermia, convulsions, renal failure, stroke and myocardial infarction (Logan, 2002; Cretzmeyer *et al*., 2003; Nordahl *et al*., 2003; ; Thiriet *et al.*, 2005; Barr *et al*., 2006; Plüdderman *et al*., 2009).

1.7 Effects of Chronic Methamphetamine Exposure

Chronic abuse results in detrimental, and sometimes fatal, effects. These effects include severe weight loss/anorexia, severe dermatological problems (“MA mouth”), higher risk of seizures and uncontrollable rage/violent behavior (Nordahl *et al*., 2003; Thiriet *et al.*, 2005; Barr *et al*., 2006; Plüdderman *et al*., 2009). Long-term use also increases the risk

of contracting human immunodeficiency virus and Hepatitis C due to drug use and increase sexual risk behavior (Cretzmeyer *et al*., 2003; Plüdderman *et al*., 2009). A shift from the favourable mode of administration to intravenous route has been observed due to physical difficulties from smoking which include; damage to the nasal tract, coughing up blood, choking and difficulty in breathing (Cretzmeyer *et al*., 2003; Plüdderman *et al*., 2009). MA is also known to affect the CNS to cause mental health deficits such confusion, impaired concentration and memory, hallucinations, insomnia, depressive and psychotic reactions, paranoid reactions and panic disorders (Logan, 2002; Cretzmeyer *et al*., 2003; Nordahl *et al*., 2003; Barr *et al*., 2006; Plüdderman *et al*., 2009). It has to cross a physiologically restrictive barrier (blood-brain barrier) in order to ultimately influence the CNS.

1.8 The Blood-Brain Barrier

1.8.1 Localization and Functions of the Blood-Brain Barrier

There are three physiological barriers that restrict and control molecular exchange at the interfaces between the blood and tissue or its fluid spaces. The blood-brain barrier (BBB) is located between the blood and brain interstitial fluid, the choroid plexus epithelium separates the blood and ventricular cerebrospinal fluid (CSF), and the arachnoid epithelium is situated between the blood and subarachnoid CSF (Abbott *et al.*, 2006; Weiss *et al.*, 2008). However, it is the BBB that exerts the most control over the immediate microenvironment of brain cells (Abbott *et al.*, 2006). The BBB functions to maintain the CNS homeostasis, which includes the regulation of inflammatory cells to act in response to the local environment (Cardoso *et al.*, 2010) and the continual turnover and drainage of CSF and interstitial fluid (ISF). Moreover, it supplies the brain with essential nutrients, mediates efflux of many waste products and importantly protects the brain from ionic concentration fluctuations that can occur after a meal or exercise which would disrupt synaptic and axonal signaling (Abbott *et al*., 2006). It also restricts ionic and fluid movements between the blood and the brain thereby regulating ionic traffic. The latter produces the ISF that provides an optimum environment for neuronal functions and is essential in protection against harmful

substances, variations in blood composition and the breakdown of concentration gradients (Abbott *et al.*, 2006; Cardoso *et al.*, 2010). Thus it serves to protect the brain against foreign material, toxins and other substrates (Weiss *et al.*, 2008; Cardoso *et al.*, 2010; Li *et al.*, 2010) including narcotics such as MA.

1.8.2 Composition of the Blood-Brain Barrier

The BBB is often considered to be three-cell archetype consisting of the supporting pericyte (PC), the astrocyte (AC) and brain microvascular endothelial cell (BMVEC), (Gumbleton and Audus, 2001). Although the biochemical properties of BMVECs controls the BBB permeability, overall brain microvascular biology results from interactions of these cells with the basement membrane and neighbouring glial cells, such as microglia and ACs, as well as neurons and perivascular PCs (Cardoso *et al.*, 2010). The various cell types (basement membrane, neurons, microglia, PCs, endothelial cells and ACs) collectively constitute the neurovascular unit (NVU) (Figure 1.3), which is required for both health and CNS function (Cardoso *et al.*, 2010) and are indirectly involved in the establishment and maintenance of the BBB (Weiss *et al.*, 2008).

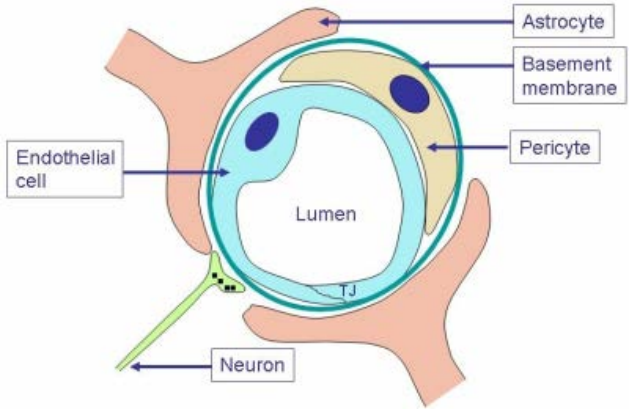

Figure 1.3 Components of the BBB constituted by endothelial cells, astrocytes and pericytes (http://home.szbk.u-szeged.hu/~krizbai/index.html).

1.8.3 The Three Main Blood-Brain Barrier Components

1.8.3.1 Pericytes

Most elements of the basement membrane including a number of proteoglycans are synthesized by vascular pericytes (PCs). It is a process thought to be a crucial step in the differentiation of the BBB (Cardoso *et al.*, 2010). PCs are integral constituents of each capillary with various frequencies in different vascular beds and are most abundant in the CNS and retina (Liebner *et al*., 2011). Along with endothelial cells (ECs), they communicate via tight junctions (TJs), gap junctions and adhesion plaques. The proper association of PCs and microvascular is essential in maintaining structural support and junctional integrity. The association with blood vessels has been suggested to regulate EC proliferation, migration and differentiation. Importantly, in response to stress stimuli, as during severe and prolonged oxygen deprivation, PCs make regulatory adjustments (Cardoso *et al.*, 2010) and have been correlated with the barrier capacity of the endothelium. PCs are actively involved in maintenance of the integrity of the vessel, vasoregulation and restricted BBB permeability (Weiss *et al.*, 2008).

1.8.3.2 Astrocytes

Astrocytes (ACs) play a major role in promoting proteoglycan synthesis with a resultant increase in BMVEC charge selectivity and the induction of BBB functions (Cardoso *et al.*, 2010). Specifically, ACs are involved in physiological and biochemical activities such as neural parenchyma compartmentalization, maintenance of the ionic homeostasis of the extracellular space, pH regulation and neurotransmitter uptake and processing. It also provides energy rich substrates to the neurons and mediates signals from the brain to the vascular system. Moreover, ACs are believed to play a decisive role in the maintenance of the BBB properties and in controlling the cerebral flow (Liebner *et al*., 2011). They are also required for proper neuronal function and the close proximity of neural bodies to brain capillaries suggests that the interactions between these elements are essential for a functional NVU (Cardoso *et al.*, 2010). Astrocyte- and glial-released factors have also been suggested to contribute to BBB integrity, including glial-derived neurotrophic factor, angiopoietin-1 and angiotensin II (Weiss *et al.*, 2008).

1.8.3.3 Endothelial Cells

Endothelial cells (ECs) present pivotal properties that restrict the free movement of molecules and are therefore considered the anatomic basis of the BBB. The restrictive function is due the presence of TJ proteins located paracellularly, between adjacent ECs (Cardoso *et al.*, 2010). One of the brain endothelium's most important characteristics in mammals is its highly restricted and controlled permeability to compounds and ions. The latter is reflected by a very high transendothelial electrical resistance (TEER). The endothelial lining presents a large surface area (total estimated interface area is 350 m^2) for the exchange of materials between the blood and the brain (Michiels, 2003). Moreover, the differences between brain and non-brain ECs allows for the necessary restrictive functioning of the BBB. The differences result in low level of non-specific transcytosis (pinocytosis) and paracellular diffusion of hydrophilic substances, strong metabolic activity due to the high number of mitochondria, and the polarized expression of membrane receptors and transporters responsible for the active transport of blood-borne nutrients as well as the efflux of potentially toxic substances from the cerebral region to the vascular compartment (Weiss *et al.*, 2008).

1.8.4 Blood-Brain Barrier Disruption and Brain Disorders

The origin of diseases may differ but the role played by the brain endothelium usually shares some basic trends such as augmented leukocyte adhesion and migration, enhanced expression of immunologically relevant antigens and changes in the BBB permeability and function, which all results in BBB disruption. Short periods of hypoxia may lead to hyperpermeability observed using mouse brain endothelial (bEnd5) cells and BBB injury is present to a varying degree in all multiple sclerotic lesions. A number of pathologies and several disorders seem to involve the disturbances of endothelial-glial interaction and may even exacerbate the adverse effects on the BBB permeability (Lundquist and Renftel, 2002; Hawkins and Davis, 2005; Abbott *et al*., 2006; Yang *et al*., 2007; Palmela *et al*., 2011).

1.8.5 The Immortalized bEnd5 Cell Line as an *In Vitro* Blood-Brain Barrier Model

The BBB is formed, in large, by the ECs that line cerebral microvessels (Abbott *et al.*, 2006) which limit solute exchange between the blood and CNS (Mahajan *et al*., 2008). In order to establish a relationship between the BBB, the brain and exogenous compounds, the bEnd5 cell line can be used to investigate transport across the BBB to the brain. These cells have a spindle-cell shape (Yang *et al*., 2007; Steiner *et al*., 2011) and were established as a cell line from isolated mouse brain endothelial cells by using Polyoma virus middle T-antigen (Williams *et al*., 1989; Reiss *et al*., 1998; Yang *et al*., 2007; Steiner *et al*., 2011; Watanabe *et al*., 2013). An immortalized cell line has the advantage of being less labor intensive and the tedious procedures of isolating the brain endothelial can be avoided, however a disadvantage may include continuous sub-culturing of the cells which could result in a change of occludin expression and incomplete TJ formation (Lundquist and Renftel, 2002). Mouse models may also prove more advantageous due to their availability of transgenic and gene-targeted animals and the wide range of antibodies (Steiner *et al*., 2011). Using *in vitro* models however, minimizes the number of animals required for experiments. The bEnd5 cell line has been shown to reach a TEER value of 121 $\Omega.cm^2$ (Audus *et al*., 1990; Yang *et al*., 2007). Furthermore, the cell line expresses three important junction proteins: claudin-5, occludins, and zona occludins-1 in addition to vascular endothelial-cadherin, von Willebrand factor, platelet endothelial cell adhesion molecule-1, endoglin, intercellular adhesion molecule-2 and transporters such as P-glycoprotein, sodium-potassium-chloride-/NKCC co-transporters, glucose transporter-1 and most protein kinase C isoforms (Yang *et al.*, 2007; Steiner *et al*., 2011; Paolinelli *et al*., 2013; Watanabe *et al*., 2013). The existence of TJs in bEnd5 cells, which is a core component in restrictive BBB function, has been clearly demonstrated. Using this proposed cell line, mechanisms involving MA and the BBB could then be elucidated.

1.8.6 Mechanisms of Methamphetamine on the Blood-Brain Barrier

MA's potent and toxic action on the sympathetic and CNS makes a strong case for the urgency in which MA use should be addressed. The adverse outcomes of MA have been

well established however the mechanisms behind these effects are poorly understood. Due to MA's high lipid solubility and the additional methyl group, large amounts of the drug can readily cross the BBB via non-specific diffusion (Syed *et al*., 2001; Nordahl *et al*., 2003; Bloom *et al*., 2008). Once in the neuronal setting, it is characterized by the disruption of monoamine neurotransmitter production, synaptic integrity of the dopaminergic system (Ramirez *et al.*, 2009) and adverse effects on the serotonin and cholinergic systems (Nordahl *et al*., 2003). Physiological concentrations have been shown to cause both short-term and persistent DA depletion as MA ultimately results in DA efflux, a consequence of transport reversal (Goodwin *et al.*, 2003; Moszczynska *et al.*, 2004; Cervinski *et al.*, 2005; Kish, 2008). Positron emission tomography imaging and post-mortem studies in humans provide evidence of MA's neurotoxicity, with regular users showing a loss of DA nerve terminals in the caudate and putamen, reduced glucose metabolism in the thalamus, caudate and putamen, and an increased glucose metabolism in the parietal cortex (Davidson *et al*., 2001; Volkow *et al*., 2001; Kish, 2008). These structural brain changes are associated with both long- and short-term impairment in cognitive processing, memory and emotion (Parry *et al.*, 2004). However, these effects become prominent only after MA affects the integrity of the BBB.

1.8.7 Methamphetamine Adversely Affects the Cell Cycle

Essentially, there are 4 phases of the cell cycle: G_1, S, G_2 and M_1 (Figure 1.4). The G_1 (gap phase) is the phase where the cells prepare for deoxyribose nucleic acid (DNA) replication. DNA synthesis occurs in the S phase and the G_2 (second gap) phase prepare the cells for division. During the M_1 (mitosis) phase, the replicated chromosomes are divided into separate nuclei and cytokinesis takes place to produce two daughter cells. There is also a G_0 phase which describes cells that have exited the cycle and become quiescent (Johnson and Walker, 1999). The timing and order of events are monitored via cell cycle checkpoints which ensure that the particular phase is completed before a new phase is initiated. This prevents the formation of genetically abnormal cells. In response to intracellular and extracellular environments, cycle progression can be ceased at these checkpoints (Murray, 1994). Apoptosis and proliferation are therefore

strongly coupled to cell cycle and can affect both cell division and cell death thus an imbalance could result in tissue atrophy or growth (King and Cidlowski, 1998). Moreover, cell proliferation is a vital mechanism for repairing the monolayer adjacent to the lesion or site of injury (Buşu *et al*., 2013) and therefore maintains a functional BBB.

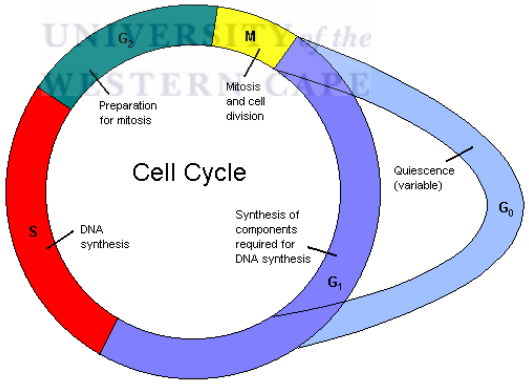

Figure 1.4 The different phases and activities that take place in the cell cycle (http://www.ch.ic.ac.uk/local/projects/s_liu/Html/Graphics/CellCycle.gif).

Cell cycle progression has been associated with an increase in intracellular glutathione/glutathione disulfide (GSH/GSSG) levels which modulates the function of redox-sensitive protein cysteines. This ultimately plays a role in cell growth, proliferation, differentiation and apoptosis. Buşu *et al*. (2013) conducted an experiment involving GSH and cell cycle activities on BMVECs and observed a decrease in nuclear GSH associated with enhanced DNA damage. This finding was coupled with the lack of endothelial GSH synthesis and a lengthened resident time of ECs in the S-phase. They concluded that the delay in S-to-G2-to-M progression allows for extended time for DNA repair and cell survival. However, MA has shown to affect the DNA synthesis in the S-phase. Yuan *et al*. (2011) demonstrated that *in vivo* MA administration resulted in a decreased pool of S-phase progenitors without specific alterations in the S-phase dynamics of the cell cycle. This result was accompanied by inhibited hippocampal proliferation coupled with immature neurons being inhibited proposed as result of maladaptive modifications in the development of neural progenitors and increases in cell death. Since MA interferes with the S-phase, the synthesis of new cells is inhibited. Maturation of hippocampal progenitors into glutamatergic neurons in adulthood is

thought to contribute to and maintain adult hippocampal structure and function (Earnhart *et al*., 2007), which may influence the relapse rates of recreational users.

In both, *in vivo* and *in vitro* models, MA cytotoxicity involves the mitochondrial-dependent death pathway which is strongly linked to DA deregulation (Genca *et al*., 2007). MA has been reported to diffuse into the mitochondria and ultimately results in the disruption of the electrochemical gradient (Chance and Williams, 1956) which in turn initiates apoptotic processes (Lemasters *et al*., 1999). In addition, various proapoptotic factors (cytochrome-c, cell death cysteine proteinases and caspases) also arise from dysfunctional mitochondria (Murphy *et al*., 1999). The resultant apoptotic cascades are irreversible once the proapoptotic factors have been released (Davidson *et al*., 2001). Necrosis could also be affiliated with MA induced excitotoxicity which is the overstimulation of nerve cells (Stout *et al*., 1998) and has been shown to occur in several brain areas (cortex, striatum and hippocampus) after MA administration (Deng *et al*., 2001). Most of the research relating to MA and its possible effects on cell cycles is largely focused on neuronal tissue with little being reported on the *in vitro* MA-induced effects on the BBB. It is however possible that these effects could also occur in ECs which would generate novel insight into the mechanisms of MA-induced cell cycle results.

1.8.8 Methamphetamine Increases Blood-Brain Barrier Permeability

The BBB's ability to sustain its obstructive function, is dependent on its low permeability which is mirrored by a very high TEER of approximately > 1000 $\Omega.cm^2$ (Gumbleton and Audus, 2001; Abbott *et al*., 2006; Martins *et al.*, 2011). TEER in principle is a quantitative measurement describing the barrier integrity which in essence is the electrical, ohmic resistance of the cell layer (Benson *et al*., 2013). Studies have illustrated MA's ability to decrease TEER readings on numerous *in vitro* monolayers (Abdul-Muneer *et al*., 2005; Mahajan *et al*., 2008; Ramirez *et al*., 2009; Zhang *et al*., 2009; Martins *et al*., 2010; Carey *et al*., 2012; Rosas-Hernandez *et al*., 2013) which was often accompanied with an increase in leukocyte migration (Afghajanian *et al*., 2008; Dietrich, 2009; Ramirez *et al*., 2009). These two MA-induced mechanisms strongly

partake in the progression of vascular endothelial dysfunction and the pathophysiology of various vascular-related diseases (Lum and Roebuck, 2001; Afghajanian *et al*., 2008). MA's adverse influence on BBB permeability is further supported by observations with increases in albumin- and Evans Blue extravasation leakages (Bowyer and Ali, 2006; Sharma and Ali, 2006; Kiyatkin and Sharma, 2009; Martins *et al*., 2011; Sharma *et al*., 2012; Kiyatkin, 2013; O'Shea *et al*., 2014) which would otherwise be detained by the presence of an intact BBB. In addition, MA has also shown to modulate TJ expression (Mahajan *et al*., 2008; Martins *et al*., 2011). Another proposed mechanism is the activation of myosin long chain kinase which increases BBB permeability through the modification of TJs and cytoskeleton thereby causes a breach in BBB integrity (Ramirez *et al.*, 2009).

There is an increasing amount of evidence suggesting that the main source for MA-induced neurotoxicity is dependent on the production of reactive oxygen species (ROS) which is suggested to be of the bi-products of DA accumulation, subsequent enzymatic oxidation, DA auto-oxidation and increased glutamate release (Davidson *et al*., 2001; Chen *et al.*, 2003). Apart from ROS, reactive nitrogen species (RNS) have also been reported to contribute to neurotoxicity caused by MA usage (Fleckenstein *et al.*, 1997; Lin *et al.*, 1999; Cervinski *et al.*, 2005; Ramirez *et al.*, 2009). ROS production initiates a cascade of events which ultimately results in BBB dysfunction. These events include nitric oxide (NO) production and excess glutamate release as well as the activation of glial cells and matrix metalloproteinases (MMP) (Oppenheim *et al*., 2013). Anderson and Itzhak (2006) reported an increase in striatal nitrate (stable NO product), neuronal nitric oxide synthase (nNOS) expression and nitration results which is coupled with MA-induced dopaminergic neurotoxicity and results in the activation of apoptotic cascades (Imam *et al*., 2005) thus NO has the ability to contribute to tissue damage (de Vries *et al*., 1997). Martins *et al*. (2013) concluded that the BBB opening they observed involves endothelium-derived NO or NO-mediated trancytosis. In addition, NO generated by nNOS has also been shown to activate MMPs (Haddad and Yu, 2009). These proteases have been reported to degrade and redistribute components of the extracellular matrix and tight junctions (van der Goes *et al*., 2001; Nordahl *et al*., 2003;

Shreibelt *et al*., 2007; Dietrich, 2009; Martins *et al*., 2011; Lakhan *et al*., 2013). MA has also been associated with increased glutamate levels (Yamamoto and Raudensky, 2008; Northrop *et al*., 2011) and microglial activation (Thomas *et al*., 2004; Sekine *et al*., 2008) which then resulted in neuroinflammation (Yamamoto and Raudensky, 2008; Coelho-Santos *et al*., 2012) and further cytokine release. These events ultimately caused neuroinflammation and TJ rearrangement thus exacerbation of BBB dysfunction (Nordahl *et al*., 2003; Martins *et al*., 2011; Martins *et al*., 2013).

The role of MA-induced oxidative stress (OS) is further supported by the finding that Trolox (Ramirez *et al*., 2009), N-Acetylcysteineamide (Zhang *et al*., 2009; Carey *et al*., 2012), metallothioneine, zinc (Ajjimaporn *et al*., 2005), melatonin (Parameyong *et al*., 2013), mannitol, ascorbic acid, vitamin E (De Vito and Wagner, 1989), phenyl-butyl-nitrone (Yamamoto and Zhu, 1998) and selenium (Imam and Ali, 2000) attenuates the increased lipid peroxidation (Zhang *et al*., 2009; Carey *et al*., 2012), monocyte migration (Ramirez *et al*., 2009), peroxynitrate generation (Imam and Ali, 2000) and cell death (Ajjimaporn *et al*., 2005; Zhang *et al*., 2009; Carey *et al*., 2012; Parameyong *et al*., 2013) as well as decreased TEER (Ramirez *et al*., 2009; Zhang *et al*., 2009; Carey *et al*., 2012), glutathione peroxidase and GSH levels (Zhang *et al*., 2009; Carey *et al*., 2012), DA and serotonin levels in the striatum (De Vito and Wagner, 1989; Yamamoto and Zhu, 1998) brought about by MA. MA-induced ROS levels were also significantly decreased as a result of these antioxidants (Ajjimaporn *et al*., 2005; Zhang *et al*., 2009; Carey *et al*., 2012; Parameyong *et al*., 2013). Since the adverse effects caused by MA are reduced by ROS scavengers and anti-oxidants, novel treatments possessing scavenging properties may have the potential to ameliorate BBB injury. Natural herbal teas, such as *Aspalathus linearis* have been reported to possess antioxidant capabilities but has as yet, not been investigated against MA.

1.9 Rooibos (*Aspalathus linearis*) Herbal tea

1.9.1 Anecdotal Properties of *Aspalathus linearis*

Aspalathus linearis is the only edible shrubby legume belonging to the genus *Aspalathus* which includes more than 270 species (Joubert and Ferreira, 1996; Villaño *et al*., 2010; Breiter *et al*., 2011; Joubert and de Beer, 2011). The plants' leaves and stems undergoes a process of fermentation (Ferreira *et al.*, 1995; Joubert, 1996) in order to manufacture the local endemic tea *viz.* rooibos herbal tea (Figure 1.5), which is a drinking beverage with acclaimed beneficial health effects (Krafczyk and Glomb, 2008). The herbal tea has been found to possess a myriad of properties which include: anti-oxidant, -atherosclerotic, -inflammatory, -mutagenic, -carcinogenic, -allergic, -tumor and -viral activities, hepatoprotective properties and immune-modulating effects (Ferreira *et al.*, 1995; Joubert and Ferreira, 1996; Nijveldt *et al.*, 2001; McKay and Blumberg, 2007; Villaño *et al*., 2010). It also has been established to have effect on dermatological diseases such as Behcet's disease, Sweet disease and photosensitive dermatitis (Ferreira *et al.*, 1995; Joubert and Ferreira, 1996). Moreover, the herbal tea is prescribed against nervous tension, allergies and various stomach and indigestion problems (Ferreira *et al.*, 1995; Joubert, 1996; Joubert and Ferreira, 1996). The potential health benefits and bioactivity of *A. linearis* have been linked to its polyphenolic content naturally occurring in the plant (Ferreira *et al.*, 1995; Joubert and Ferreira, 1996; McKay and Blumberg, 2007; Joubert and de Beer, 2011)

Fig A. Unfermented (green) tea Fig B. Fermented (red) tea

Figure 1.5 Physical characteristics of the two forms of rooibos (*A. linearis*) herbal tea: **A**. Unfermented form also known as green tea (http://www.carmientea.co.za/tea-variants/rooibos/). **B**. Resulting form after fermentation also known as red tea (the beverage) (http://amavida.com/learn/).

1.9.2 Chemistry of *Aspalathus linearis*

1.9.2.1 The Polyphenolic Contents of *Aspalathus linearis*

Antioxidant activity is reported to be the result of polyphenols present in the herbal tea (Ferreira *et al.*, 1995; Joubert and Ferreira, 1996). Polyphenols, a class of phytochemicals include classes of chromones, coumarins, lignans, stilbenes, xanthones and the ubiquitous flavonoids (McKay and Blumberg, 2007). *A. linearis* boasts a large yield of flavonoids with very high contents of C-glycosides. It also possesses minerals, ascorbic acid, is caffeine-free and has low tannin levels (Ferreira *et al.*, 1995; van der Merwe *et al.*, 2006; Krafczyk and Glomb, 2008; Joubert and de Beer, 2011). A study done by Krafczyk and Glomb (2008) characterized the phenolic compounds in processed *A. linearis* (Table 1). In addition, lignans, flavones diglycosides, (+)-catechin, a phenylpyruvic acid glycoside, the flavonol quercetin-3-O-robinobioside and the coumarins, esculetin and esculin, have also been identified in *A. linearis* (Krafczyk and Glomb, 2008; Joubert and de Beer, 2011). Infusion of fermented rooibos herbal tea has also been reported to contain 1.29 µg/ml fluoride, a sodium content of 43.33 µg/ml, and minute amounts of aluminium (Joubert and de Beer, 2011). Green tea (*Camelia sinensis*) is also known to contain a high phenolic content and was compared to rooibos herbal tea. There was a significant difference in total polyphenols (41%-green vs. 29%-rooibos) with lower percentages of flavonoids and non-flavonoids in rooibos. These differences may relate to the difference in enzymatic and chemical modifications occurring during fermentation and processing (McKay and Blumberg, 2007).

Table 1 Polyphenols present in *A. linearis*

Class of Phytochemicals	Individual component
Flavan-3-ols	Catechin
Flavanones	Eriodictyol
Flavones	Chrysoeriol, iso-orientin, iso-vitexin, luteolin, orientin and vitexin
Flavonols	Quercetin, iso-quercetin and rutin
Dihydrochalcones	Aspalathin and nothofagin
Proanthocyanadins	Present
Phenolic acids	Caffeic, ferulic, p-coumaric, p-hydroxybenzoic, 4-hydroxy-3,5-dimethoxycinnamic, protocatechuic acid, syringic and vanillic acid

(Ferreira *et al*., 1995; McKay and Blumberg, 2007)

1.9.2.2 Flavonoids Present in *Aspalathus linearis*

The polyphenol group can be further divided into the subgroups of flavonoids. The flavonoid content of *A. linearis* has been described by Van der Merwe *et al*. (2010) and Joubert and Ferreira (1996) (Figure 1.6). However, rooibos herbal tea is unique since it contains large amounts of aspalathin (2'.3,4,4',6'-penthydroxy-3-*C*-β-D-glycopyranosyldihydrochalcone) that can only be isolated from *A. linearis* and is the one of two known sources of nothofagin in much lower quantities (Joubert, 1996; Joubert and Ferreira, 1996; McKay and Blumberg, 2007; Snijman *et al*., 2009; Villaño *et al*., 2010; Joubert and de Beer, 2011). The two C-linked dihydrochalcone glycosides are the major flavonoid constituents in unfermented (green) rooibos herbal tea (van der Merwe *et al*., 2010). Aspalathin contributes ~43% of the total antioxidant capacity of aqueous extracts of unfermented rooibos and has comparable radical scavenging potency to the well-known flavonoid antioxidants namely quercetin and epigallocatechin gallate. Aspalathin also constitutes *ca*. 0.55% of soluble solids of the processed herbal tea and in unprocessed tea aspalathin comprises as much as 9.3% of the plant material (Joubert, 1996) as it is greatly reduced via the oxidative process of fermentation. This process

results in the formation of the two flavones analogues, iso-orientin and orientin as major products which also contributes to antioxidant potency (Joubert *et al.*, 2008; Krafczyk and Glomb, 2008; Snijman *et al.*, 2009; Joubert *et al.*, 2010; Joubert and de Beer, 2011). The presence of flavonoids are presumed to contribute significantly to the scavenging effects on active oxygen species (Ferreira *et al.*, 1995). Therefore, an important property of polyphenols is their ability to scavenge of ROS (Ferreira *et al.*, 1995; Nijveldt *et al.*, 2001).

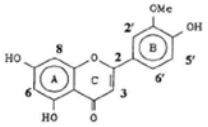

Fig A. Chrysoeriol

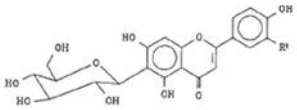

Fig B. Orientin R1=OH
Vitexin R1= H

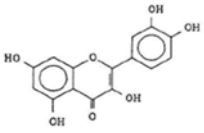

Fig C. Quercetin

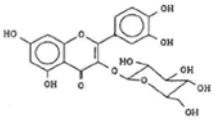

Fig D. Iso-quercetin

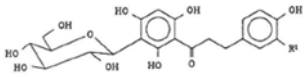

Fig E. Aspalathin R1=OH
Nothofagin R1= H

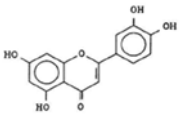

Fig F. Luteolin

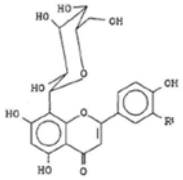

Fig G. Iso-orientin R1=OH
Iso-vitexin R1= H

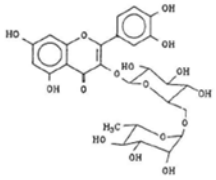

Fig H. Rutin

Figure 1.6 Molecular structures of the flavonoids present in *A. linearis*: **A** Chrysoeriol. **B** Orientin. **C** Quercetin. **D** Iso-quercetin. **E** Aspalathin and nothofagin. **F** Luteolin. **G** Iso-orientin and iso-vitexin. **H** Rutin (van der Merwe *et al.*, 2010; Joubert and Ferreira, 1996).

1.9.3 Metabolism and Bioavailability of Rooibos (*A. linearis*) Herbal Tea

After consumption of *A. linearis*, flavonoids are predominantly metabolized in the colon and liver. Phase II biotransformations in the liver include glucuronidation, sulfation or methylation of the phenolic hydroxyl groups. Variables such as absorption, inter-individual variability, bioavailability and mechanism of redox endogenous regulation, play an important role in defining the absorption and the efficiency of dietary antioxidants *in vivo* (Villaño *et al.*, 2010). Stalmach *et al*. (2009) conducted a study using ten volunteers who ingested 500 ml herbal tea containing total fermented flavonoid contents of 84 µmol. In the collected urine, 8 metabolites were identified. Two of the main compounds identified were O-methyl-aspalathin-O-glucuronide and eriodictyol-O-sulfate, whereas no metabolites were detected in the plasma samples. The overall metabolite levels excreted were 82 nmol, accounting for 0.09% of the flavonoids

in the fermented beverages. Most of the aspalathin metabolites (80-90%) were excreted within 5 hours of herbal tea consumption with a urinary recovery of 15 ± 3.5 nmol of metabolites which corresponded to 0.18% of intake suggesting that aspalathin absorption took place in the small intestine with a very limited bioavailability. Moreover, excretion of eriodictyol-O-sulfate metabolites occurred mainly during the 5-12 hour collection period with relatively low recoveries of 0.3% following consumption of 23 µmol of eriodictyol-O-sulfate in fermented beverages suggesting that absorption had occurred in the large intestine (Stalmach *et al.*, 2009).

Breiter *et al*. (2011) observed seven derived metabolites, aspalathin and nothofagin were identified including their unchanged forms in pig and human urine samples. It was also concluded that the dihydrochalcone, flavone-C, and flavanol-O-glycosides in unfermented rooibos herbal tea are bioavailable to a certain extent and as a consequence, it is assumed that the main constituents of flavonoids directly reach the large intestine. Furthermore, the flavonoids not absorbed in the upper gastrointestinal tract are degraded by bacteria residing in the colon, with subsequent hydrolysis of conjugates and glycosides, and ring fusion of the aglycones to phenolic acids, followed by reabsorption (Villaño *et al.*, 2010). Aspalathin is not subject to the degradation in the stomach as a 100% recovery rate was observed when incubated with artificial gastric juice for up to 2 hours (Stalmach *et al.*, 2009). In addition, the absence of detectable quantities of metabolites of dihydrochalcones and flavanone C-glycosides in plasma most probably reflects their rapid removal from circulation (Villaño *et al.*, 2010). However, unmetabolized compounds were recently confirmed in plasma (Breiter *et al.*, 2011). Despite low bioavailability of aspalathin, its *in vivo* bioactivity confirms the importance and relevance of this flavonoid as a potent ROS scavenger (Stalmach *et al*., 2009; Joubert *et al.*, 2010; Breiter *et al*., 2011; Joubert and de Beer, 2011).

1.9.4 The Antioxidative Properties of *Aspalathus linearis*

Antioxidants have a similar “preservative” effect on biological systems and particularly on human life (Joubert and Ferreira, 1996). Interaction of the phenolic constituents with free radical species in different phases provides different perspectives on their anti- or

pro-oxidant properties (Joubert, 1996). Primary or chain-breaking antioxidants interfere with lipid peroxidation which is followed by the chelation of metals, scavenging of oxygen, quenching of singlet oxygen and reduction of hydroperoxides to non-radical products which contribute in retarding the rate of lipid peroxidation (Joubert and Ferreira, 1996). Flavonoids have been described as antioxidants by means of their superoxide dismutase mimetic substances (Ferreira *et al.*, 1995; Nijveldt *et al.*, 2001). Aspalathin, catechins, phenolic carboxylic acids (protocatechuic acid, ferulic acid and caffeic acid), flavones (luteolin), flavanones (quercetin, iso-quercetin and rutin) and phenolic carboxylic acids (protocatechuic acid, ferulic acid and caffeic acid) in *A. linearis* possess antioxidant properties and contribute to the powerful scavenging abilities for protection of the body against ROS (Ferreira *et al.*, 1995; Joubert and Ferreira, 1996; Nijveldt *et al.*, 2001). A mechanisms by which flavonoids function is direct through scavenging where they are oxidized by radicals which then results in a more stable, less-reactive radical (Nijveldt *et al.*, 2001).

A. linearis has been shown to scavenge the physiologically relevant ROS, superoxide anion (Joubert *et al.*, 2008), peroxynitrate ($ONOO^-$) and interfere with nitric oxide synthase activity which reacts with free radicals to produce $ONOO^-$ radicals which then ultimately results in cell membrane damage. Rutin and quercetin inhibit xanthine oxidase which serves as an oxygen free radicals source. Luteolin was reported to be the most powerful inhibitor of the enzyme (Nijveldt *et al.*, 2001). *A. linearis* displays superior scavenging activity for both the xanthine or xanthine oxidase-generated superoxide and hydrogen peroxide (Fernandes *et al.*, 2004). *A. linearis* also protects against lipid peroxidation and scavenges alkyl peroxyl radicals, reduces compliment activation, and the release of peroxidase and arachidonic acid (Joubert *et al.*, 2008), thus ultimately preventing inflammatory responses and the production of ROS. ROS and inflammation has been strongly linked to tumor progression to which rooibos has also been associated with.

Studies report the ability of rooibos to inhibit cancer progression by reducing cancer-associated changes in animal cells induced by mutagens benzo[a]pyrene and mitomycin

C (Sasaki *et al*., 1993), cancerous transformations of mouse cells exposed to x-rays (Komatsu *et al*., 1994), age-related lipid peroxide accumulation in rat brains (Inanami *et al*., 1995) and the development of large esophageal papillomas by decreasing the number and size (Sissing *et al*., 2011). Rooibos also showed chemoprotective effects against cancer promotion in a liver carcinogenic model and skin cancer in mouse models (Marnewick *et al*., 2005; Petrova, 2009). Moreover, numerous positive effects of rooibos have also been shown against cardiovascular disease (CVD) by illustrating a decrease in lipid peroxidation (Inami *et al*., 2008; O'Keefe *et al*., 2008), atherosclerosis (Basu and Lucas, 2007), myocardial infarction occurrence (Mukamal *et al*., 2002) and angiotensin-converting enzyme (Samani *et al*., 1996; Persson *et al*., 2010) which is linked to CVD. In essence, *A. linearis* demonstrated protective effects in studies relating to cancer and CVD disease in which it is proposed that ROS played a critical role. It is therefore plausible that rooibos could protect against MA-induced OS and thus help maintain the integrity of the BBB.

Reports strongly suggest that rooibos could potentially protect against MA-induced effects on the integrity of the BBB which can be attributed to MA's potential to compromise the BBB's permeability. The presence of high levels of anti-oxidants aid in maintaining an intact BBB (Plateel *et al*., 1995), however, the lipophilic nature of MA allows it to readily cross the BBB in which its effects have been linked to excess ROS and RNS. These molecules give rise to cascades involving NO, MMP, increased glutamate, mitochondrial dysfunction, lipid peroxidation and, microglial and cytokine activation which in turn activates additional ROS and vice versa (Sekine *et al*., 2008; Yamamoto and Raudensky, 2008; Oppenheim *et al*., 2013; Northrop *et al*., 2011). Thus, it may be proposed that BBB dysfunction may be a result of a combination of events caused indirectly by MA. Interaction of rooibos polyphenols and/or non-polyphenolic compounds with ROS may prove to be useful in ameliorating BBB dysfunction brought about by MA and provide a foundation for natural therapeutic targets against narcotics.

1.10 Aims

The aim of the study was to determine the *in vitro* effects of pure methamphetamine on the blood-brain barrier in a cell culture model using the bEnd5 cell line, and investigate the potential protective effects of fermented rooibos (*Aspalathus linearis*) herbal tea.

1.11 Objectives

The following parameters were investigated in order to determine the effects of MA and R_f, individually and in combination, on bEnd5 cells over selected time intervals:

1. To determine cell numbers and % viability using, the trypan blue viability assay at 24, 48, 72 and 96 hours using selected concentrations of MA, R_f and combinations of the compounds. The conditions used in this assay included only 24 hour (once-off) exposure to the compounds.

2. To analyze the compounds effects on bEnd5 cell metabolic activity and viability using, the MTT/XTT viability assay at 24, 48, 72 and 96 hours using selected concentrations of MA, Rf and combinations of the compounds. The conditions used in this assay included 24 hour (once-off) and daily exposure to the compounds.

3. To investigate the permeability status in response to compound exposure using transendothelial electrical resistance (TEER) at 24, 48, 72, 96, 120 and 144 hours with exposure to selected concentrations of MA, Rf and combinations of the compounds. The conditions used in this assay included only daily exposure to the compounds.

4. To determine the compounds effects on bEnd5 cell cycles using flow cytometry at 24, 48, 72 and 96 hours using selected concentrations of MA, Rf and combinations of the compounds. The conditions used in this assay included only 24 hour (once-off) exposure to the compounds.

1.12 Hypothesis

The working hypothesis is that the adverse effects of pure methamphetamine on the blood-brain barrier will be ameliorated by fermented rooibos herbal tea.

CHAPTER 2

2 Methods and Materials

The aim of the study was to determine the effects that 24 hour (hr) and daily exposure of methamphetamine (MA) and fermented rooibos (R_f) has on mouse brain endothelial (bEnd5) cells over selected time intervals. bEnd5 cells were also subjected to a combination of the compounds to investigate potential mitigating effects of R_f against MA on the endothelial cells. The chemical analysis of the R_f sample was achieved by determining the polyphenol, flavonol and flavanol quantities expressed against a selected standard in addition to investigating the antioxidant activities using FRAP, ORAC and ABTS/TEAC assays. The chemical analysis is discussed in more detail below.

2.1 Preparation of Aqueous Infusion of *A. linearis*

A. linearis (South African Rooibos Council, Batch no. P06/02KK) was prepared by steeping the dried leaves in boiling water for 30 minutes (min). A 20% aqueous extract was pre-filtered through cheesecloth and subsequently through Whatman no. 4 followed by no. 1 filter paper. The filter extract was stored at -20 degrees Celsius (°C) and protected from light.

2.2 Chemical Analysis of Fermented Rooibos

Chemical analysis of the R_f aqueous extract was carried out under the supervision of Prof J. Marnewick at Cape Peninsula University of Technology (CPUT)'s Oxidative Stress Research Centre (Bellville, Cape Town, South Africa) with the following routine and standardizing tests: measurement of flavonols and flavanols (Wallace and Giusti, 2010; Li *et al*., 1996), ferric reducing antioxidant power (FRAP) assay (Benzie and Strain, 1996), oxygen radical absorbance capacity assay (ORAC) assay (Huang *et al*., 2005), ABTS (2,2'-azino-di-3-ethylbenzthialozine sulphonate) or Trolox equivalent antioxidant capacity (TEAC-total antioxidant status) assay (Zulueta *et al*., 2009) and the measurement of polyphenols (Schofield *et al*., 2001; Blainski *et al*., 2013; Berker *et al*., 2013).

2.2.1 Measurement of Polyphenols

2.2.1.1 Principle

This method made use of the redox reagent Folin Ciocalteu which oxidizes the polyphenols present in the tea extract. The redox reagent is formed by a blue chromophore complex consisting of a mixture containing phosphotungstic acid and phosphomolybdic acid. After oxidation, the previous mentioned acids are reduced to tungsten and molybdenum, respectively. The blue colouration can be quantified by visible-light spectrophotometry with a maximum absorbance in the region of 750 nm and is directly proportional to the total quantity of phenolic compounds originally present (Schofield *et al*., 2001; Blainski *et al*., 2013; Berker *et al*., 2013).

2.2.1.2 Chemicals Required for the Measurement of Polyphenols

The chemicals used in order to measure polyphenols included: 10% ethanol (EtOH) (Saarchem, Cat no. 2233540 LP), Folin Ciocalteu reagent (Merck, Cat no. 109001), 7.5% sodium carbonate (Na_2CO_3) (Sigma Aldrich, Cat no. 223530), gallic acid (Sigma, Cat no. G7384) was used as standard with which to determine the polyphenols in the extract. Stock standard concentrations were prepared as follows: 40 mg gallic acid was dissolved in 50 ml 10% EtOH to give a gallic acid stock standard concentration of 800 mg/l. The gallic acid stock control was prepared as follows: 10 mg gallic acid was dissolved in 50 ml 10% EtOH. All solutions were prepared on the day of analysis.

2.2.1.3 Sample Preparation and Analysis

The 20% R_f aqueous extract sample was directly used in the analysis. To avoid precipitates, the sample was centrifuged for 3 min at 4300.8 G-force (G) (4000 revolutions per minute (rpm)) and the supernatant was used in the analysis. Preparation of the sample was done on ice throughout the procedure. All samples were stored at -40 °C. The gallic acid stock standard concentrations were prepared (See Appendix A: Table 2.1) and 25 µl of the standard, control and sample was added (in triplicate) to designated wells, respectively. This was followed by the addition of 125 µl Folin Ciocalteu reagent to each well. The plate was left for 5 min at room temperature (RT)

and 100 µl Na_2CO_3 was added to each well. The plate was then left for an additional 2 hours (hrs) at RT before reading, using a Multiskan™ plate reader (Fisher Scientific) at 760-765 nm.

2.2.2 Measurement of Flavonols

2.2.2.1 Principle

The analysis made use of quercetin as the standard which was used to determine total phenolic subgroup within the R_f extract at 360 nm.

2.2.2.2 Chemicals Required for the Measurement of Flavonols

The chemicals necessary for the measurement of flavonols included: 10% EtOH, 95% EtOH, 0.1% hydrogen chloride (HCl) (Saarchem, Cat no. 100319 LP) in 95% EtOH, 2% HCl, The quercetin stock standard solution (80 mg/l) was prepared as follows: 4 mg quercetin (Sigma, Cat no. Q0125) was weighed and added to 50 ml 95% EtOH. The quercetin stock control was prepared as follows: 1.5 mg quercetin was weighed and added to 50 ml 95% EtOH. All solutions were prepared on the day of analysis.

2.2.2.3 Sample Preparation and Analysis

The 20% R_f aqueous extract sample was directly used in the analysis. To avoid precipitates, the sample was centrifuged for 3 min at 4300.8 G (4000 rpm) and the supernatant was used in the analysis. All samples were stored at -40 °C. The quercetin acid stock standard concentrations were prepared (See Appendix A: Table 2.2) and 12.5 µl added to designated wells, respectively. In addition, 12.5 µl of the control and sample (in triplicate) was added to designated wells. The solution, which contained 12.5 µl 0.1% HCl in 95% EtOH, was then added followed by the addition of 225 µl 2% HCl to each well. The plate was then left for 30 min at RT and read at 360 nm with the temperature set to 25 °C using a Multiskan™ spectrum plate reader.

2.2.3 Measurement of Flavanols

2.2.3.1 Principle

This assay was employed for the detection and quantification of proanthocyanidins (PAs). PAs (also known as condensed tannins) are polymeric condensation products of flavanols and the aromatic aldehyde, 4-dimethylaminocinnamaldehyde (DMACA), has an affinity for the C8 position of the A-ring and thus reacts with the terminal units of PAs. Specifically, aldehydes react with *m*-diphenol present in the A-ring of flavanols, which forms the blue coloured carbonium ion in acidic environment observed when using the assay. The method has a maximum absorbance of 640 nm (Li *et al*., 1996; Wallace and Giusti, 2010).

2.2.3.2 Chemicals Required for the Measurement of Flavanols

The chemicals utilized to determine the amount of flavanols in the extract included: 32% HCl-methanol (MeOH) solution prepared as follows: 250 ml HCl was added to 750 ml MeOH (Saarchem, Cat no. 4164080 LC) and mixed thoroughly. 4-Dimethylamino-cinnamaldehyde (DMACA) (Merck, Cat no. 822034) was prepared as follows: 0.25 g DMACA was dissolved in 500 ml HCl-MeOH mixture. Catechin hydrate (Sigma, Cat no. C1251) was used as a standard with which to measure the flavanols in the extract. The 1 mM catechin stock standard was prepared as follows: 0.0145 g catechin hydrate added to 50 ml methanol. The 200 µM catechin stock control was prepared as follows: 0.0029 g catechin hydrate was added to 50 ml MeOH. All solutions were prepared on the day of analysis.

2.2.3.3 Sample Preparation and Analysis

The 20% R_f aqueous extract sample was directly used in the analysis. To avoid precipitates, the sample was centrifuged for 3 min at 4300.8 G (4000 rpm) and the supernatant was used in the analysis. All samples were stored at -40 °C. The catechin acid stock standard concentrations were prepared (See Appendix A: Table 2.3) and 50 µl of the standard, control and sample was added (in triplicate) to designated wells, respectively. 250 µl DMACA was added to all wells for reaction initiation. The plate

was then left for 30 min at RT and absorbance was read at 640 nm using a Multiskan™ spectrum plate reader (After reading, if any of the flavanol values were greater than the standard curve range, a 10-fold dilution was performed on the samples by using 100 µl of the sample supernatant and 900 µl of MeOH. The flavanol assay with the diluted sample was then repeated).

2.2.4 Oxygen Radical Absorbance Capacity (ORAC) assay

2.2.4.1 Principle

The ORAC method was used to analyze the lipid-soluble antioxidant samples by introducing randomly methylated beta-cyclodextrin in 50% acetone water mixture. The mixture made lipid-soluble antioxidants soluble in phosphate buffer. This method is unique in its analysis as it takes into account the inhibition time and degree into a single quantity by measuring the area under the curve. Antioxidant capacity is measured by the inhibition of free radical damage. It is reflected by protection against probe fluorescent change and the fluorescent intensity changes indicate the degree of free radical damage (Huang *et al*., 2005).

2.2.4.2 Chemicals Required for the ORAC assay

The chemicals utilized for the ORAC assay included: hexane (Saarchem, Cat no. 2868040 LC) which was stored at RT. Acetone/water/acetic acid (AWA) solution stored at RT comprised of 700 ml acetone (Saarchem, Cat no. 1022040 LC), 295 ml distilled water (dH_2O) and 5 ml glacial acetic acid (Saarchem, Cat no. 1021000). The 75 mM, pH 7.4 phosphate buffer consisted of 2 solutions. The first solution consisted of 1.035 g sodium di-hydrogen orthophosphate-1-hydrate ($NaH_2PO_4.H_2O$) (Sigma Aldrich, Cat no. S9638) and 100 ml double distilled water (ddH_2O) which was mixed until dissolved. The second solution consisted of 1.335 g di-sodium hydrogen orthophosphate dihydrate ($Na_2HPO_4.2H_2O$) (Merck, Cat no. 5822880EM) added to 100 ml ddH_2O and was mixed until dissolved. 18 ml of the first solution and 82 ml of the second solution was then mixed to obtain 75 mM, pH 7.4 phosphate buffer. The phosphate buffer was stored at 4 °C and the pH of the solution was always re-checked for consistency before use.

Fluorescein sodium salt ($C_{20}H_{10}Na_2O_5$) (Sigma, Cat no. F6377) stock stored at 4 °C in a dark container consisted of 0.0225 g $C_{20}H_{10}Na_2O_5$ dissolved in 50 ml phosphate buffer. The 25 mg/ml peroxyl radical which is AAPH (2, 2'-Azobis (2-methylpropionamidine) dihydrochloride (Sigma Aldrich, Cat no. 440914). 0.5 M perchloric acid (PCA) (Saarchem, Cat no. 494612) which consists of 195 ml dH_2O mixed with 15 ml 70% PCA and stored at RT. Trolox (Sigma Aldrich, Cat no. 238831) was used as a standard in this assay. The 500 µM Trolox stock standard solution was prepared by the addition of 0.00625 g 6-hydroxy-2,5,7,8-tetra-methylchroman-2-carboxylic acid (Sigma Aldrich, Cat no. 238831) to 50 ml phosphate buffer which was mixed until dissolved. The 250 µM Trolox stock control comprised 0.00312 g 6-hydroxy-2,5,7,8-tetra-methylchroman-2-carboxylic acid added to 50 ml phosphate buffer and was mixed until dissolved).

2.2.4.3 Sample Preparation and Analysis

The 20% R_f aqueous extract sample was directly used in the analysis. To avoid precipitates, the sample was centrifuged for 3 min at 4300.8 G (4000 rpm) and the supernatant was used in the analysis. All samples were stored at -40 °C. The Trolox stock standard concentrations were prepared (See Appendix A: Table 2.4) and 12 µl of the standard, control and sample was added (in triplicate) to designated wells, respectively. From the fluorescein stock solution, 10 µl was added into 2 ml phosphate buffer. This solution was then diluted as follows: 240 µl of the fluorescein-phosphate buffer mixture was added to 15 ml phosphate buffer. 138 µl of this diluted solution was added into each well. 6 ml of the phosphate buffer was added to the 25 mg/ml AAPH (prepared fresh) and was mixed well until dissolved. 50 µl of this solution was transferred to each well and the final volume of the assay was 200 µl. The plate was then read using a Multiskan™ plate reader with an excitation wavelength set at 485 nm and the emission wavelength at 530 nm.

2.2.5 ABTS (2,2'-azino-di-3-ethylbenzthialozine sulphonate) (TEAC) radical cation scavenging assay

2.2.5.1 Principle

This method was used to estimate antioxidant capacity based on scavenging of the $ABTS^{+}$ radical cation, typically has bluish-green colour, by the antioxidants present in a sample. Antioxidants present in the reaction medium capture the free radical, which is translated into a loss of colour and therefore a reduction in absorbance. The latter corresponds quantitatively to the concentration of antioxidants present, thus a decrease in colour indicates a stronger antioxidant presence and vice versa (Zulueta *et al*., 2009).

2.2.5.2 Chemicals Required for the ABTS (TEAC) assay

The chemicals required for the ABTS assay included: 7mM ABTS (2,2'-azino-bis(3-ethylbenzothiazoline-6-sulfonic acid) diammonium salt (Sigma, Cat no. A1888) and 140 mM potassium-peroxodisulphate (Merck, Cat no. 105091) using dH_2O. ABTS mix was prepared 24 hrs before starting the assay in a dark room as follows: 88 µl of potassium-peroxodisulphate solution was added to 5 ml ABTS and was mixed well. Trolox was used as a standard in this assay. The 1 mM Trolox stock standard was prepared as follows: 0.0125 g Trolox was added to 50 ml of EtOH. The 200 µM Trolox stock control was comprised of 0.0025 g Trolox dissolved in 50 ml of EtOH. Both Trolox stock standard and control was prepared on the day of analysis.

2.2.5.3 Sample Preparation and Analysis

The 20% R_f aqueous extract sample was directly used in the analysis. To avoid precipitates, the sample was centrifuged for 3 min at 4300.8 G (4000 rpm) and the supernatant was used in the analysis. Preparation of the sample was done on ice throughout the whole procedure. All samples were stored at -40 °C. The Trolox stock standard concentrations were prepared (See Appendix A: Table 2.5) and 25 µl of the standard, control and sample was added (in triplicate) to designated wells, respectively. The ABTS mix solution was diluted as follows: 1 ml ABTS mix was added and mixed with 20 ml EtOH which read an absorbance of approximately 2 (±0.1). Of this diluted

ABTS mix, 300 µl was added to each well. The plate was then left for 30 min at RT before taking a reading. The plate was read using a Multiskan™ plate reader at 734 nm with a temperature set to 25 °C.

2.2.6 Ferric Reducing Antioxidant Power (FRAP) assay

2.2.6.1 Principle

The FRAP assay uses antioxidants as reductants in a redox-linked colorimetric method, employing an easily reduced oxidant present. At low pH, reduction of a ferric tripyridyltriazine (Fe^3-TPTZ) complex to the ferrous form, results in an intense blue colour. The reaction is non-specific, in that any half-reaction that has a lower redox potential than that of the ferric or ferrous half-reaction will drive the ferric (Fe^{3+}) to ferrous (Fe^{2+}) reaction. The change in absorbance is therefore directly related to the reducing power of the antioxidants present in the reaction mixture (Benzie and Strain, 1996).

2.2.6.2 Chemicals Required for the FRAP assay

The chemicals necessary to perform the FRAP assay included: acetate buffer 300 mM, pH 3.6 comprised of 1.627 g sodium acetate and 16 ml glacial acetic acid which was made up with dH_2O to 1 litre. 40 mM HCl and 10 mM TPTZ (2, 4, 6-tri [2-pyridyl]-s-triazine) (Sigma, Cat no. T1253) comprised of 0.0093 g TPTZ and 3 ml of 40 mM HCl. 20 mM iron (III) chloride hexahydrate ($FeCl_3.6H_2O$) (Sigma, Cat no. F2877) which was comprised of 0.054 g $FeCl_3.6H_2O$ and 10 ml dH_2O L-ascorbic acid (Sigma, Cat no. A5960) was used as a standard in this assay. The 1 mM L-ascorbic acid stock standard solution was prepared as follows: 0.0088 g ascorbic acid was weighed and dissolved in 50 ml dH_2O. The 400 µM L-ascorbic acid stock control was prepared as follows: 0.00352 g ascorbic acid was added to 50 ml dH_2O and mixed until dissolved. All solutions were prepared on the day of analysis.

2.2.6.3 Sample Preparation and Analysis

The 20% R_f aqueous extract sample was directly used in the analysis. To avoid precipitates, the sample was centrifuged for 3 min at 4300.8 G (4000 rpm) and the supernatant was used in the analysis. All samples were stored at -40 °C. The straw-coloured FRAP reagent was prepared in a 50 ml conical tube which contained the following reagents: 30 ml Acetate buffer, 3 ml TPTZ solution, 3 ml iron chloride solution, and 6.6 ml dH_2O. The ascorbic acid stock standard concentrations were prepared (See Appendix A: Table 2.6) and 10 µl of the standard, control and sample was added (in triplicate) to designated wells, respectively. Moreover, 300 µl of the FRAP reagent was then added to each well with a multichannel pipette and the final volume of the assay was 310 µl. The plate was incubated for 30 min in an incubating oven set at 37 °C. The plate was then read using a Multiskan™ plate reader at 593 nm.

2.3 Experiments Performed on the Blood-Brain Brain (bEnd5) Model

2.3.1 Chemicals Required for *In Vitro* Analysis

The following reagents were required for *in vitro* analysis: 10 % fetal bovine serum (FBS) (Whitehead Scientific (Pty) Ltd, Cat no. DE 14-801 FI), 1 % non-essential amino acids (NEAA) (Whitehead Scientific (Pty) Ltd, Cat no. BE 13-114E), 1 % antibiotic *Penicillin-Streptomycin* Amphotericin B mixture (Whitehead Scientific (Pty) Ltd, Cat no. 17-745E), 1 % sodium pyruvate (Whitehead Scientific (Pty) Ltd, Cat no. BE 13-115E), 500 ml Dulbecco's modified eagle medium (DMEM) (Whitehead Scientific (Pty) Ltd, Cat no. BE 12-719F). Mouse brain endothelial (bEnd5) cell line (Highvelt Biological, agents for ATCC), 0.25% trypsin (Whitehead Scientific (Pty) Ltd, Cat no. BE 02-007E), phosphate buffer serum (PBS) (Sigma, Cat no. D8662), trypan blue (Sigma Cell Culture Reagents®, T-8154), fermented rooibos (R_f) (South African Rooibos Council, Batch no. P06/02KK), pure methamphetamine (MA) (Sigma Aldrich, CAS no. 51-57-0), 20 µl MTT (5 mg/ml) (Promega, Cat no. G4000), cell proliferation kit XTT II (Roche Products (Pty) Ltd, Cat no. 11465015001), 500 nM hydrocortisone (Sigma, Cat no. H0888), 500 µl dimethyl Sulfoxide (Whitehead Scientific (Pty) Ltd, Cat no. sc-358801), 70% EtOH (Saarchem, Cat no. 2233540 LP), RNase (20 mg/ml)

(Invitrogen life technologies, Cat no. 12091-039), propidium iodide (PI) (Fluka, CAS no. 25535-16-14).

2.3.2 Mouse Brain Endothelial (bEnd5) Cell Culturing

2.3.2.1 Principle

The *in vitro* analysis made use of cell culturing which produces a 2-dimensional cell growth with gene expression signaling that is advantageous in being more quantifiable. It allows for the development of optimized culture conditions, initially for cell proliferation but ultimately for functional expression (Freshney *et al*., 2007; Souza *et al*., 2010). By removing and subculturing from the *in vivo* host, the cultured cells portray events that would ultimately occur in that *in vivo* setting. Endothelial cells are the core component of the BBB and our model uses an established brain endothelial cell line namely mouse brain endothelial (bEnd5) cells. The bEnd5 cells display both morphological (ECs comprise of different vascular beds or undergo different vascular processes which employs a myriad of mechanisms) and functional characteristics (the barrier properties of these specialized ECs notably depend on TJs between adjacent cells) of cells in the *in vivo* state. These cells are grown on cellulose membrane (insert) which mimics the *in vivo* basement membrane where the apical compartment of the bicameral chamber represents the circulatory environment (blood) and the basolateral compartment (brain parenchyma) is represented by the well.

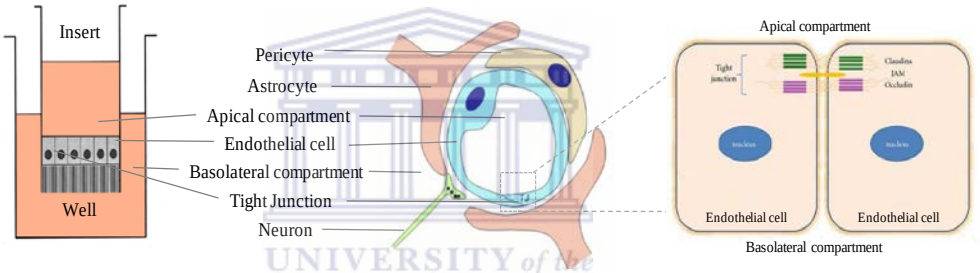

Figure 2A. *In vitro* BBB model Figure 2B. *In vivo* BBB Figure 2C. Endothelial TJ proteins

Figure 2 The BBB model and its closely related *in vivo* BBB components. **A** The bicameral chamber consisting of the well and insert which represent the basolateral and apical compartments, respectively (http://www.biocompare.com/Editorial-Articles/147111-Cells-on-the-Go-Cellular-Migration-Assays/). **B** The major components of the in vivo BBB: endothelial cells, pericytes and astrocytes (http://home.szbk.u-szeged.hu/~krizbai/index.html). **C** The endothelial TJ proteins in the paracellular compartment of adjacent ECs (http://imgarcade.com/1/junction-proteins/).

2.3.2.2 Method

The Tissue Culture medium (complete medium) was supplemented by adding 10% FBS, 1% NEAA, 1% antibiotic *Penicillin-Streptomycin* Amphotericin B mixture and 1% sodium pyruvate to 500 ml DMEM as previously described (Reiss *et al*., 1998). The mouse brain endothelial (bEnd5) cell line was removed from the liquid nitrogen store and thawed. Cells were centrifuged for 5 min at 268.8 G (1000 rpm) at RT and the top was wiped off with 70% ethanol. The supernatant was then discarded. The cell pellet was re-suspended in 1 ml complete medium and then transferred to a 25 cm^2 tissue culture treated (TC) flask containing the desired amount of complete medium. Incubation at 37 ºC then proceeded and the cell cultures were checked after 24 hrs to ensure attachment, using the Inverted Phase Contrast Microscope.

After attachment, the medium was poured off and 2-3 ml PBS were used to rinse the attached cells. The PBS was then aspirated. Trypsin (1 ml of 0.25%) was added which dislodges the attached cells from the TC flask surface (Huang *et al*., 2010) and incubated at 37 ºC for 10-15 min, after which 1 ml of medium (the same volume as trypsin added in the previous step) was added. The dislodged cells were then aspirated

into a 15 ml conical tube and centrifuged at 1680 G (2500 rpm) for 5 min at RT. After centrifuging, the supernatant was poured off and the desired amount of medium was then added to the cell pellet and re-suspended. A cell count was done using trypan blue in order to seed the required amount of cells necessary for the selected assays. For each assay, the cells were seeded and allowed to attach for 24 hrs. The cells were exposed to selected concentrations of MA and R_f which was made up following suitable dilutions (MA: 10-fold and Rf: 2-fold dilutions) using complete medium from a 20% R_f and 99.9% MA stock, respectively.

2.3.3 Trypan Blue Exclusion assay

2.3.3.1 Principle

Trypan Blue is a carcinogenic dye used to determine the amount of viable cells present in a sample. It does so by non-viable cells absorbing the trypan blue due to their non-selective permeability, whereas viable cells will not absorb the dye, thus when viewed under a light microscope, non-viable cells were stained blue while viable cells were translucent and fluoresce (Mascotti *et al.*, 2000).

2.3.3.2 Method

Cells were seeded at 5 x 10^4 cells per ml/35 mm petri dishes (n = 5, day = 0) . Selected MA concentrations (0.1, 1, 10, 100, 1000 µM) and R_f concentrations (1, 0.5, 0.25, 0.125, 0.0625 and 0.05%) were added (day = 1), respectively. In addition, the cells were also exposed to a combination of MA (0.1, 1, 10 and 100 µM) and R_f (0.05 and 0.1%). The R_f concentrations used in the combinations were selected based on the viability results after R_f exposure. After 24 hr (only) exposure to the compounds, the cells were incubated at 37 ºC, 5% carbon dioxide (CO_2). Results were recorded at 24, 48, 72 and 96 hrs. An established ratio of cells, trypan blue dye and complete medium was used to determine cell viability (0.4% trypan blue was made up in isotonic buffer i.e. PBS, pH 7.2 to 7.3). Since trypan blue results in cell death after prolonged exposure, the cells were added last to the complex. This was followed by the addition of 10 µl to the appropriate sections on the Neubauer hemocytometer and observed under an Inverted

Phase Contrast Microscope (Zeiss) for cell counts. The following equation was used in order to determine % cell viability:

$$\text{Cell Viability (\%)} = \frac{\text{Number of unstained (live) cells}}{\text{Total number of (live and dead) cells}} \text{ x } 100$$

2.3.4 3-(4, 5-Dimethylthiazol-2-YI)-2, 5 Diphenyltetrazoium Bromide (MTT) Viability assay

2.3.4.1 Principle

The 3-(4, 5-Dimethylthiazol-2-YI)-2, 5 Diphenyltetrazolium Bromide (MTT) assay is a colorimetric assay that makes use of the water-soluble, yellow MTT dye which is converted to water-insoluble, purple formazan derivative by mitochondrial dehydrogenases via reduction cleavage of the tetrazolium ring in living cells. The formazan product is impermeable to the cell membranes and therefore accumulates in healthy cells. The intensity of the colour is directly proportional to the amount of viable cells or metabolic activity present (Edmondson *et al*., 1988; Lappalainen *et al.*, 1994; Fotakis and Timbrell, 2005; Funk *et al*., 200,).

2.3.4.2 Method

A 96-well flat bottomed, clear microtiter plate was seeded with 2 x 10^3 cells/well (n = 5, day = 0) and exposed to the selected concentrations (as per trypan blue viability assay) of MA (day = 1) which was followed by incubation for 24, 48, 72 and 96 hrs at 37 ºC, 5% CO_2. The cells underwent both 24 hr and daily exposure to the compound with the addition of 2000 and 3000 µM for once-off exposure only. After incubation, 20 µl MTT (5 mg/ml) were added and the plate was re-incubated for 2 hrs at 37 ºC, 5% CO_2. The plate was then read at 490 nm on a microtiter plate reader (Glomax, Promega).

2.3.5 2,3-bis-(2-methoxy-4-nitro-5-sulfophenyl)-2H-tetrazolium-5-carboxanilide (XTT) Viability assay

2.3.5.1 Principle

The XTT assay is a colorimetric assay where viable cells reduce the tetrazolium salt 2,3-bis-(2-methoxy-4-nitro-5-sulfophenyl)-2H-tetrazolium-5-carboxanilide **(**XTT) to an orange-coloured water-soluble formazan product. This assay makes use of an electron coupling agent for optimal formazan yield. Mitochondrial succinate dehydrogenase, cytochrome P450 and flavoprotein oxidases contribute to the formation of the formazan. The formazan is quantified photometrically and correlates with the number of viable cells (Altman, 1976; Stevens and Olsen, 1993; Funk *et al*., 2007; Smith and Hunter, 2008).

2.3.5.2 Method

Cells were seeded at 2 x 10^3 cells/well in a 96-well flat bottomed (n = 5, day = 0), clear microtiter plate. The cells were then exposed to MA (0.1, 1, 10, 100, 1000 µM) R_f and (0.1, 0.05, 0.025%, 0.0125, 0.00625 and 0.003125%). In addition, the cells were also exposed to a combination of MA (0.1, 1, 10, 100 µM) and R_f (0.05 and 0.1%) concentrations. Care was taken to control for false positives resulting from the concentrations of R_f used in this particular experiment. The cells underwent both 24 hr and daily exposure to the compounds with the exception of MA exposure which was only daily. After the compound exposure, the plate was incubated at the selected time intervals as per MTT assay protocol. Reconstituted XTT (50 µl) was added to each well and further incubated for 4 hrs at 37 ºC, 5% CO_2. The plate was then read at 450 nm on a microtiter plate reader. The following equation was used in order to determine % cell viability for both the MTT and XTT viability assay:

$$\text{Cell Viability (\%)} = \frac{\text{Experimental absorbance (abs)} - \text{Experimental media abs}}{\text{Control abs} - \text{Control media abs}}$$

2.3.6 Transendothelial Electrical Resistance (TEER)

2.3.6.1 Principle

Using an Ohm Millicell-Electrical Resistance System (ERS) ®, the integrity of the cell membrane is assessed (Verma *et al*., 2009) by measuring electrical resistance across a cell monolayer *in vitro* in order to investigate changes in resistance and transendothelial permeability. It qualitatively measures cell monolayer health and quantitatively measures cell confluence across an *in vitro* monolayers. Furthermore a decrease in TEER is inversely proportional to an increase in paracellular permeability of tight junction indicators and vice versa (Konsoula and Barile, 2007).

2.3.6.2 Method

Cells were seeded at a density of $1x10^6$ cells/matrigel coated, Millicell inserts (Bio-Smart Scientific, Cat no. 35024) in a 24-well flat bottomed, clear microtiter plate (n = 4, day = 0) and incubated at 37 ºC, 5% CO_2. The ranges of MA (0.1, 1, 10 and 100 µM) and R_f (0.1, 0.05, 0.025, 0.0125 and 0.00625%) concentrations (respectively) were added in the presence of 500 nM hydrocortisone which was dissolved in 500 µl dimethyl sulfoxide to the cells as described (Hoheisel *et al*., 1998; Schrot *et al*., 2005). Cells were also exposed to a combination of MA (0.1, 1, 10 µM) and R_f (0.05 and 0.1%) concentrations. The cells were exposed to the compounds daily. TEER for cell monolayers was measured every 3 hrs with the Millicell electrical resistance system (Millicell®-ERS, Millipore), for 24, 48, 72, 96, 120, 144 hrs. Cell measurements were recorded 3 times/day.

The resistance mode of the voltohmeter was used for measurements. In brief, the short electrode was immersed in the apical compartment (insert) while the long electrode was immersed in the basolateral compartment (well of the plate). Care was taken to avoid contact with cells growing on the membrane to prevent piercing the cell monolayer and insert membrane, thus creating an open circuit. The resistance was then measured and recorded. Resistance measurements were corrected by subtracting the resistance reading

of the blank wells (inserts without cells) from the experimental wells (insert with cells). These measurements were further standardized for the surface area of the insert.

2.3.7 Flow Cytometry: Cell Cycle Analysis

2.3.7.1 Principle

This method is used to determine cell repartition in the various cell cycle phases and allows for the accurate determination of drugs effects in the cycle. Furthermore, it is performed using propidium iodide which is used for nuclear staining. The fluorescence emitted is proportional to the DNA content present in the cells, provided that RNA has been removed (Jayat and Ratinaud, 1993; Riccardi and Nicoletti, 2006).

2.3.7.2 Method

Cells were seeded at 5 x 10^5 cells/25 cm^2 TC flasks (n = 3, day = 0) and incubated overnight at 37 °C, 5% CO_2. The cells were the exposed (day = 1) to selected concentrations of MA (0.1, 1 and 10µM), R_f (0.1 and 0.05%), and combinations of the latter compounds for 24 hrs (once-off) only. This was followed by incubation for 24, 48, 72, 96, 120 and 144 hrs at 37 °C, 5% CO_2. The cells were exposed to the compounds for only 24 hrs (once-off). At the respective time interval, the medium was aspirated into 15 ml centrifuge tubes. The cells were then washed with 1 ml PBS and the PBS transferred into the respective centrifuge tubes. Trypsin (0.5 ml of 0.25%) was added to the flasks followed by incubation for 15 min at 37 °C, 5% CO_2. To neutralize the cells, 1 ml complete medium was added and the suspension transferred to the conical tubes followed by centrifuging for 5 min at 268.8 G (1000 rpm). The supernatant was poured of and the pellet resuspended in 2 ml medium followed by a cell count using trypan blue for each sample. EtOH (70%) was added to a final volume of 10 ml and stored at -20 °C for a minimum of 2 hrs.

2.3.7.3 Cell Cycle Analysis by Propidium Iodide Staining

On the day of the analysis, the cells were centrifuged for 5 min at 268.8 G (1000 rpm) and the supernatant was carefully removed leaving approximately 1 ml EtOH. The cells

were re-centrifuged for 1 min at 268.8 G (1000 rpm) and most of the remaining EtOH was removed without disturbing the pellet. PBS (1 ml) was added and centrifuged for 1 min at 268.8 G (1000 rpm) followed by the removal of the PBS. The latter step was repeated. RNase (20 mg/ml) diluted in PBS at a ratio of 1: 199 was prepared and the required volume (50 µl/5 x 10^5 cells) added and incubated at RT for 30 min or at 37 °C, 5% CO_2 for 15 min. PI staining solution was made up (1 mg/ml) and added (450 µl/5 x 10^5 cells) 20 min prior to analysis. The samples were analysed using the Becton Dickinson FACS (fluorescence activated cell sorter) Calibur flowcytometer with a 488 nm Argon laser. Each analysis was based on 10 000 events and the software used for the acquisition of the data was Cellquest Pro version 5. 2. 1. The cell population was identified and gated (R1) on a forward scatter (FSC) vs. side scatter (SSC) dot plot in acquisition mode. Fluorescent Channel 2 (FL2) at 575 nm was used for PI detection. A dot plot of FL2A (area) vs. FL2W (width) was used to identify single cells (R2) and thus eliminate doublets. A histogram plot of FL2A was used to enumerate G1/G0, S-phase and G2/M populations. The combined parameters of FSC, SSC, FL2A and FL2W displayed the results. A threshold of 53 on the FSC channel was set to remove sample debris. Nile Red fluorescent particles were used for instrument standardization, stability and reproducibility. Analysis of the results was performed using Modfit version 2.0 software (Verity Software House).

2.4 Statistical Analysis

Statistical analysis of the data yielded was done using the MedCalc (version 11.5.1) program (Medcalc Software Company). Normality was determined using the Kolmogorov-Smirnov test followed by use of the Wilcoxon Rank Sum test for not-normally distributed paired samples. Outliers were statistically determined using the Box-and-Whisker plot and removed prior to determining significance, where $P<0.05$ was denoted as being significantly different.

CHAPTER 3

3 Results

3.1 The Effects of Methamphetamine on bEnd5 Cells

3.1.1 Effects of 24 hr-MAE on Cell Numbers using the Trypan Blue Exclusion Method

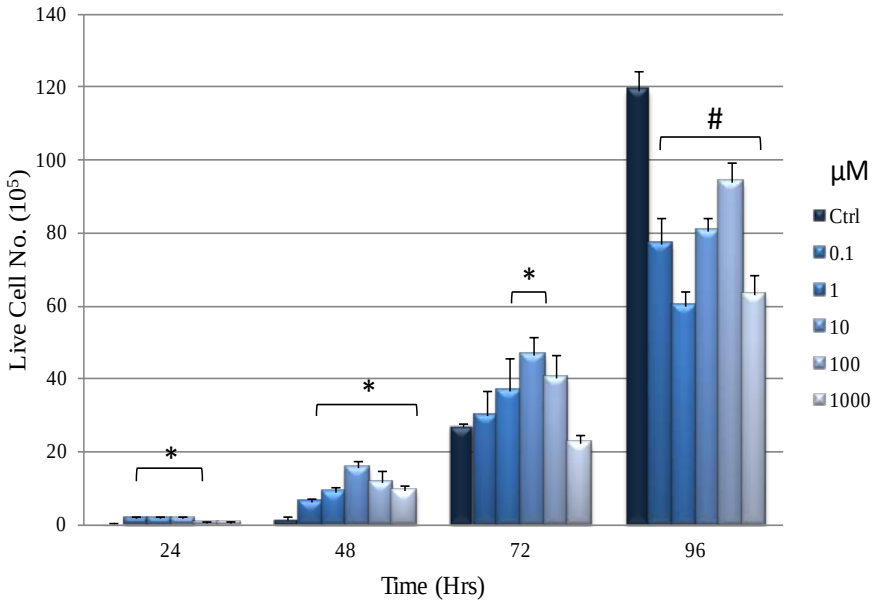

Figure 3.1 Live cell number in response to 24 hr exposure of selected MA concentrations and time. Results are expressed as mean ± SEM (n=5). Significant ($P<0.05$) increases in live cell number are denoted with * whereas significant decreases are denoted with #.

From 24 to 72 hrs, exposure of the cells to MA significantly increased cell growth ($P\leq0.0495$) coupled with biphasic growth expressions at the latter time intervals. In contrast, at 96 hrs, exposure to the entire range of MA concentrations resulted in significant growth suppression ($P\leq0.0399$). Specifically, significant increases in the live cell numbers were observed at 0.1, 1 and 10 µM ($P\leq0.0143$) after 24 hr exposure. Exposure to all MA concentrations at 48 hrs resulted in an increase in cell numbers ($P\leq0.0253$). The intermediate concentrations resulted in elevated cell growth at 72 hrs

(P≤0.0495). Exposure to 10 µM MA at both 48 (15.52±2.11 live cell no.) and 72 hrs (46.66±5.00 live cell no.) resulted in the highest increase in comparison to their controls. At 96 hrs a significant decrease in cell numbers was observed when exposed to all MA concentrations (P≤0.0339). Moreover, 1 µM MA at the 96 hr time period significantly decreased (P=0.0253) the cell numbers to approximately half (59.90±4.06 live cell no.) that of the controls (119.22±5.35 live cell no.). In addition, no dose-response trend was observed at 96 hrs (See Figure 3.1 and Appendix B: Table 3.2).

3.1.2 Effects of 24 hour-Methamphetamine-Exposure (24 hr-MAE) on Cell Viability (%) using the Trypan Blue Exclusion Method

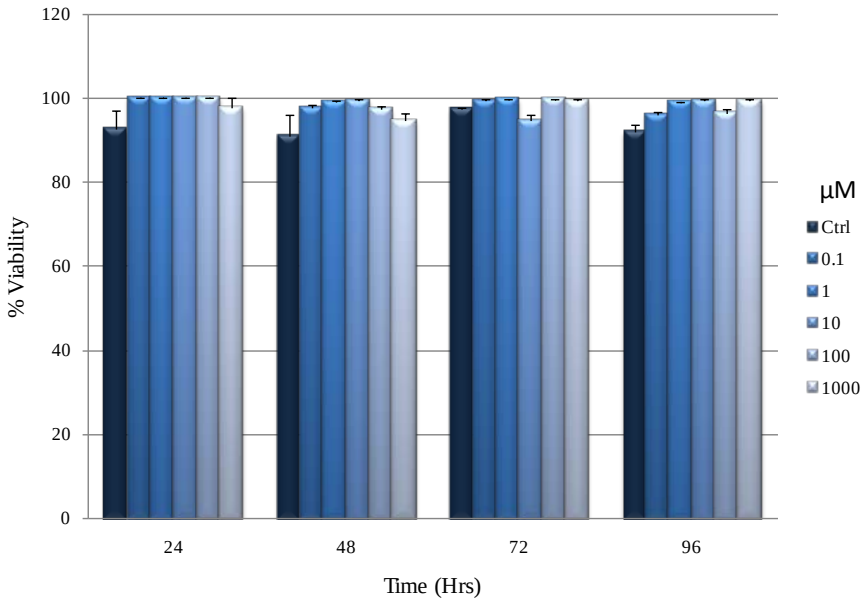

Figure 3.2 Cell Viability (%) in response to 24 hr exposure of selected MA concentrations and time. Results are expressed as mean ± SEM (n=5). Significant (P<0.05) increases in cell viability are denoted with * whereas significant decreases are denoted with #.

Exposure to different concentrations of MA resulted in no statistical significant differences in cell viability from the controls for all MA exposed concentrations across all the time intervals. This, therefore, illustrated a non-toxic effect in response to the selected MA concentrations as seen with an overall cell toxicity of <5.22% (cell toxicity was determined by expressing the dead cell numbers over an entire (live and dead cells)

population). Furthermore, the non-toxic effect was also clearly demonstrated at 96 hrs (See Figure 3.2 and Appendix B: Table 3.3).

3.1.3 Effects of 24 hr-MAE on Cell Viability (%) using the Reduced Formazan Method (Observing Metabolic Activity)

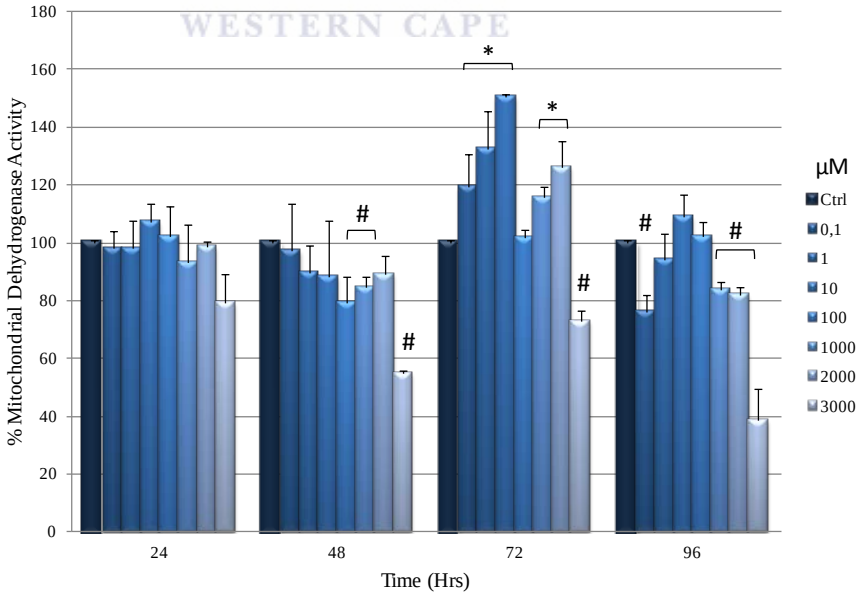

Figure 3.3 Mitochondrial dehydrogenase activity (%) in response to 24 hr exposure of selected MA concentrations and time. Results are expressed as mean ± SEM (n=5). Controls were normalized to 100% and experimental groups expressed relative to controls. Significant ($P<0.05$) increases in cell viability are denoted with * whereas significant decreases are denoted with #.

The functional state of MA is a reflection of the viability of a cell. The XTT assay measures the mitochondrial state by evaluating the mitochondrial dehydrogenase (MDH) activity, thus by definition viability will therefore be referred to as MDH activity. MA exposure at 24 hrs resulted in no statistical significant differences in viability when compared to the controls. At 48 hrs, small statistical significant decreases in MDH activity were observed after exposure to 100 and 1000 µM MA ($P \leq 0.0105$). However, when exposed to the range of 0.1-2000 µM MA at 72 hrs, a marked elevation in MDH activity ($P \leq 0.0463$) was observed (with the exception of 100 µM). The highest

viability (150.51±1.09%) across all time intervals was observed at 10 µM MA at 72 hrs. At 96 hrs, a significant decline was observed in response to the lowest (P=0.0071) MA concentrations. The lowest viability across all time intervals was also observed at 96 hrs (36.60±10.97%). Exposure to 3000 µM MA resulted in consistently lower viability than all selected concentrations for all time intervals (P≤0.0105) (See Figure 3.3 and Appendix B: Table 3.4).

3.1.4 Effects of Daily-MAE on Cell Viability (%) using the Reduced Formazan Method (Observing Metabolic Activity)

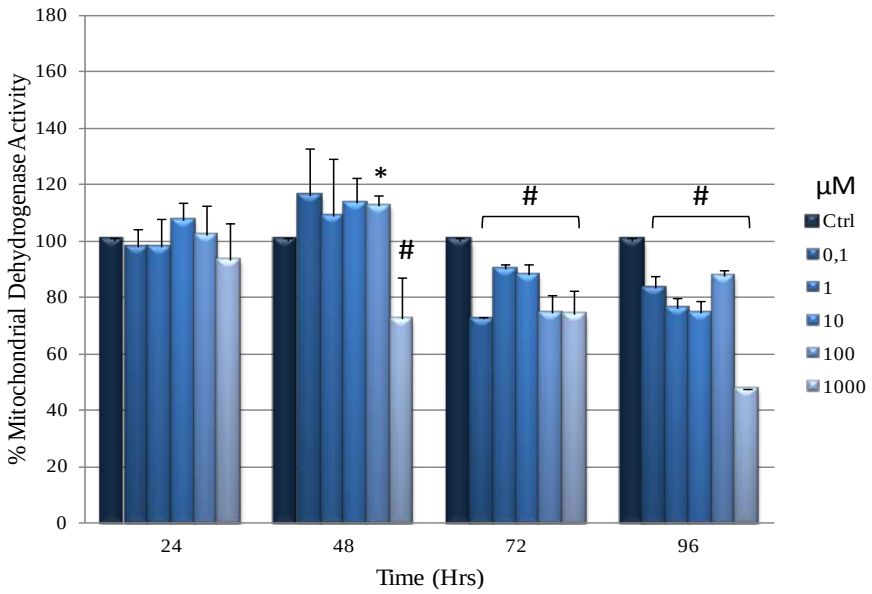

Figure 3.4 Mitochondrial dehydrogenase activity (%) in response to daily exposure of selected MA concentrations and time. Results are expressed as mean ± SEM (n=5). Controls were normalized to 100% and experimental groups expressed relative to controls. Significant (P<0.05) increases in cell viability are denoted with * whereas significant decreases are denoted with #.

There were no statistical differences observed at 24 hrs when comparing the MA-exposed cells to the control (as was observed with the once-off (24 hr) exposure). At 48 hrs, a small statistically significant increase in viability was observed at 100 µM MA (P=0.0028). At 72 and 96 hrs, exposure to the entire range of MA resulted in a

statistically significant decrease (P≤0.0063) in viability. The highest concentration of MA resulted in the lowest viability ((P≤0.0463) for all timelines except at 24 hrs. The lowest viability across all time intervals was observed at 96 hrs (47.47±0.24%). When comparing the cell viability in response daily exposure to that of once-off, suppression was observed at both 72 and 96 hrs as opposed to suppression displayed occurring at only 96 hrs with once-off exposure (See Figure 3.4 and Appendix B: Table 3.5).

3.1.5 Effects of Daily-MAE on Monolayer Electrical Resistance (TEER)

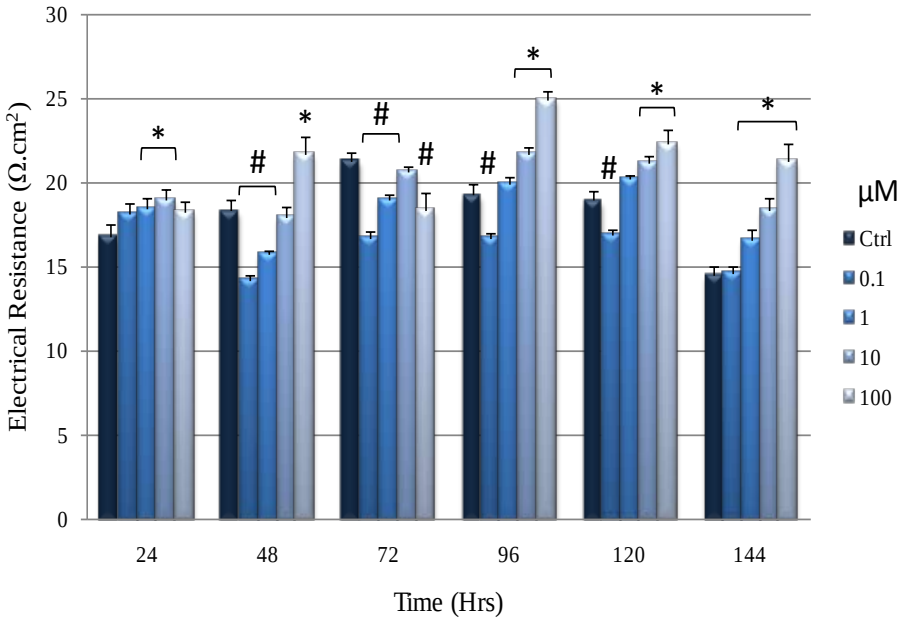

Figure 3.5 Transendothelial electrical resistance in response to daily exposure of selected MA concentrations and time. Results are expressed as mean ± SEM (n=4). Significant (P<0.05) increases in TEER are denoted with * whereas significant decreases are denoted with #.

The permeability across the monolayer was analysed by measuring the electrical resistance across this monolayer. Increases in electrical resistance indicated a decrease in permeability across the monolayer whereas a decrease would indicate an increase in permeability. Dose-dependent increases (P≤0.0302) were observed across all time intervals after exposure of the cells to MA. The highest MA concentration (100 μM) resulted in the highest electrical resistance (P≤0.0068) across all time intervals with

exception to 24 and 72 hrs where exposure to 100 µM MA resulted in decreased resistance ($P \leq 0.0432$) at 72 hrs. In addition, the lowest MA concentration (0.1µM) resulted in the lowest TEER ($P \leq 0.0064$) across all time intervals with exception to 96 hrs. The highest TEER reading was observed at 96 hrs (24.96±0.56 $\Omega.cm^2$) and the lowest at 48 hrs (14.23±0.30 $\Omega.cm^2$) when exposed to 100 and 0.1 µM, respectively. Thus, there permeability of the monolayer was increased by the lowest MA concentrations with exposure to the higher concentrations resulting in a less permeable monolayer (See Figure 3.5 and Appendix B: Table 3.6).

3.1.6 Effects of Methamphetamine Exposure on bEnd5 Cell Cycles

The flow cytometry analysis is depicted from a profile of cell cycle phases of a population of cells at a predefined point of time.

3.1.6.1 Effects of 24 hr-MAE on bEnd5 Cell Cycles at 24 hours

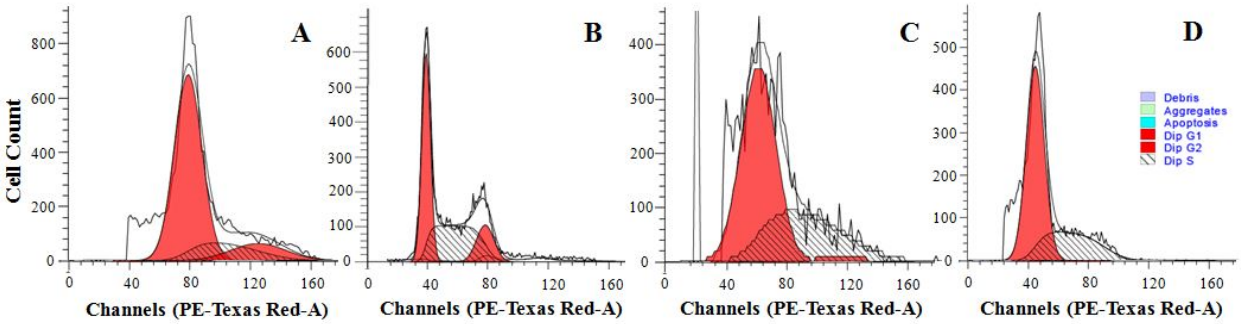

Figure 3.6 Histograms illustrating cell cycle results after 24 hr exposure to selected MA concentrations at 24 hrs using flow cytometry (≥ 10 000 events analysed). **A** Control. **B** Exposure to 0.1 µM MA. **C** Exposure to 1 µM MA. **D** Exposure to 10 µM MA.

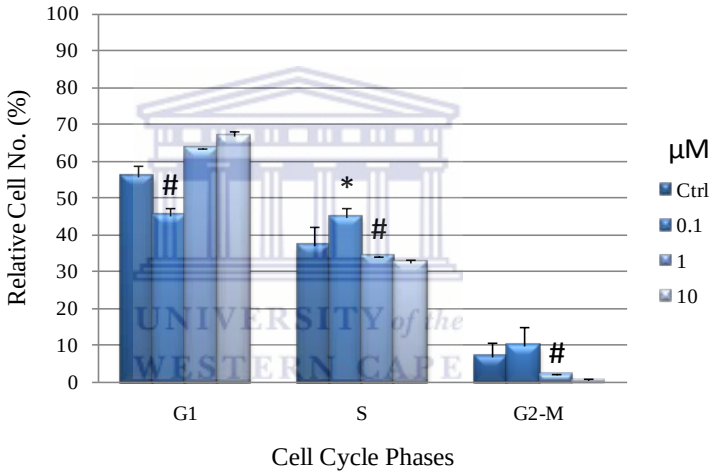

Figure 3.7 Relative cell numbers (%) at distinct phases of the cell cycle after exposure to selected MA concentrations at 24 hrs. Results are expressed as mean ± SEM (n=3). Significant ($P<0.05$) increases in relative cell no. are denoted with * whereas significant decreases are denoted with #.

Majority of the cells for both controls and exposed cells were detected in the G1-phase (≥45.19±2.40%) while the least amount of cells was observed in the G2-M phase (≤9.99±5.00%), at 24 hrs. In addition, a significant decrease ($P<0.0495$) was observed when exposed to 0.1 µM MA in G1-phase which also resulted in an increase ($P<0.0495$) in the S-phase. Significant decreases ($P\leq0.0317$) were displayed at 1 µM MA in both the G2-M- and S-phase. Despite the small statistical significant differences, the data depicts a normal profile of cell division (See Figure 3.6 and 3.7, Appendix B: Table 3.7 and Appendix F).

3.1.6.2 Effects of 24 hr-MAE on bEnd5 Cell Cycles at 48 hours

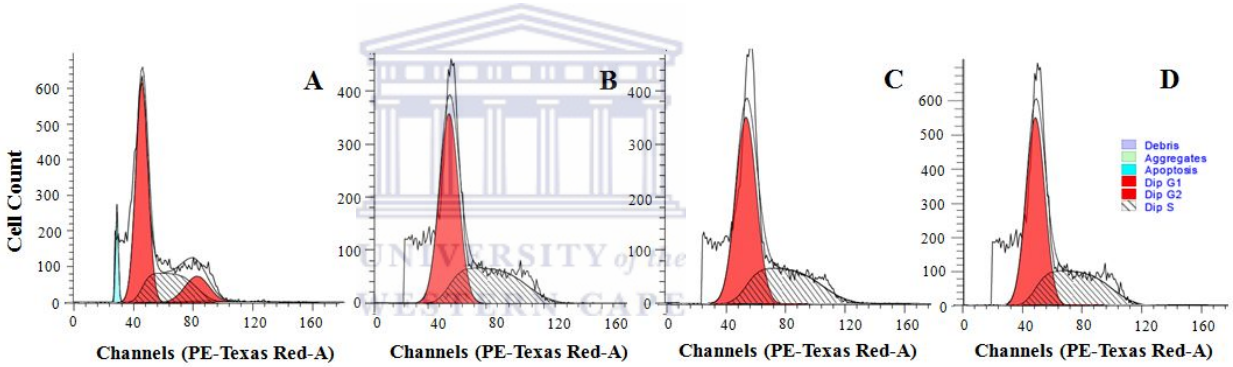

Figure 3.8 Histograms illustrating cell cycle results after 24 hr exposure to selected MA concentrations at 48 hrs using flow cytometry (≥ 10 000 events analysed). **A** Control. **B** Exposure to 0.1 µM MA. **C** Exposure to 1 µM MA. **D** Exposure to 10 µM MA.

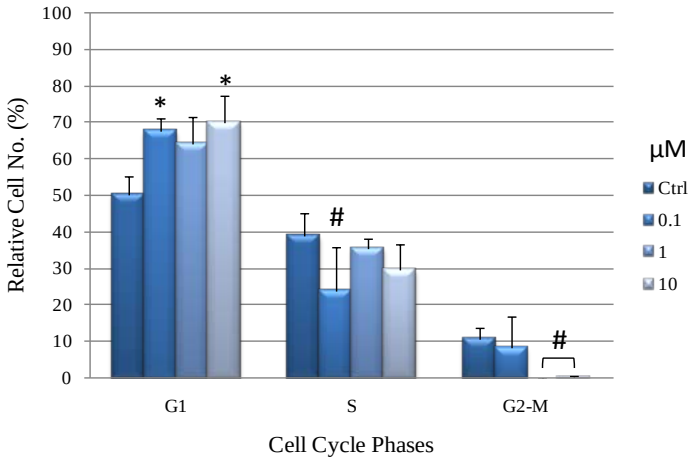

Figure 3.9 Relative cell numbers (%) at distinct phases of the cell cycle after exposure to selected MA concentrations at 48 hrs. Results are expressed as mean ± SEM (n=3). Significant ($P<0.05$) increases in relative cell no. are denoted with * whereas significant decreases are denoted with #.

More than 50% of the controls and MA-exposed cells were detected in the G1-phase at 48 hrs. The lowest numbers were detected in the G2-M phase (≤10.75±3.13%). In addition, significant increases ($P\leq0.0430$) were observed in the G-phase when cell were exposed to 0.1 and 10 µM MA. The lowest MA concentration also resulted in a decrease ($P=0.0356$) in S-phase. Significant decreases ($P\leq0.0440$) in the G2-M phase occurred at 1 and 10 µM. Despite the small statistical significant differences, the data

depicts a normal profile of cell division (See Figure 3.8 and 3.9, Appendix B: Table 3.8 and Appendix G).

3.1.6.3 Effects of 24 hr-MAE on bEnd5 Cell Cycles at 72 hours

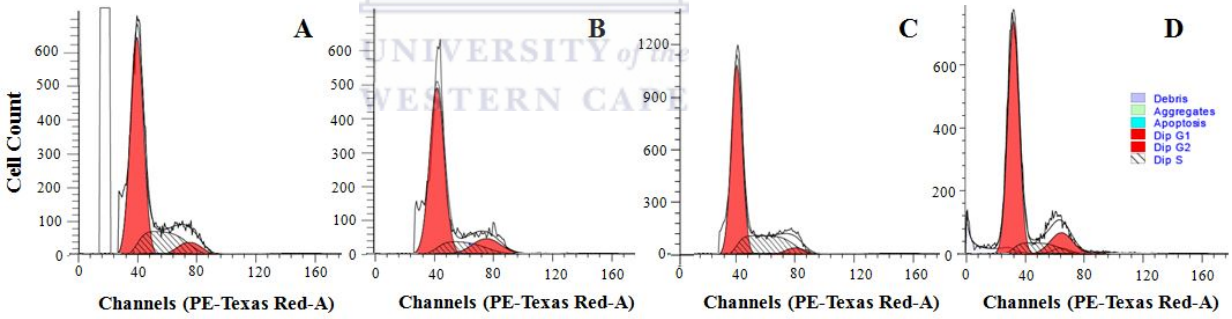

Figure 3.10 Histograms illustrating cell cycle results after 24 hr exposure to selected MA concentrations at 72 hrs using flow cytometry (≥ 10 000 events analysed). **A** Control. **B** Exposure to 0.1 µM MA. **C** Exposure to 1 µM MA. **D** Exposure to 10 µM MA.

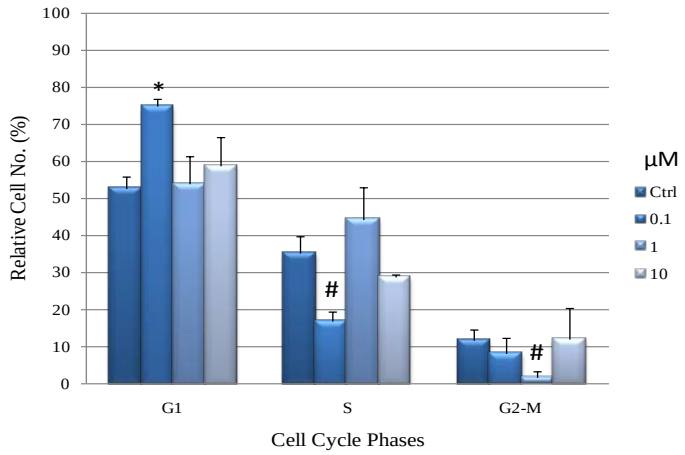

Figure 3.11 Relative cell numbers (%) at distinct phases of the cell cycle after exposure to selected MA concentrations at 72 hrs. Results are expressed as mean ± SEM (n=3). Significant ($P<0.05$) increases in relative cell no. are denoted with * whereas significant decreases are denoted with #.

At 72 hrs, G1-phase contained the most cells (≥52.71±3.06%) with the least cells observed in the G2-M phase (≤12.22±8.34%). Exposure to 0.1 µM MA resulted in a marked increase ($P=0.0186$) and decrease ($P=0.0264$) in the G1- and S-phase. The

intermediate concentration displayed a marked decrease (P=0.0498) in the G2-M phase. Despite the small statistical significant differences, the data depicts a normal profile of cell division (See Figure 3.10 and 3.11, Appendix B: Figure 3.9 and Appendix H).

3.1.6.4 Effects of 24 hr-MAE on bEnd5 Cell Cycles at 96 hours

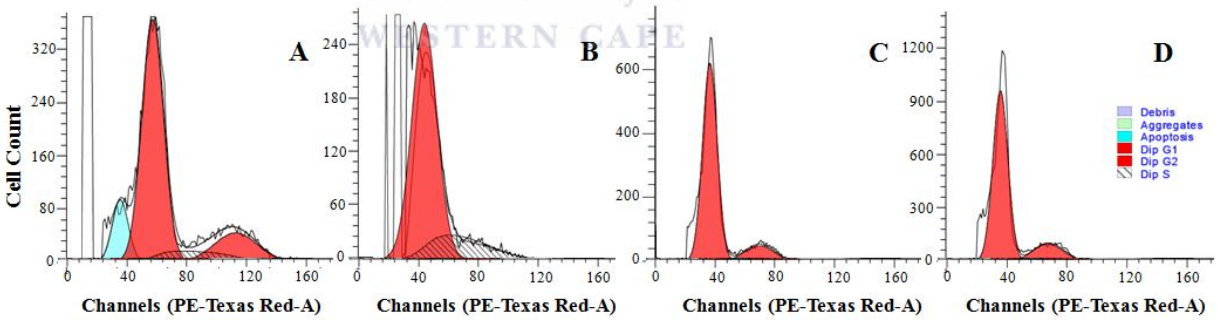

Figure 3.12 Histograms illustrating cell cycle results after 24 hr exposure to selected MA concentrations at 96 hrs using flow cytometry (≥ 10 000 events analysed). **A** Control. **B** Exposure to 0.1 µM MA. **C** Exposure to 1 µM MA. **D** Exposure to 10 µM MA.

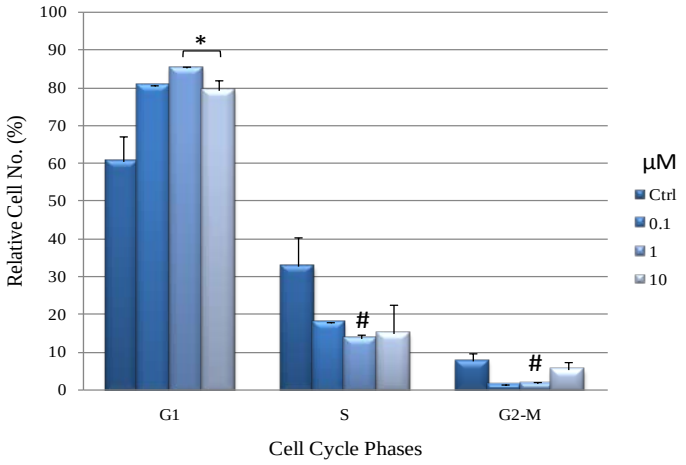

Figure 3.13 Relative cell numbers (%) at distinct phases of the cell cycle after exposure to selected MA concentrations at 96 hrs. Results are expressed as mean ± SEM (n=3). Significant (P<0.05) increases in relative cell no. are denoted with * whereas significant decreases are denoted with #.

The G1 phase at 96 hrs had the highest amount of detected cells (≥60.66±6.65). The lowest numbers were detected in the G2-M phase (≤7.70±2.00). In the G1-phase, 1 and

10 µM displayed significant increases (P≤0.0299) in % relative cell numbers whereas only 1 µM resulted in the decreases at both the S- (P=0.0299) and G2-M-phases (P=0.0239) when compared to controls. Moreover, a dose-dependent increase was observed in the G2-M phase. The data clearly suggests the accumulation of cells in the G1-phase thus, subsequently preventing entry into the S1- and G2-M phase at 96 hrs (See Figure 3.12 and 3.13, Appendix B: Table 3.10 and Appendix I).

3.2 The Effects of Fermented Rooibos Herbal Tea on bEnd5 Cells

3.2.1 Chemical Analysis of Fermented Rooibos Extract

Table 3.1 Constituents present in the fermented *A.linearis* aqueous extract divided into **A**. Analysis for components with respect to standards, and **B**. Total antioxidant activity/property analysed with respect to standards.

Analysis Performed	Quantity expressed against standard	
	Expressed as standard/aqueous R_f	*Expressed as standard/dried R_f*
***A**. Analysis for components with respect to standards*		
Aspalathin	mg/100ml 21.30	mg/g 1.07
Polyphenols	mg GAE/100ml 1086.24	mg GAE/g 54.34
Flavonols	mg QE/100ml 90.96	mg QE/g 4.55
Flavanols	mg CE/100ml 156.05	mg CE/g 7.80
***B**. Total antioxidant activity/property analysed with respect to standards*		
ORAC	µmol TE/100ml 21148.92	µmol TE/g 1057.45
ABTS (TEAC)	µmol TE/100ml 4905.80	µmol TE/g 245.29
FRAP	µmol AAE/100ml 7395.24	µmol AAE/100g 369.76

GAE-Gallic acid equivalents, AAE-ascorbic acid equivalents, TE-Trolox equivalents, QE-quercetin equivalents, CE-catechin equivalents), FRAP-ferric reducing antioxidant power, ORAC-oxygen radical absorbance capacity, ABTS-2,2'-azino-di-3-ethylbenzthialozine sulphonate, TEAC-trolox equivalent antioxidant capacity.

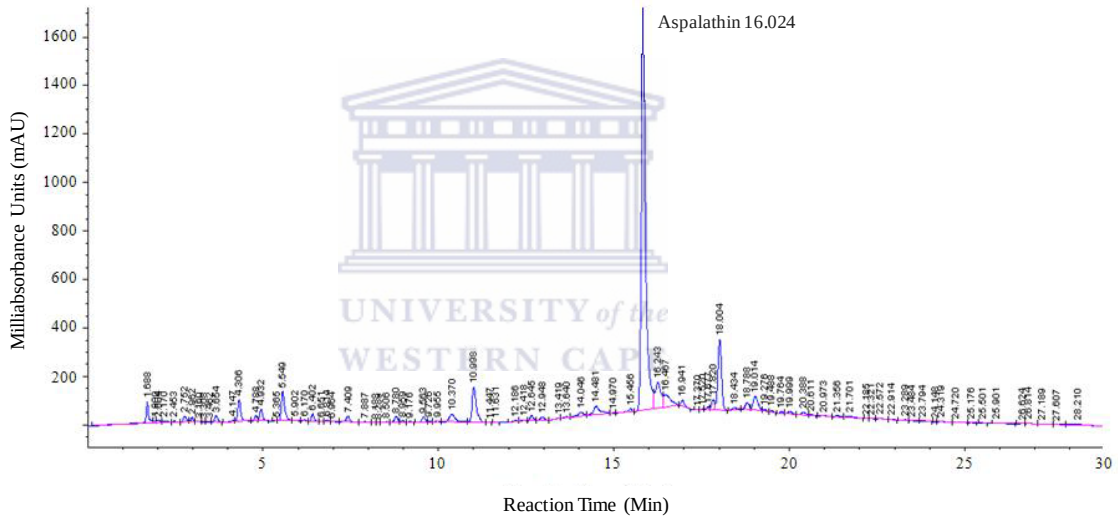

Figure 3.14 The data obtained from high performance liquid chromatography analysis illustrated the large amount of Aspalathin at 16.024 mAU (Analysis performed by Oxidative Stress Research Centre, CPUT).

Table 3.1 displays the constituents of the fermented *A. linearis* producing standardized information necessary for this study. Polyphenols as a group of compounds were expressed in terms of gallic acid equivalents yielding 1086.24 mg GAE/100 ml and 54.34 mg GAE/g. The two flavonoid subgroups, flavonols and flavanols, are expressed in terms of catechin and quercetin, respectively. Flavonols yielded 90.96 mg CE/100 ml and 4.55 mg CE/g. Flavanols yielded 156.05 mg QE/100 ml and 7.80 mg QE/g. There was also 21.30 mg/100ml and 1.07 mg/g dihydrochalcone aspalathin detected in the sample (see also figure 3.17).

The ABTS and ORAC analyses measured the antioxidant strength based on trolox equivalents resulting in 21148.92 µmol TE/100 ml and 1057.45 µmol TE/g for ORAC, and 4905.80 µmol TE/100ml and 245.29 µmol TE/g for ABTS/TEAC. FRAP results, expressed in terms of ascorbic acid equivalents were 7395.24 µmol AAE/100ml and 369.76 µmol AAE/g.

3.2.2 Effects of 24 hr-R_fE on Cell Numbers using the Trypan Blue Exclusion Method

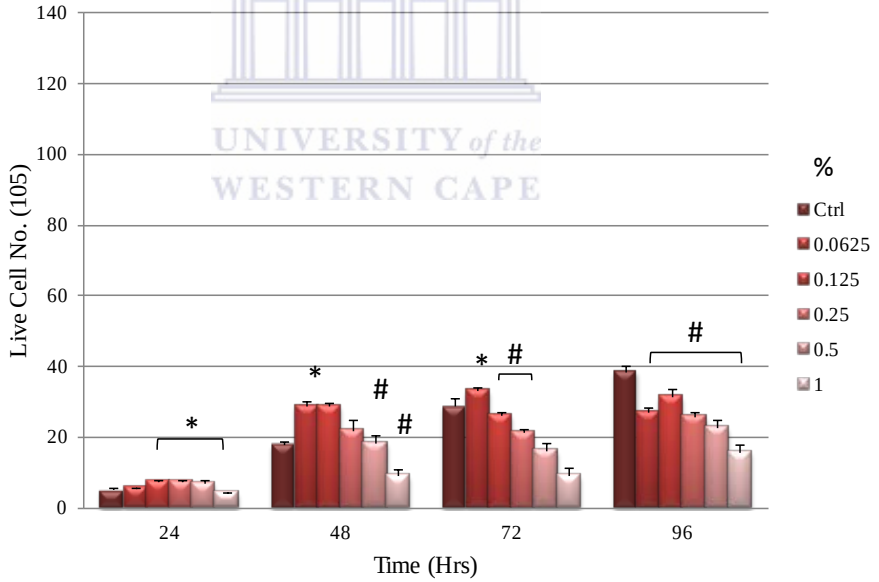

Figure 3.15 Live cell number in response to 24 hr exposure of selected R_f concentrations and time. Results are expressed as mean ± SEM (n=5). Significant ($P<0.05$) increases in live cell number are denoted with * whereas significant decreases are denoted with #.

A biphasic growth expression was observed after exposing the cells to an R_f range of 0.0625-1% with small statistically significant increases observed ($P\leq0.0494$) in response to all concentrations with exception to lowest R_f concentration (0.0625% R_f). In contrast, significant dose-dependent growth suppression ($P\leq0.0032$) was observed at the remaining time intervals (48-96 hrs). At 48 hrs, a significant increase ($P=0.0003$) was observed at 0.0625%, coupled with decreases observed at 0.5% and 1% ($P\leq0.0015$). The lowest concentration (0.0625%) resulted in an increase ($P=0.0002$) at 72 hrs while 0.125 and 0.25% resulted in decreases ($P\leq0.0041$). All R_f concentrations resulted in significant decreases ($P\leq0.0073$) in cell numbers at 96 hrs in comparison to controls. Exposure to 1% R_f resulted in the greatest suppression ($P\leq0.0032$) in contrast to the lowest concentration (0.0625%) at all time intervals (Figure 3.15 and Appendix C: Table 3.11).

3.2.3 Effects of 24 hour Fermented-Rooibos-Exposure (24 hr-R_fE) on Cell Viability (%) using the Trypan Blue Exclusion Method

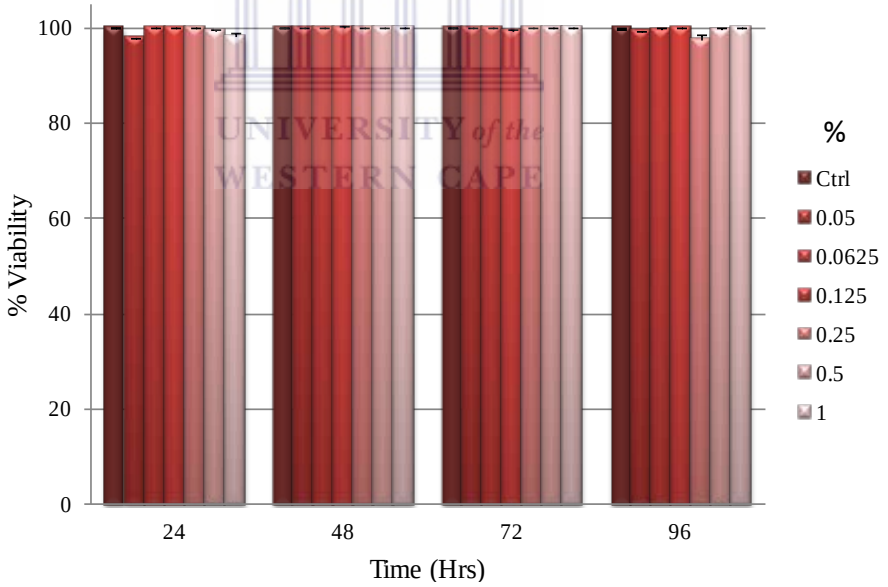

Figure 3.16 Cell Viability (%) in response to 24 hr exposure of selected R_f concentrations and time. Results are expressed as mean ± SEM (n=5). Significant ($P<0.05$) increases in cell viability are denoted with * whereas significant decreases are denoted with #.

Exposure of cells to all R_f concentrations resulted in cell viability similar to that of the controls across all the time intervals. This, as with exposure to the selected MA concentrations, illustrated a non-toxic effect in response to the selected R_f concentrations as seen with an overall cell toxicity of <2.47% (cell toxicity was determined by expressing the dead cell numbers over an entire (live and dead cells) population) (Figure 3.16 and Appendix C: Table 3.12).

3.2.4 Effects of 24 hr-R_fE on Cell Viability (%) using the Reduced Formazan Method (Observing Metabolic Activity)

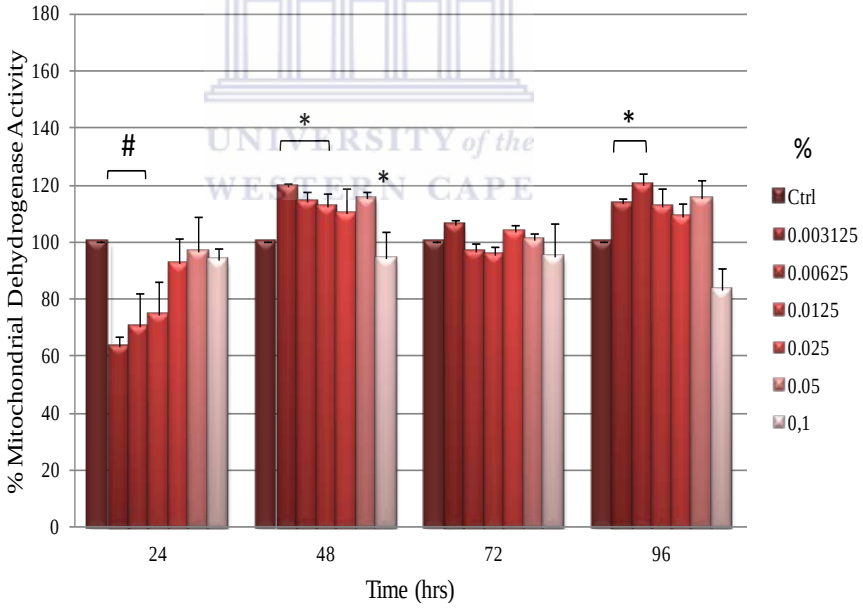

Figure 3.17 Mitochondrial dehydrogenase activity (%) in response to 24 hr exposure of selected R_f concentrations and time. Results are expressed as mean ± SEM (n=5). Controls were normalized to 100% and experimental groups expressed relative to controls. Significant ($P<0.05$) increases in cell viability are denoted with * whereas significant decreases are denoted with #.

R_f exposure at 24 hrs resulted in a dose-dependent increase ($P\leq0.0030$), however, these doses initially displayed suppressed MDH activity with the lowest concentrations (0.003125-0.0125% R_f) displaying the greatest suppression ($P<0.0001$). Exposure at the remaining time intervals resulted in small statistical significant elevation in MDH activity at 48 and 96 hrs ($P\leq0.0105$) when compared to respective controls. Significant increases ($P\leq0.0105$) in viability was observed in response to 0.003125-0.05% at 48 hrs coupled with a small statistical significant decrease at 0.1% ($P=0.0071$). Similarly, the two lowest concentrations (0.003125 and 0.00625%) resulted in the significant increases ($P\leq0.0071$) observed at 96 hrs. No significant differences were observed 72 hrs (Figure 3.17 and Appendix C: Table 3.13).

3.2.5 Effects of Daily-R_fE on Cell Viability (%) using the Reduced Formazan Method (Observing Metabolic Activity)

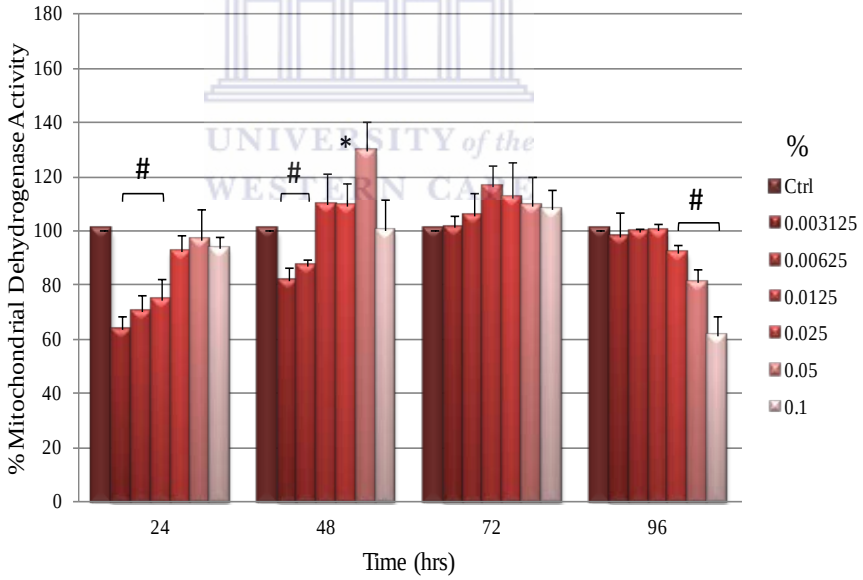

Figure 3.18 Mitochondrial dehydrogenase activity (%) in response to daily exposure of selected R_f concentrations and time. Results are expressed as mean ± SEM (n=5). Controls were normalized to 100% and experimental groups expressed relative to controls. Significant ($P<0.05$) increases in cell viability are denoted with * whereas significant decreases are denoted with #.

Dose-dependent increases ($P\leq0.0165$) were observed at 24 and 48 hrs however, these doses initially displayed suppressed MDH activity when the cells were exposed to the R_f range of 0.003125-0.1%, with the lowest concentration displaying the greatest suppression ($P\leq0.0165$) (as seen with 24 hr-R_fE). A small statistically significant increase ($P<0.0001$) was also observed at 48 hrs after exposure to 0.025% R_f. Furthermore, at 72 and 96 hrs, exposure to R_f resulted in no statistical significant differences with significant decreases ($P\leq0.0188$) occurring at only 96 hrs when exposed to the higher R_f concentrations (0.025, 0.05 and 0.1%). The highest viability (129.43±10.88) was observed at 48 hrs when exposed to 0.05% and the lowest viability (61.19±7.58) was observed at 96 hrs when exposed to 0.1% R_f (Figure 3.18 and Appendix C: Table 3.14).

3.2.6 Effects of Daily-R_fE on Monolayer Electrical Resistance (TEER)

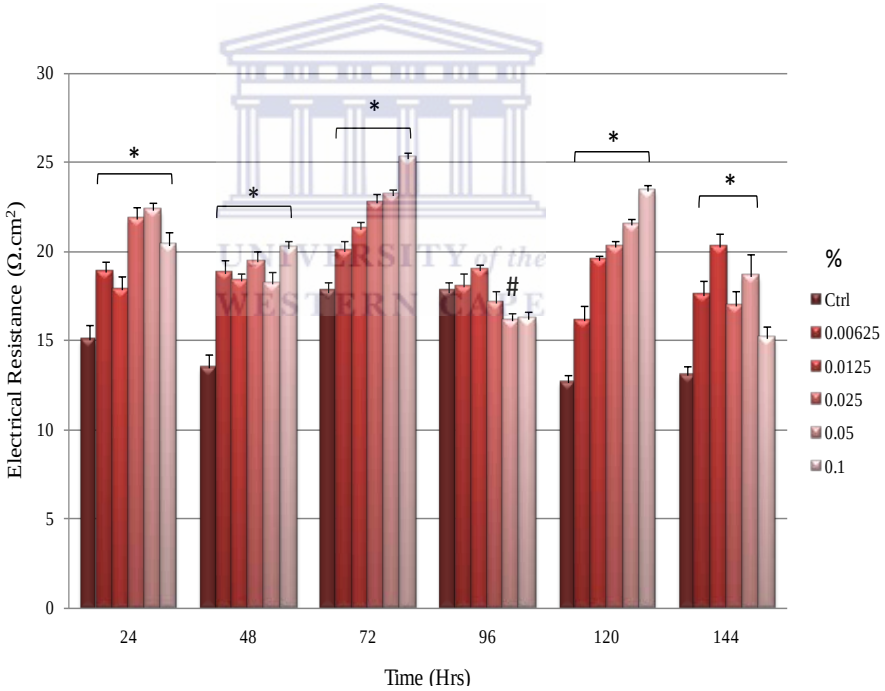

Figure 3.19 Transendothelial electrical resistance in response to daily exposure of selected R_f concentrations and time. Results are expressed as mean ± SEM (n=4). Significant (P<0.05) increases in TEER are denoted with * whereas significant decreases are denoted with #.

Exposure of the cells to an R_f range of 0.00625-0.1% at 24 hrs resulted in a dose-dependent increase (P≤0.0167) in resistance with the lowest concentration (0.00625% R_f) displayed the lowest TEER (P≤0.0100) and the highest concentration (0.1% R_f) displaying the highest TEER (P≤0.0001). However, despite observing a lower TEER, it was consistently greater than the controls. The significant dose-related trend was also observed at 72 (P≤0.0100) and 120 hrs (P≤0.0071). On the alternative days, a statistically significant flat-increase (P≤0.0418) was observed with a small statistical significant decrease (P=0.0418) in TEER observed at 96 hrs, at only 0.05% R_f (Figure 3.19 and Appendix C: Table 3.15).

3.2.7 Effects of Fermented Rooibos Exposure on bEnd5 Cell Cycles

3.2.7.1 Effects of 24 hr-R_fE on Cell Cycles at 24 hours

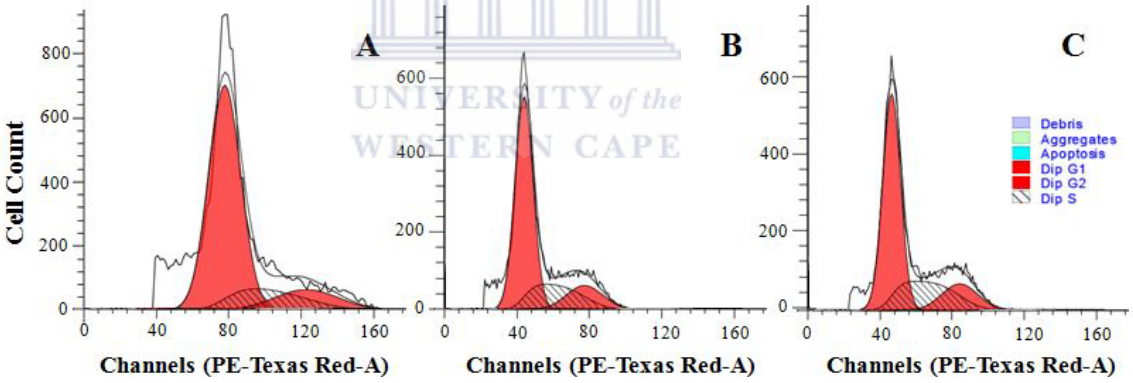

Figure 3.20 Histograms illustrating cell cycle results after 24 hr exposure to selected R_f concentrations at 24 hrs using flow cytometry (≥ 10 000 events analysed). **A** Control. **B** Exposure to 0.05% R_f. **C** Exposure to 0.1% R_f.

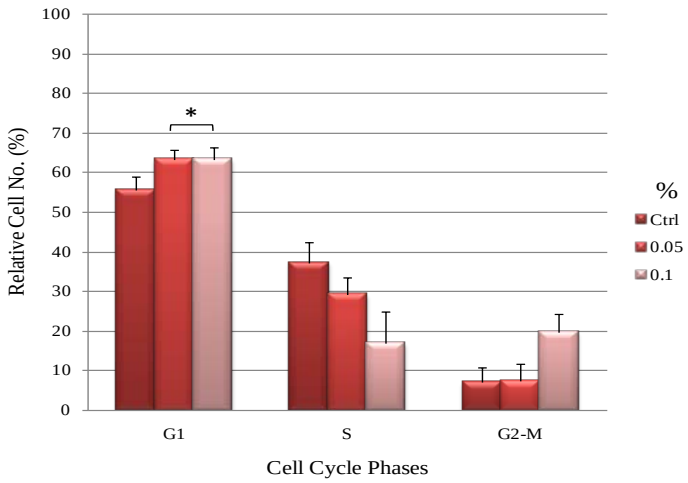

Figure 3.21 Relative cell numbers (%) at distinct phases of the cell cycle after exposure to selected R_f concentrations at 24 hrs. Results are expressed as mean ± SEM (n=3). Significant ($P<0.05$) increases in relative cell no. are denoted with * whereas significant decreases are denoted with #.

The highest cell numbers for both controls and exposed cells were observed in the G1-phase (≥55.79±3.29%) while the least amount of cells were observed in the G2-M phase

(7.47±4.20%) at 24 hrs. In addition, significant increases (P≤0.0031) were observed at G2-M phase when exposed to both R_f concentrations in comparison to controls. Despite the small statistical significant differences, the data depicts a normal profile of cell division (See Figure 3.20 and 3.21, Appendix C: Table 3.16 and Appendix J).

3.2.7.2 Effects of 24 hr-R_fE on Cell Cycles at 48 hours

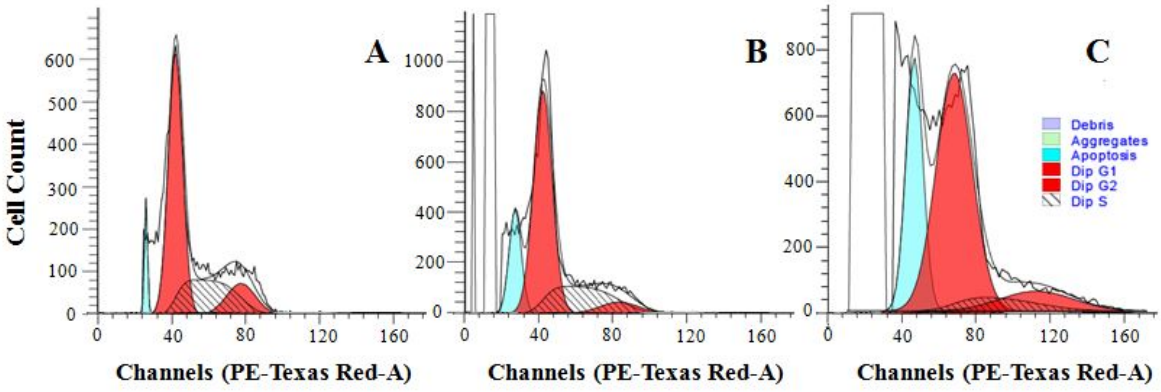

Figure 3.22 Histograms illustrating cell cycle results after 24 hr exposure to selected R_f concentrations at 48 hrs using flow cytometry (≥ 10 000 events analysed). **A** Control. **B** Exposure to 0.05% R_f. **C** Exposure to 0.1% R_f.

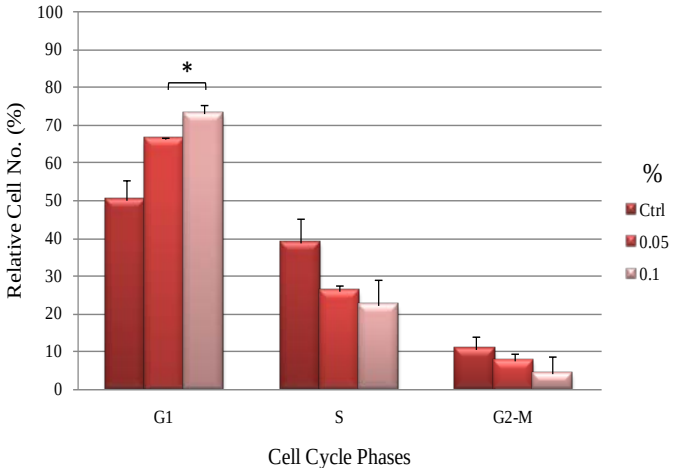

Figure 3.23 Relative cell numbers (%) at distinct phases of the cell cycle after exposure to R_f selected concentrations at 48 hrs. Results are expressed as mean ± SEM (n=3). Significant (P<0.05) increases in relative cell no. are denoted with * whereas significant decreases are denoted with #.

The G2-M phase displayed the least amount of cells detected (≤7.62±1.87%) with the most cells detected at the G1 phase (≥73.18±2.26%). Moreover, significant increases (P≤0.0356) were observed at G2-M phase when exposed to both R_f concentrations in comparison to controls. As with 24 hrs, the small statistical significant differences, the data depicts a normal profile of cell division (See Figure 3.22 and 3.23, Appendix C: Table 3.17 and Appendix K).

3.2.7.3 Effects of 24 hr-R_fE on Cell Cycles at 72 hours

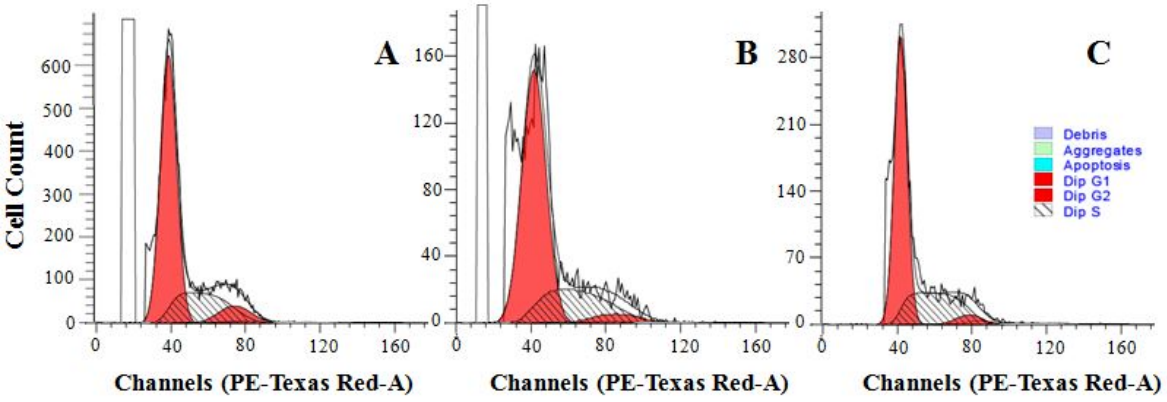

Figure 3.24 Histograms illustrating cell cycle results after 24 hr exposure to selected R_f concentrations at 72 hrs using flow cytometry (≥ 10 000 events analysed). **A** Control. **B** Exposure to 0.05% R_f. **C** Exposure to 0.1% R_f.

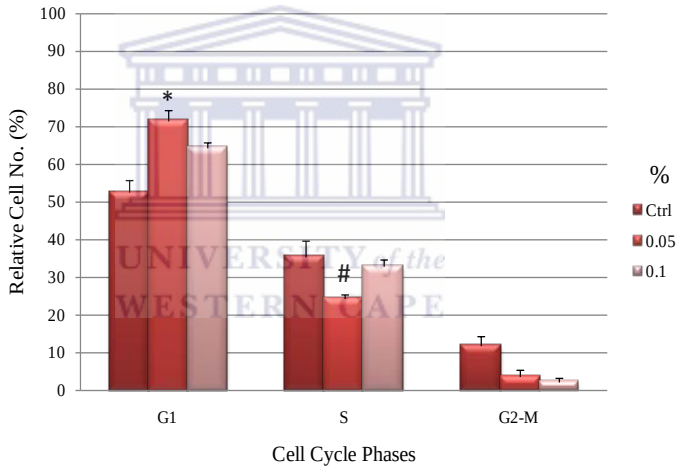

Figure 3.25 Relative cell numbers (%) at distinct phases of the cell cycle after exposure to selected R_f concentrations at 72 hrs. Results are expressed as mean ± SEM (n=3). Significant ($P<0.05$) increases in relative cell no. are denoted with * whereas significant decreases are denoted with #.

The most cells were recorded in the G1-phase (≥ 52.71±3.06%) and the least in the S-phase (≤3.82±1.59%). Exposure to 0.05% R_f resulted in a marked increase (P=0.0062) and decrease (P=0.0087) in the G1- and S-phase, respectively. The data depicts a normal profile of cell division despite the small statistical significant differences (See Figure 3.24 and 3.25, Appendix C: Table 3.18 and Appendix L).

3.2.7.4 Effects of 24 hr-R_fE on Cell Cycles at 96 hours

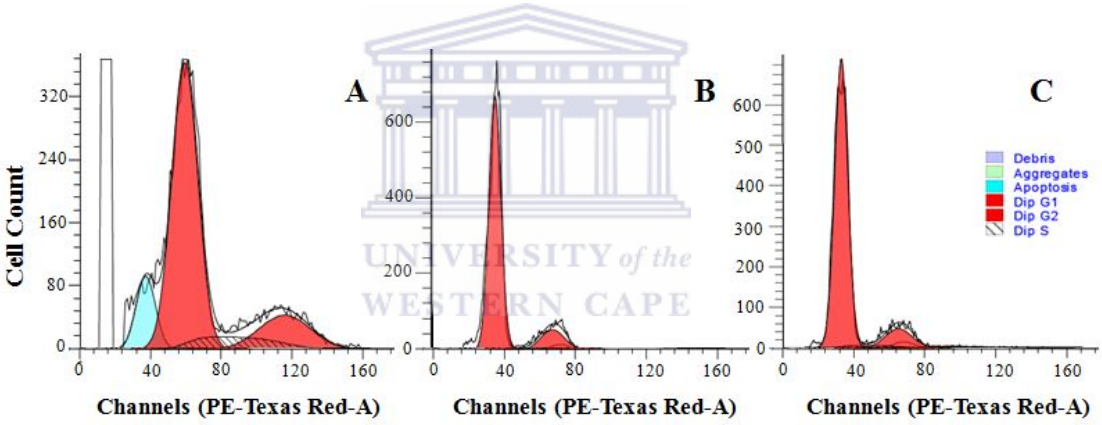

Figure 3.26 Histograms illustrating cell cycle results after 24 hr exposure to selected R_f concentrations at 96 hrs using flow cytometry (≥ 10 000 events analysed). **A** Control. **B** Exposure to 0.05% R_f. **C** Exposure to 0.1% R_f.

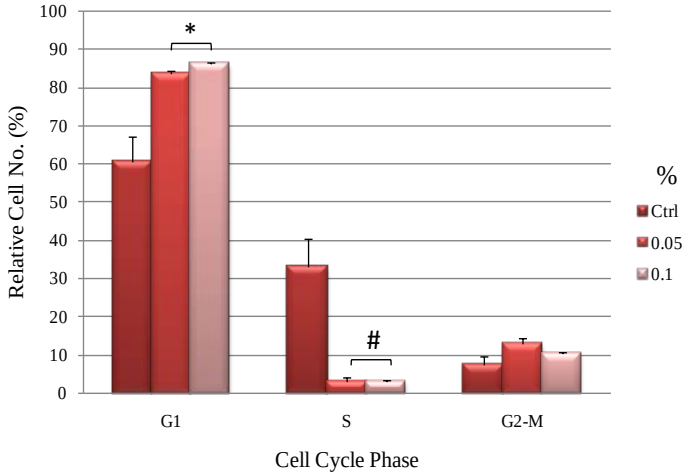

Figure 3.27 Relative cell numbers (%) at distinct phases of the cell cycle after exposure to selected R_f concentrations at 96 hrs. Results are expressed as mean ± SEM (n=3). Significant ($P<0.05$) increases in relative cell no. are denoted with * whereas significant decreases are denoted with #.

At 96 hrs, G1-phase had the highest relative cell numbers (≥86.41±0.13), with the S-phase having the least (≤33.04±7.34%). Exposure to both R_f concentrations resulted in a marked increases ($P\leq0.0158$) and decreases ($P\leq0.0240$) in the G1- and S-phase, respectively. A normal cell division profile was not observed at 96 hrs since the cells

have accumulated in the G1-phase preventing DNA synthesis as seen with S-phase cell population suppression (See Figure 3.26 and 3.27, Appendix C: Table 3.19 and Appendix M).

3.3 Effects of the Methamphetamine and Fermented Rooibos Combinations

Note: In order to prevent confusion for the reader the combination of various methamphetamine concentrations combined with two selected concentrations of R_f (0.05 and 0.1%), were catagorised into Combination 1 (0.05% with selected MA concentrations) and Combination 2 (0.1% with selected MA concentrations)

3.3.1 Effects of 0.05% Fermented Rooibos and Selected Methamphetamine Concentrations (Combination 1)

3.3.1.1 Effects of 24 hr Exposure to Combination 1 on Cell Numbers using the Trypan Blue Exclusion Method

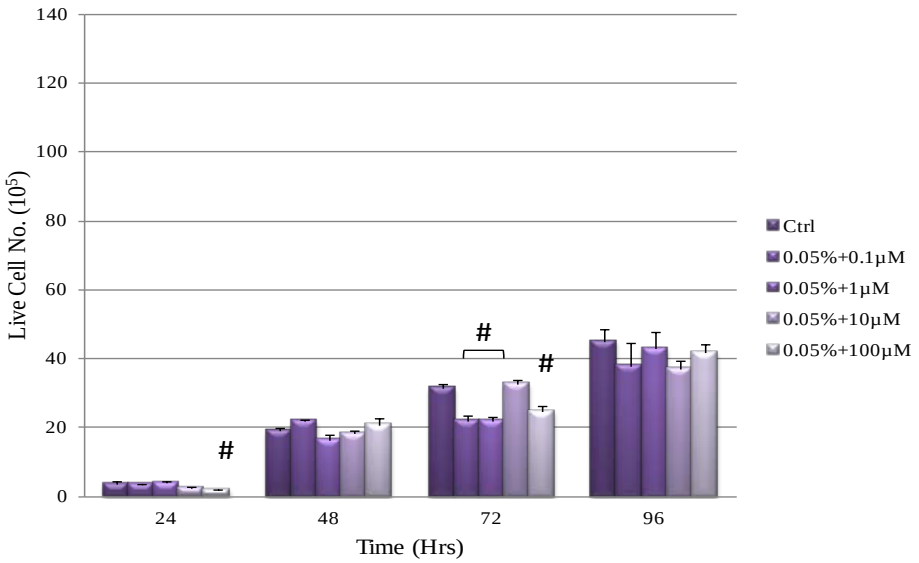

Figure 3.28 Live cell number in response to 24 hr exposure of 0.05% fermented rooibos in combination with selected methamphetamine concentrations, and time. Results are expressed as mean ± SEM (n=5). Significant ($P<0.05$) increases in live cell number are denoted with * whereas significant decreases are denoted with #.

After exposure to the combinations of R_f and MA, no statistically significant decreases were observed at 48 and 96 hrs, with a small significant decrease observed at 24 hrs when exposed to only 0.05% R_f and 100 µM MA (P=0.0012). However, at 72 hrs, exposure to all combinations displayed statistically significant decreases (P≤0.0059) with exception to 0.05% R_f and 10 µM MA when compared to the controls. (Figure 3.28 and Appendix D: Table 3.20).

3.3.1.2 Effects of 24 hr exposure to Combination 1 on Cell Viability (%) using the Trypan Blue Exclusion Method

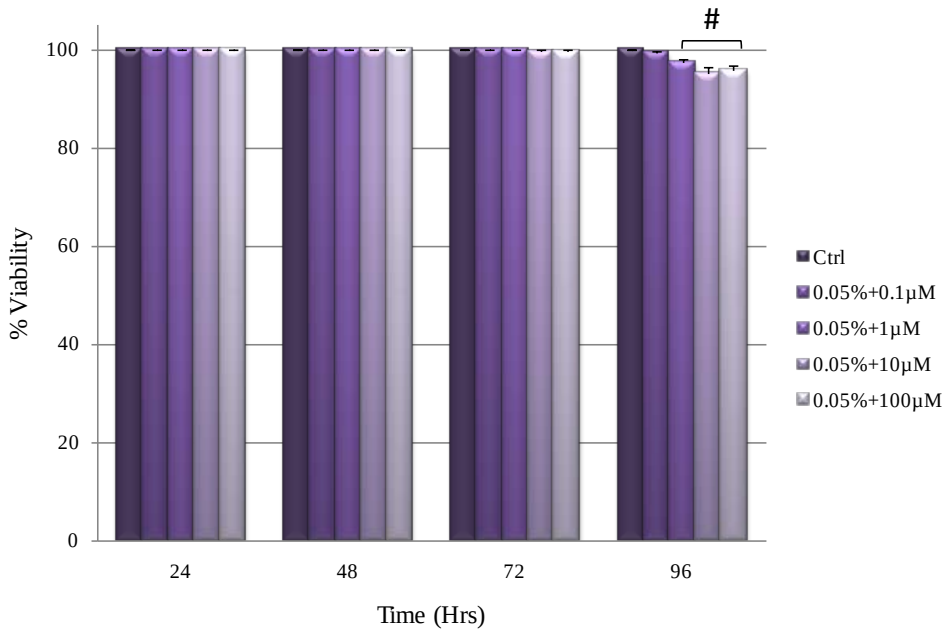

Figure 3.29 Cell Viability (%) in response to 24 hr exposure of 0.05% fermented rooibos in combination with selected methamphetamine concentrations, and time. Results are expressed as mean ± SEM (n=5). Significant (P<0.05) increases in cell viability are denoted with * whereas significant decreases are denoted with #.

No significant differences were observed for all exposed concentrations at 24, 48 and 72 hrs. However at 96 hrs, exposure to the combination containing 1, 10 and 100 µM MA resulted in significant decreases (P≤0.0024) in cell viability in comparison to controls Despite the small statistically significant decreases observed at 96 hrs, the results illustrated a non-toxic effect in response to the 0.05% R_f and the selected MA

concentrations as seen with an overall cell toxicity of <4.82% (cell toxicity was determined by expressing the dead cell numbers over an entire (live and dead cells) population) (Figure 3.29 and Appendix D: Table 3.21).

3.3.1.3 Effects of 24 hr exposure to Combination 1 on Cell Viability (%) using the Reduced Formazan Method (Observing Metabolic Activity)

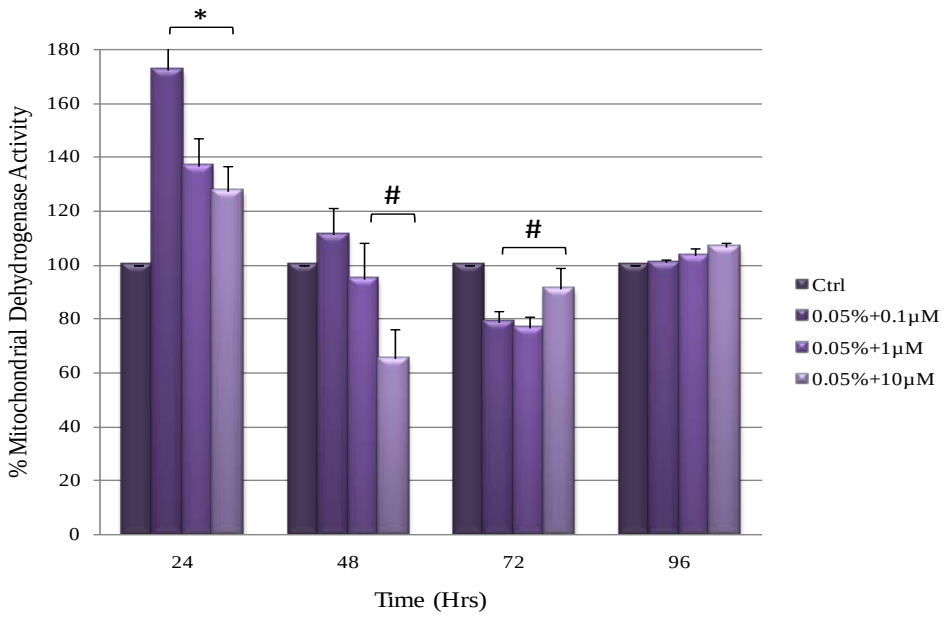

Figure 3.30 Mitochondrial dehydrogenase activity (%) in response to 24 hr exposure of 0.05% fermented rooibos in combination with selected methamphetamine concentrations, and time. Results are expressed as mean ± SEM (n=5). Controls were normalized to 100% and experimental groups expressed relative to controls. Significant ($P<0.05$) increases in cell viability are denoted with * whereas significant decreases are denoted with #.

Exposure of cells to all concentrations of R_f resulted in statistically significant increases ($P\leq0.0174$) in MDH activity at 24 hrs. However, marked decreases ($P\leq0.0105$) were observed when exposed to R_f and 1 and 10 µM MA at 48 hrs. The MDH activity was especially suppressed after exposure to 10 µM MA. All concentrations resulted in significant decreases ($P\leq0.0180$) at 72 hrs in comparison to controls. In addition, no statistically significant differences were observed at 96 hrs when compared to controls (Figure 3.30 and Appendix D: Table 3.22).

3.3.1.4 Effects of Daily Exposure to Combination 1 on Cell Viability (%) using the Reduced Formazan Method (Observing Metabolic Activity)

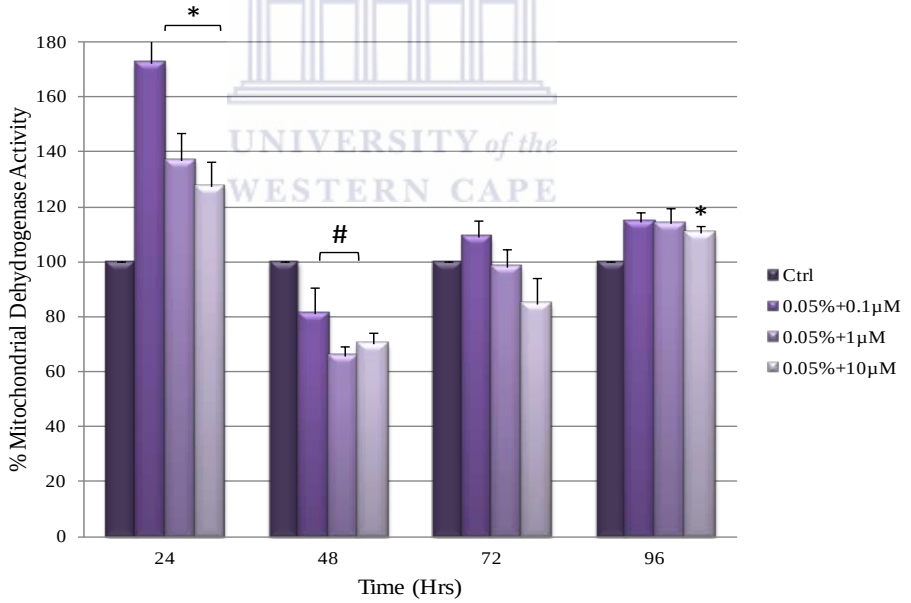

Figure 3.31 Mitochondrial dehydrogenase activity (%) in response to daily exposure of 0.05% fermented rooibos in combination with selected methamphetamine concentrations, and time. Results are expressed as mean ± SEM (n=5). Controls were normalized to 100% and experimental groups expressed relative to controls. Significant ($P<0.05$) increases in cell viability are denoted with * whereas significant decreases are denoted with #.

As seen with 24 hr (once-off) exposure, there were significant increases in % viability at 24 hrs after the cells were exposed to all combinations of R_f and MA ($P \leq 0.0174$). However, the combinations containing 0.1 and 1 µM MA displayed marked suppression ($P \leq 0.0071$) at 48 hrs when compared to the controls. No statistical significant differences were observed at 72 and 96 hrs, however, a small statistical significant increase ($P=0.0071$) in MDH activity was observed in response to the highest MA-containing combination. When comparing once-off exposure to that of daily, the MDH activity in response to the R_f and MA combinations resulted in similar observations at 24, 48 and 96 hrs. In contrast to 72 hrs, which displayed decreased MDH activity when the cells were exposed to singular combinations (Figure 3.31 and Appendix D: Table 3.23).

3.3.1.5 Effects of Daily Exposure to Combination 1 on Monolayer Electrical Resistance (TEER)

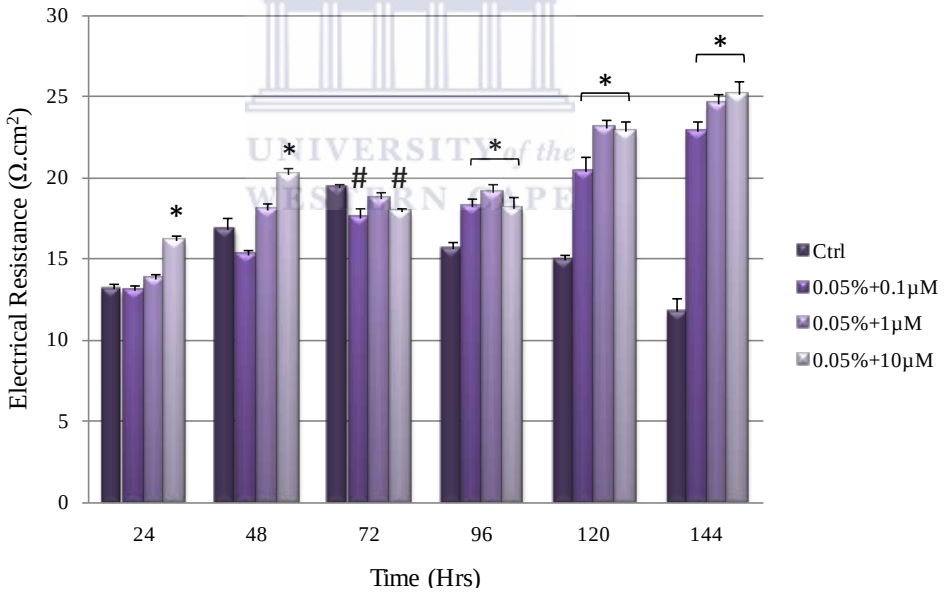

Figure 3.32 Electrical resistance in response to daily exposure of 0.05% fermented rooibos in combination with selected methamphetamine concentrations, and time. Results are expressed as mean ± SEM (n=4). Significant (P<0.05) increases in TEER are denoted with * whereas significant decreases are denoted with #.

Exposure of cells to the combinations resulted on dose-dependent increases (P<0.0001) across the time intervals with exception to 72 and 96 hrs which displayed small statistically significant decreases (P≤0.0128) and a flat-patterned increase (P≤0.0066), respectively. The lowest MA-containing combination displayed the lowest TEER (P≤0.0128) with highest MA-containing combination (P≤0.0066) resulting in the highest resistance across all time intervals with exception to 96 hrs (Figure 3.32 and Appendix D: Table 3.24).

3.3.1.6 Effects of Combination 1 on bEnd5 Cell Cycles

3.3.1.6.1 Effects of 24 hr Exposure to Combination 1 on Cell Cycles at 24 hours

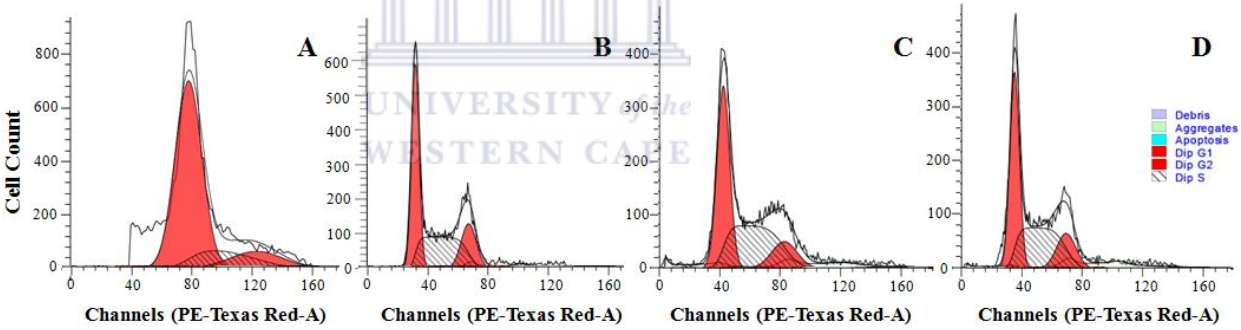

Figure 3.33 Histograms illustrating cell cycle results after exposure to 0.05% fermented Rooibos in combination with selected methamphetamine concentrations at 24 hrs using flow cytometry as follows (≥ 10 000 events analysed). **A** Control. **B** 0.05% R_f and 0.1 µM MA. **C** 0.05% R_f and 1 µM MA. **D** 0.05% R_f and 10 µM MA.

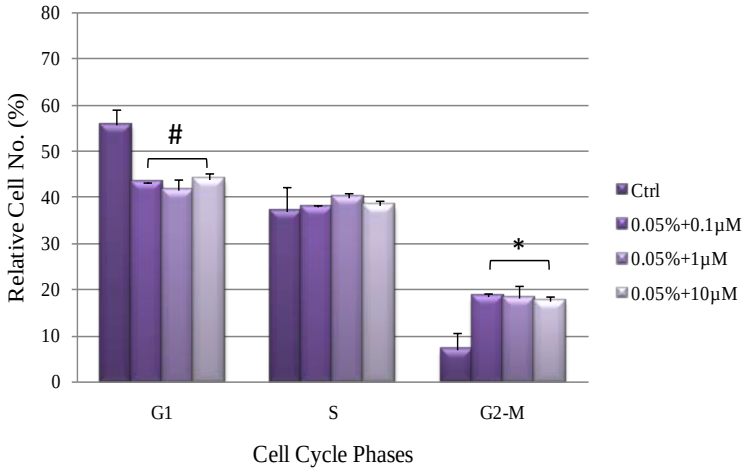

Figure 3.34 Relative cell numbers (%) at distinct phases of the cell cycle after 24 hr exposure to a combination of 0.05% fermented rooibos and selected MA concentrations at 24 hrs. Results are expressed as mean ± SEM (n=3). Significant ($P<0.05$) increases in relative cell no. are denoted with * whereas significant decreases are denoted with #.

The G1-phase contained the highest relative cell number (≥41.56±2.47%) and G2-M phase possessed the least amount of cells (≤18.75±0.41%). All combination concentrations resulted in marked decreases ($P\leq0.0495$) and increases ($P\leq0.0275$) in the

G1- and G2-M-phases, respectively. Experimental groups were similar to that of controls in the S-phase. The experimental groups in the G1- and S-phases were also similar (See Figure 3.33 and 3.34, Appendix D: Table 3.25 and Appendix N).

3.3.1.6.2 Effects of 24 hr Exposure to Combination 1 on Cell Cycles at 48 hours

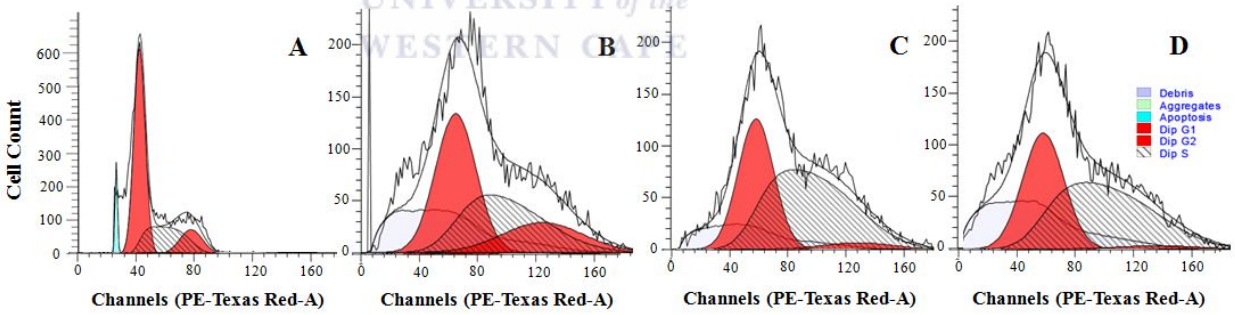

Figure 3.35 Histograms illustrating cell cycle results after exposure to 0.05% fermented Rooibos in combination with selected methamphetamine concentrations at 48 hrs using flow cytometry as follows (≥ 10 000 events analysed). **A** Control. **B** 0.05% R_f and 0.1 µM MA. **C** 0.05% R_f and 1 µM MA. **D** 0.05% R_f and 10 µM MA.

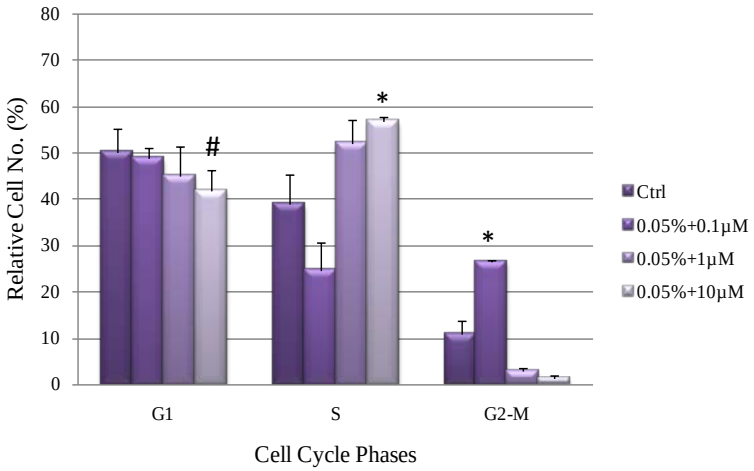

Figure 3.36 Relative cell numbers (%) at distinct phases of the cell cycle after 24 hr exposure to a combination of 0.05% fermented rooibos and selected MA concentrations at 48 hrs. Results are expressed as mean ± SEM (n=3). Significant ($P<0.05$) increases in relative cell no. are denoted with * whereas significant decreases are denoted with #.

The S-phase contained the highest amount of cells (≥24.56±6.27%). The experimental groups in the G1- and S-phases were similar with exception to the lowest MA-

containing combination in the S-phase. The least cells were detected in the G2-M phase (1.39±0.57%) after exposure to the 10 µM MA combination. A significant decrease (P=0.0356) and increase (P=0.0356) was observed when exposed to the highest MA combination in the G1- and S-phases, respectively. R_f and 0.1 µM MA exposure in the G2-M phase displayed a marked increase (P=0.0430) in comparison to controls (See Figure 3.35 and 3.36, Appendix D: Table 3.26 and Appendix O).

3.3.1.6.3 Effects of 24 hr Exposure to Combination 1 on Cell Cycles at 72 hours

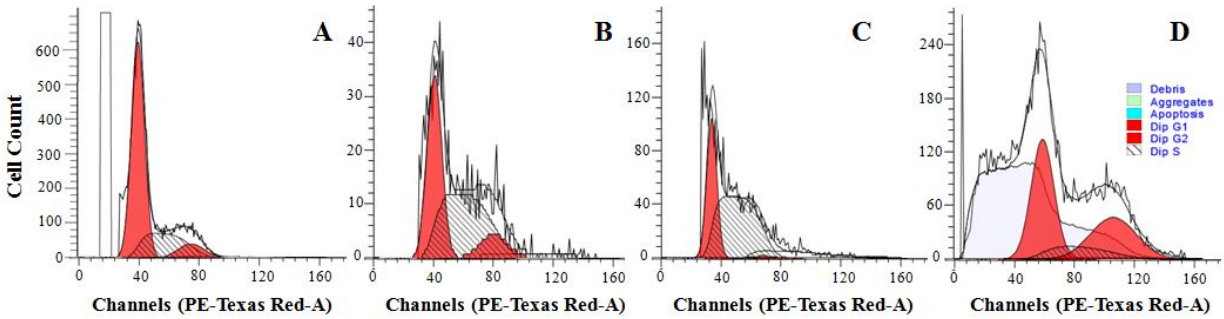

Figure 3.37 Histograms illustrating cell cycle results after exposure to 0.05% fermented Rooibos in combination with selected methamphetamine concentrations at 72 hrs using flow cytometry as follows (≥ 10 000 events analysed). **A** Control. **B** 0.05% R_f and 0.1 µM MA. **C** 0.05% R_f and 1 µM MA. **D** 0.05% R_f and 10 µM MA.

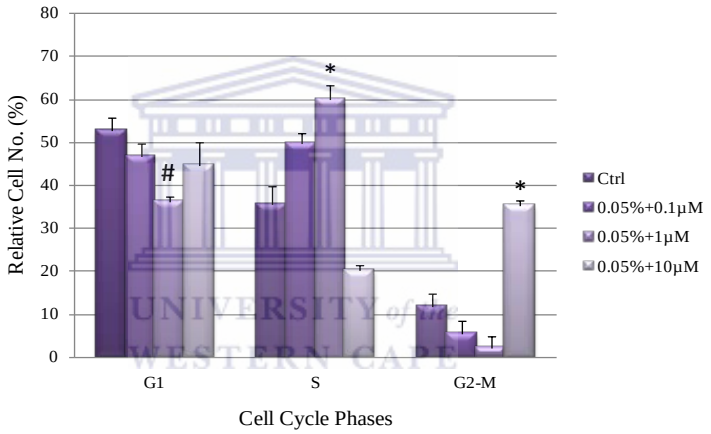

Figure 3.38 Relative cell numbers (%) at distinct phases of the cell cycle after 24 hr exposure to a combination of 0.05% fermented rooibos and selected MA concentrations at 72 hrs. Results are expressed as mean ± SEM (n=3). Significant ($P<0.05$) increases in relative cell no. are denoted with * whereas significant decreases are denoted with #.

At 72 hrs, the highest cell number was observed in the S-phase (59.81±3.46%) when exposed to the 1 µM MA combination with the least cells detected in the G2-M phase at 2.15±2.63% after exposure to the R_f and 10 µM MA combination. A significant decrease ($P=0.0128$) was observed at the G1-phase when exposed to the intermediate combination. The highest combinations resulted in marked increases at both S- ($P=0.0415$) and G2-M-phases ($P=0.0025$) when compared to controls (See Figure 3.37 and 3.38, Appendix D: Table 3.27 and Appendix P).

3.3.1.6.4 Effects of 24 hr Exposure to Combination 1 on Cell Cycles at 96 hours

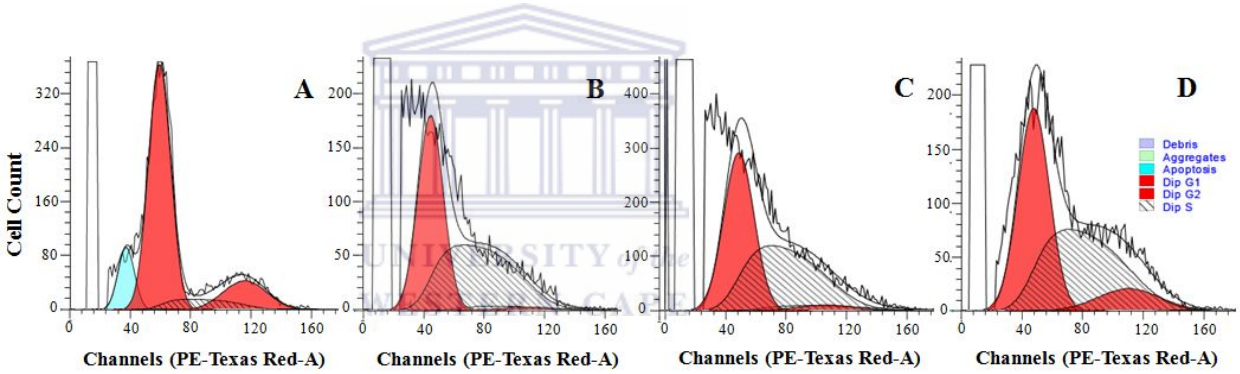

Figure 3.39 Histograms illustrating cell cycle results after exposure to 0.05% fermented Rooibos in combination with selected methamphetamine concentrations at 96 hrs using flow cytometry as follows (≥ 10 000 events analysed). **A** Control. **B** 0.05% R_f and 0.1 µM MA. **C** 0.05% R_f and 1 µM MA. **D** 0.05% R_f and 10 µM MA.

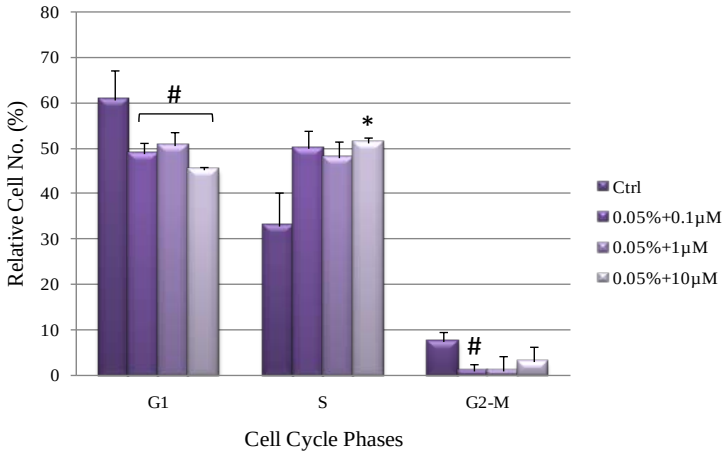

Figure 3.40 Relative cell numbers (%) at distinct phases of the cell cycle after 24 hr exposure to a combination of 0.05% fermented rooibos and selected MA concentrations at 96 hrs. Results are expressed as mean ± SEM (n=3). Significant ($P<0.05$) increases in relative cell no. are denoted with * whereas significant decreases are denoted with #.

Experimental groups in the G1- and S-phase were similar in relative cell number. However, the highest numbers (51.22±1.21%) were detected in the S-phase when exposed to the intermediate-MA combination. Exposure to all combinations in the G1-phase resulted in marked decreases ($P\leq0.0436$). The highest combination displayed a marked increase ($P=0.0243$) in the S-phase. The least amount of cells was observed in

the G2-M phase at 1.21±1.30% and 1.21±3.15% when exposed to combinations containing 0.1 and 1 µM MA, respectively. Moreover, the lowest combination resulted in a marked decrease (P=0.0420) when compared to controls (See Figure 3.39 and 3.40, Appendix D: Table 3.28 and Appendix Q).

3.3.2 Effects of 0.1% Fermented Rooibos and selected Methamphetamine Concentrations (Combination 2)

3.3.2.1 Effects of 24 hr Exposure to Combination 2 on Cell Numbers using the Trypan Blue Exclusion Method

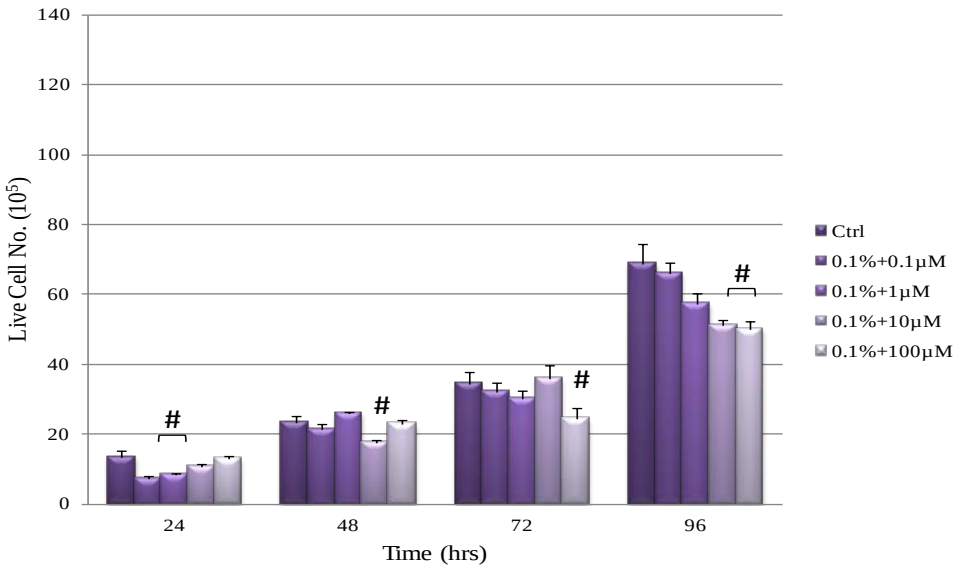

Figure 3.41 Live cell number in response to 24 hr exposure of 0.1% fermented rooibos in combination with selected methamphetamine concentrations, and time. Results are expressed as mean ± SEM (n=5). Significant (P<0.05) increases in live cell number are denoted with * whereas significant decreases are denoted with #.

A dose-dependent increase was observed at 24 hrs however exposure of the cells to these combinations initially displayed decreased cell numbers with the two lowest MA-containing (0.1 and 1 µM MA) combinations displaying statistically significant decreases (P≤0.0273) when compared to controls. No statistically significant differences were observed at 48 and 72 hrs with exception to the MA-containing combinations of

10 µM MA and 100 µM MA, respectively, which resulted in small statistically significant decreases (P≤0.0233). This effect was also observed at 96 hrs with the two higher MA-containing combinations causing cell suppression (P≤0.0371) (Figure 3.41 and Appendix E: Table 3.29).

3.3.2.2 Effects of 24 hr Exposure to Combination 2 on Cell Viability (%) using the Trypan Blue Exclusion Method

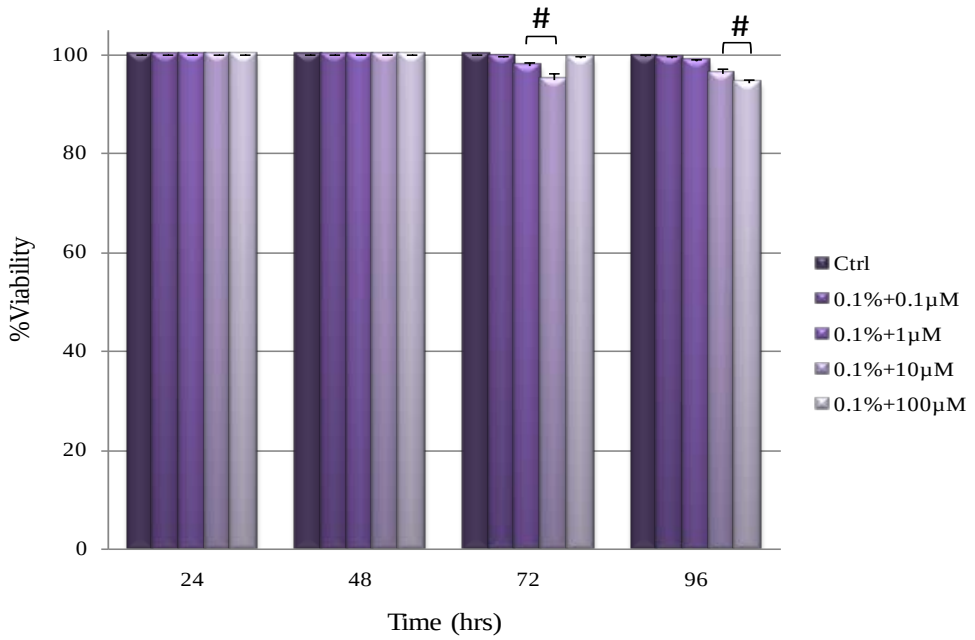

Figure 3.42 Cell Viability (%) in response to 24 hr exposure of 0.1% fermented rooibos in combination with selected methamphetamine concentrations, and time. Results are expressed as mean ± SEM (n=5). Significant (P<0.05) increases in cell viability are denoted with * whereas significant decreases are denoted with #.

There were no statistically significant differences observed when the cells were exposed to all 0.1% R_f and MA combinations at 24 and 48 hrs. However, at 72 and 96 hrs, exposure to R_f in combination with 1 and 10 µM MA (P≤0.0096), and 10 and 100 µM (P≤0.0113) MA respectively, resulted in small statistically significant decreases in cell viability. Despite the small statistically significant decreases observed at 72 and 96 hrs, the results illustrated a non-toxic effect in response to the 0.1% R_f and the selected MA concentrations as seen with an overall cell toxicity of <5.77% (cell toxicity was

determined by expressing the dead cell numbers over an entire (live and dead cells) population) (Figure 3.42 and Appendix E: Table 3.30).

3.3.2.3 Effects of 24 hr Exposure to Combination 2 on Cell Viability (%) using the Reduced Formazan Method (Observing Metabolic Activity)

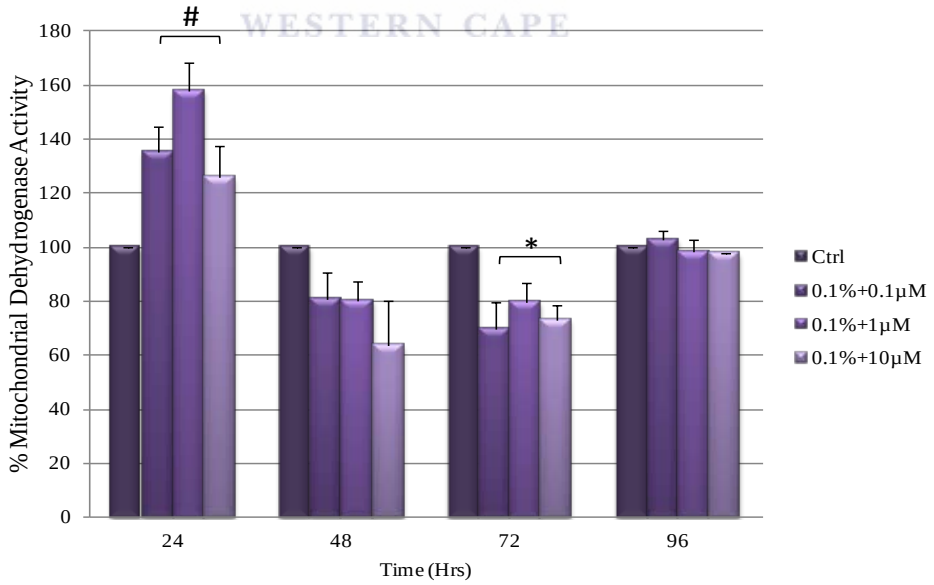

Figure 3.43 Mitochondrial dehydrogenase activity (%) in response to 24 hr exposure of 0.1% fermented rooibos in combination with selected methamphetamine concentrations, and time. Results are expressed as mean ± SEM (n=5). Controls were normalized to 100% and experimental groups expressed relative to controls. Significant ($P<0.05$) increases in cell viability are denoted with * whereas significant decreases are denoted with #.

Similar to combination 1, statistically significant increases ($P\leq0.0220$) in MDH activity were observed after exposure of cells to all 0.1% R_f and MA combinations. There were no statistically significant differences observed at 48 and 96 hrs when compared to the respective controls. However, 72 hr exposure to all combinations resulted in a statistically marked decline ($P\leq0.0071$) (Figure 3.43 and Appendix E: Table 3.31).

3.3.2.4 Effects of Daily Exposure to Combination 2 on Cell Viability (%) using the Reduced Formazan Method

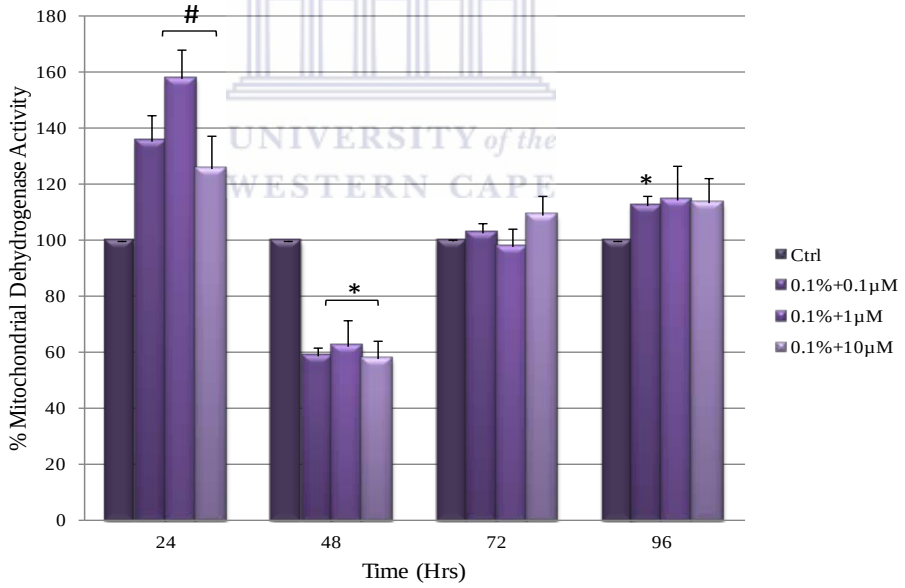

Figure 3.44 Mitochondrial dehydrogenase activity (%) in response to daily exposure of 0.1% fermented rooibos in combination with selected methamphetamine concentrations, and time. Results are expressed as mean ± SEM (n=5). Controls were normalized to 100% and experimental groups expressed relative to controls. Significant ($P<0.05$) increases in cell viability are denoted with * whereas significant decreases are denoted with #.

As was observed with once-off (24 hr) exposure, exposure of the cells to all 0.1% R_f and MA combinations displayed statistically significant increases ($P\leq0.0220$) in comparison to controls. However, exposure to all combinations at 48 hrs resulted in statistically significant decreases ($P\leq0.0105$). No differences were observed at 72 and 96 hrs, however, a small statistically significant increase ($P=0.0025$) was observed at the lowest MA (0.1 µM) combination when compared to controls (Figure 3.44 and Appendix E: Table 3.32).

3.3.2.5 Effects of Daily Exposure to Combination2 on Monolayer Electrical Resistance (TEER)

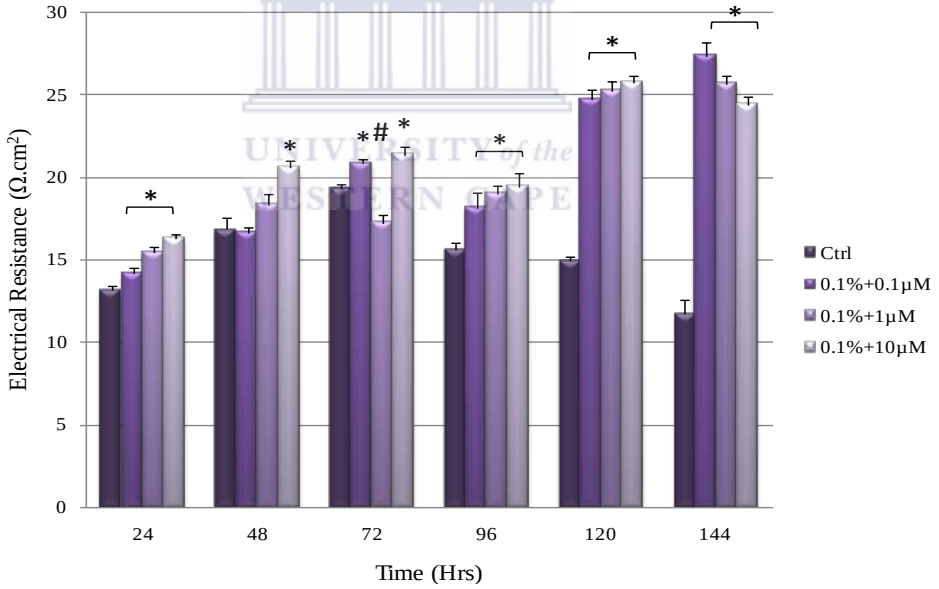

Figure 3.45 Electrical resistance in response to daily exposure of 0.1% fermented rooibos in combination with selected methamphetamine concentrations, and time. Results are expressed as mean ± SEM (n=5). Significant (P<0.05) increases in TEER are denoted with * whereas significant decreases are denoted with #.

Exposure of the cells to the combination range of R_f and MA resulted in statistically significant increases (P≤0.0210) in TEER across all time intervals with exception to 72 hrs in which Rf and 1 µM MA exposure resulted in a small statistically significant decrease (P<0.0062). In addition, a dose-dependent increase (P≤0.0210) in TEER at 24, 48, 96 and 120 hrs was observed. Although the TEER was significantly greater (P≤0.0001) than the controls at 96 hrs, it should be noted that the data took form of a dose-dependent decreased trend (Figure 3.45 and Appendix E: Table 3.33).

3.3.2.6 Effects of Combination 2 on bEnd5 Cell Cycles

3.3.2.6.1 Effects of 24 hr Exposure to Combination 2 on Cell Cycles at 24 hours

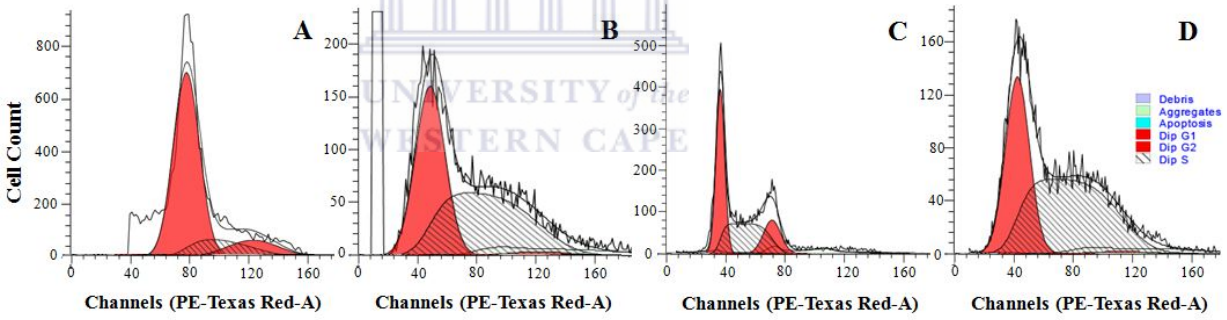

Figure 3.46 Histograms illustrating cell cycle results after 24 hr exposure to 0.1% fermented rooibos in combination with selected methamphetamine concentrations at 24 hrs using flow cytometry as follows (≥ 10 000 events analysed). **A** Control. **B** 0.1% R_f and 0.1 µM MA. **C** 0.1% R_f and 1 µM MA. **D** 0.1% R_f and 10 µM MA.

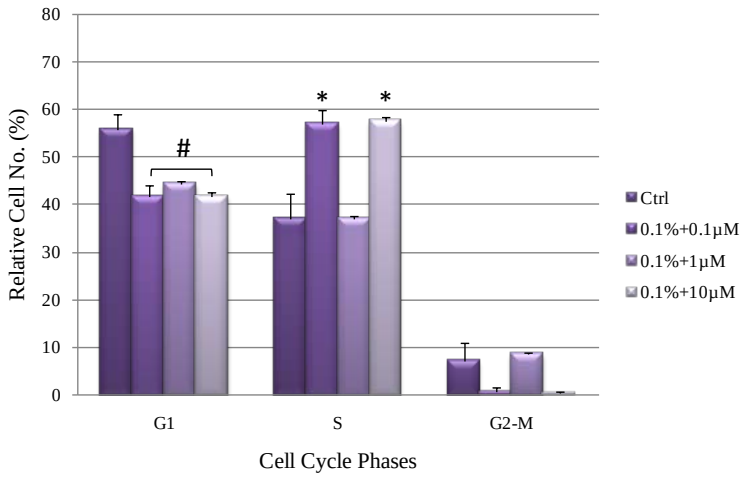

Figure 3.47 Relative cell numbers (%) at distinct phases of the cell cycle after 24 hr exposure to a combination of 0.1% fermented rooibos and selected MA concentrations at 24 hrs. Results are expressed as mean ± SEM (n=3). Significant ($P<0.05$) increases in relative cell no. are denoted with * whereas significant decreases are denoted with #.

The highest relative cell numbers were detected in the S-phase at 57.76±0.77% when exposed to the highest MA-containing (10 µM) combination which also resulted in least

detected cell populations in the G2-M phase at 0.46±0.33%. Exposure of the cells to all combinations in the G1-phase resulted in significant decreases (P≤0.0346) with marked increases occurring in the S-phase when exposed to 0.1% R_f in combination with 0.1 µM MA (P=0.0346) and 10 (P=0.0108) µM MA (See Figure 3.46 and 3.47, Appendix E: Table 3.34 and Appendix R).

3.3.2.6.2 Effects of 24 hr Exposure to Combination 2 on Cell Cycles at 48 hours

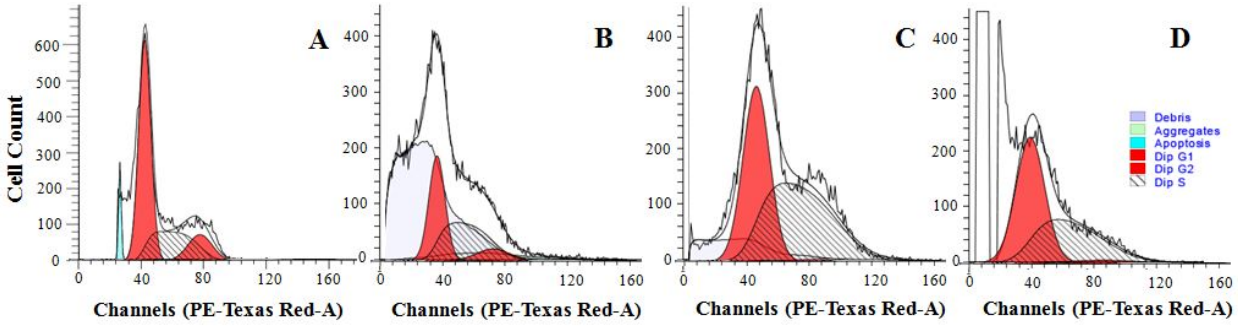

Figure 3.48 Histograms illustrating cell cycle results after exposure to 0.1% fermented rooibos in combination with selected methamphetamine concentrations at 48 hrs using flow cytometry as follows (≥ 10 000 events analysed). **A** Control. **B** 0.1% R_f and 0.1 µM MA. **C** 0.1% R_f and 1 µM MA. **D** 0.1% R_f and 10 µM MA.

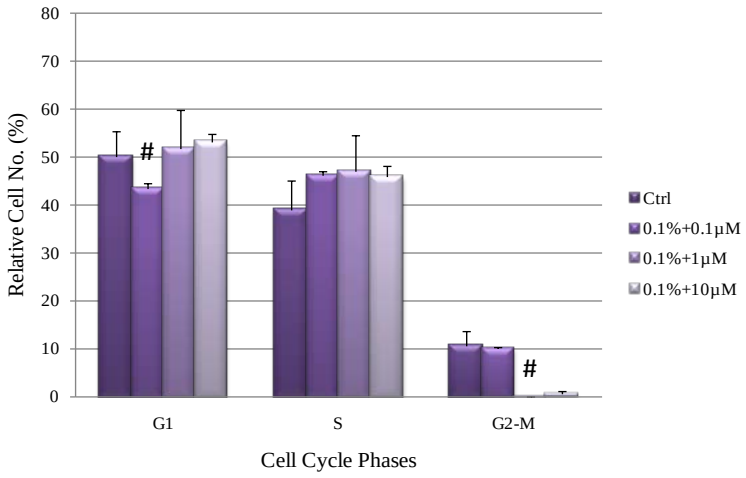

Figure 3.49 Relative cell numbers (%) at distinct phases of the cell cycle after 24 hr exposure to a combination of 0.1% fermented rooibos and selected MA concentrations at 48 hrs. Results are

expressed as mean ± SEM (n=3). Significant (P<0.05) increases in relative cell no. are denoted with * whereas significant decreases are denoted with #.

The greatest relative cell numbers were detected in the G1 phase (≥43.57±1.09%) while the least amount was observed at the G2-M phase (≤10.75±3.13%). Significant decreases were observed in the G1- and G2-M-phases when exposed to 0.1 (P=0.0436) and 1 (P=0.0406) µM MA combinations, respectively. It was noted that the experimental groups in the G1-phase were similar to that in the S-phase (See Figure 3.48 and 3.49, Appendix E: Table 3.35 and Appendix S).

3.3.2.6.3 Effects of 24 hr Exposure to Combination 2 on Cell Cycles at 72 hours

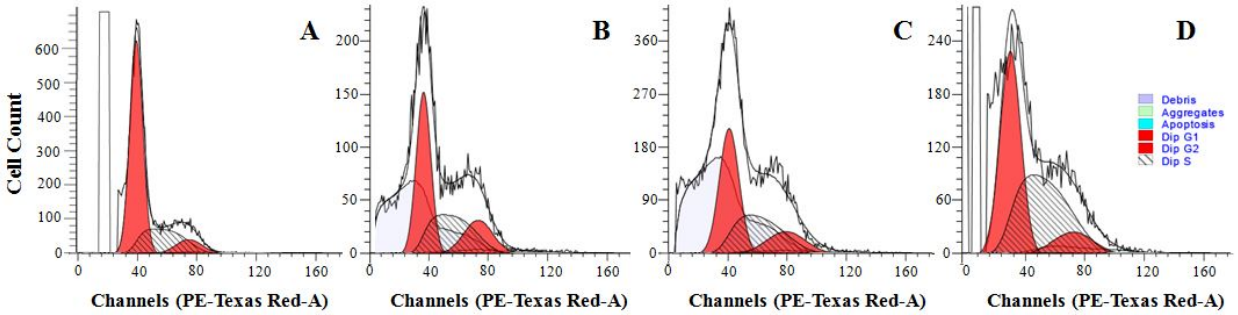

Figure 3.50 Histograms illustrating cell cycle results after exposure to 0.1% fermented rooibos in combination with selected methamphetamine concentrations at 72 hrs using flow cytometry as follows (≥ 10 000 events analysed). **A** Control. **B** 0.1% R_f and 0.1 µM MA. **C** 0.1% R_f and 1 µM MA. **D** 0.1% R_f and 10 µM MA.

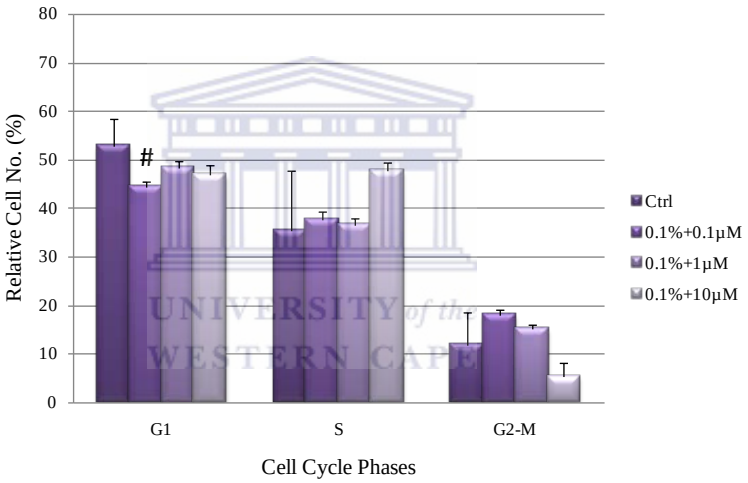

Figure 3.51 Relative cell numbers (%) at distinct phases of the cell cycle after 24 hr exposure to a combination of 0.1% fermented rooibos and selected MA concentrations at 72 hrs. Results are expressed as mean ± SEM (n=3). Significant (P<0.05) increases in relative cell no. are denoted with * whereas significant decreases are denoted with #.

The G1-phase displayed the greatest relative cell numbers (≥44.36±1.16%) with the G2-M phase displaying the least (≤18.12±0.90%). A significant decrease (P=0.0309) was observed when exposed to only lowest combination in the G-phase (See Figure 3.50 and 3.51, Appendix E: Table 3.36 and Appendix T).

3.3.2.6.4 Effects of 24 hr Exposure to Combination 2 on Cell Cycles at 96 hours

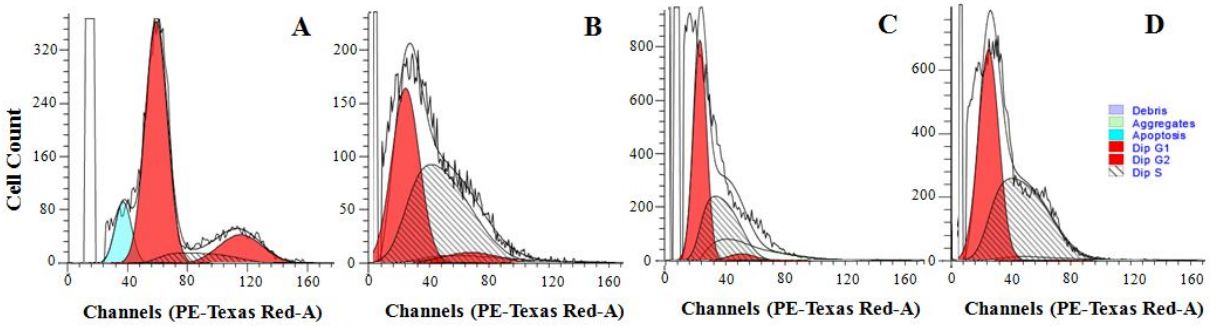

Figure 3.52 Histograms illustrating cell cycle results after exposure to 0.1% fermented rooibos in combination with selected methamphetamine concentrations at 96 hrs using flow cytometry as follows (≥ 10 000 events analysed). **A** Control. **B** 0.1% R_f and 0.1 µM MA. **C** 0.1% R_f and 1 µM MA. **D** 0.1% R_f and 10 µM MA.

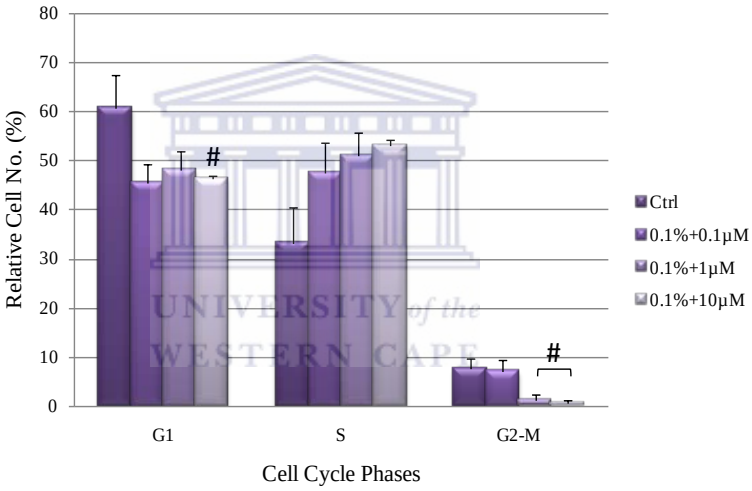

Figure 3.53 Relative cell numbers (%) at distinct phases of the cell cycle after 24 hr exposure to a combination of 0.1% fermented rooibos and selected MA concentrations at 96 hrs. Results are expressed as mean ± SEM (n=3). Significant ($P<0.05$) increases in relative cell no. are denoted with * whereas significant decreases are denoted with #.

When he cells were exposed to the combinations containing 0.1% R_f and the selected MA concentrations, the S-phase displayed the highest relative cell numbers at 53.14±1.20% when compared to the controls. The least cells detected were observed at the G2-M phase (≤7.70±2.00). The highest MA-containing combination resulted in a marked decrease ($P=0.0483$) in the G1-phase. In the G2-M phase, the combinations containing 1 µM MA ($P=0.0422$) and 10 µM MA ($P=0.0208$) also resulted in decreases when compared to controls (See Figure 3.52 and 3.53, Appendix E: Table 3.37 and Appendix U).

CHAPTER 4

4. Discussion and Conclusions

The blood-brain barrier (BBB) is important as it protects the brain from the circulatory environment and subsequent disturbance in this structure results in detrimental effects. Methamphetamine (MA) is known for its adverse effects on the brain since it easily passes through the BBB of which the precise mechanisms have not been fully elucidated. However, oxidative stress has been reported to be a contributing factor. Numerous studies have illustrated herbal teas to be potential treatments in the elimination or inhibition of the reactive oxygen species (ROS) which in turn protects against the detrimental physiological effects of the oxidants. To date, very few studies have investigated possible mechanistic approaches of MA on endothelial cells of the BBB, and even more so analysed the potential beneficial effects that fermented rooibos (R_f) herbal tea may have against MA on these endothelial cells.

In this study, physiologically relevant MA concentrations (0.1-11.1 µM) as well as supraphysiological (supra) concentrations (>11.1 µM) (Melega *et al*., 2007), were used. In addition, a broad R_f range (0.00325-0.1%) was utilized in order to establish the appropriate concentrations at which the bEnd5 cells would display above 50% viability. These concentrations were then used in combination with physiological MA concentrations for the analysis of the monolayer permeability and cell cycles.

Of great concern noted at MA rehabilitation centres as well as out-patient programmes are the number of patients who relapse which is the main hurdle in the treatment of drug dependence (Huber *et al*., 1997; Anggadiredja *et al*., 2004). It is reported that since the monoaminergic (MOA) systems are disturbed as a result of MA-induced oxidative stress (Nordahl *et al*., 2003; Ramirez *et al*., 2009), it increases the chances of patients relapsing. Studies have demonstrated that anti-oxidants have the ability to reverse the negative effects that MA has on the MOA systems which lends merit to the administration of R_f during this sensitive time of recovery. Since MA has potent ROS

production potential, it is possible that these radicals may also contribute to the change in the properties of the BBB and thus compromise its protective functions.

In the viability (%) assays, the bEnd5 cells were exposed to selected MA, and R_f concentrations as well as their combinations for 24 hrs only (once-off) at various time intervals (24-96 hrs). Viability based on intact cell membranes, were similar to that of the control cells for both single compounds and their combination at all, time intervals. Toxicity reflected <5.33%, which further validated the viability results (*data not shown*). Chen *et al*. (2012) observed similar results also incorporating the exclusion assay in which no difference was observed between the viability and cell survival rates when exposing adenocarcinomic human alveolar basal epithelial (A549) cells and Madin-Darby canine kidney cells to 25-250 µM for 72 hrs. To date, there are no studies reporting on the effects of once-off exposure to R_f on viability. A study by Macharia *et al*. (2008), however, confirmed that 6 cups of R_f consumption exerted no toxicity on kidney and liver function after illustrating that liver and kidney function enzymes (aspartate transferase, alanine amino transferase, alkaline phosphatase etc.) were not associated with any adverse effects.

Although viability (%) was not affected by exposure to the compounds, distinct differences were observed in live cell numbers across the time intervals. All MA concentrations decreased cell numbers at 96 hrs. Interestingly, R_f (0.0625-0.1%) also decreased cell numbers at this time interval which also occurred at the preceding time intervals in a dose-dependent manner. It should be noted that when exposed to the combination consisting of 0.05% R_f and MA, the cell numbers were similar to the controls at 96 hrs. This was also seen when exposed to 0.1% R_f in combination with 0.1, and 1 µM, however, the remaining concentrations resulted in a decrease. The potential of R_f to ameliorate MA effects on cell numbers at 96 hrs was seen with the combinations, which was interesting since cells exposed to R_f alone especially at the higher concentrations (0.25-1%) illustrated a greater inhibitory effect on cell numbers after exposure. Further studies needs to be conducted in order to explain these results and the possible mechanisms involved will be proposed towards the end of this section.

Viability (%) was also investigated under daily exposure conditions, in which the cells received fresh compounds from 24 through to 96 hrs. For chronic MA exposure, a decrease in viability at 72 and 96 hrs was observed which was accompanied by a similar trend in live cell numbers. Exposure at the earlier time intervals showed higher viability compared to the controls while the live cell numbers also correlated to the trend. The increased viability observed may be an indication of cellular stress as a result of MA-induced insult. Numerous studies (Zhang *et al*., 2009; Martins *et al*., 2010; Martins *et al*., 2013) involving the viability of endothelial cells assessed the effects that MA had for 24 hrs. Using rat brain vascular endothelial (GPNT) cells, Martins *et al*. (2010) observed low cell death when exposed to 0.1, 1, 10, 30 and 100 µM MA. Another study performed by Martins *et al*. (2013) using primary brain microvascular endothelial cells exposed to MA concentrations up to 100 µM showed that the cell viability was unaffected. This study at 24 hrs supports findings of Zhang *et al*., 2009; Martins *et al*., 2010 and Martins *et al*., 2013

Since the selected concentrations of MA had no effect on the viability (%) of the bEnd5 cells under both 24 hr as well as chronic exposure, it was of interest to determine which supraphysiological concentrations of MA would result in a significant change in the viability. In this study, 24 hr exposure to supra concentrations resulted in a marked decrease in viability specifically at 2000 and 3000 µM. Chronic exposure already displayed a significant decline in viability at 1000 µM when compared to controls which may be attributed to the constant presence of the MA unlike that of the once off exposure which required higher concentrations to exert similar inhibitory effects. Exposures using high MA concentrations are commonly used to investigate potential toxicity of selected compounds. Zhang *et al*. (2009) exposed human brain microvascular endothelial cells (hBMVECs) for 24 hrs and observed no differences in cell viability at MA concentrations of 100 and 500 µM. They did, however, report that the cells exposed to supraphysiological concentrations of 2500, 5000 and 10 000 µM resulted in significant decreases in the viability, with the minimum dose being 2500 µM (20% cell death). Moreover, 5000 µM and 10 000 µM resulted in 40% and 80% cell death, respectively. These findings correlated with the results of this study. Although *in vitro*

studies may use different endothelial cell line models, bEnd5 cells share structural similarities with other endothelial models which therefore explain the similar effects observed with the hBMVECs model.

Apart from experiments involving endothelial cell lines, MA's effects on other cell lines have also been documented with results similar to that of the endothelial cells. Carey *et al*. (2012) investigated the effects of 200, 500, 750, 1000 and 2000 µM MA on retinal pigment epithelial (ARPE-9) cells after 24 hrs. Exposure to 200 µM resulted in no effect. However, a marked decrease was observed when exposed to the higher concentrations with 500 µM having the least effect. Furthermore, Chen *et al*. (2012) used a high concentration range of 1250 and 2500 µM in addition to 2.5, 25, 125, 250, on A549- and Madin-Darby canine cells for 72 hrs. Treatment with 2.5-250 µM resulted in no differences in comparison to untreated groups. When exposed to 1250 and 2500 µM, a notable decrease in cell viability (%) was observed, however, dead cell counts were not notably significant between 2.5 and 2500 µM. Moreover, the cell survival rates were not markedly different for the range 2.5-250 µM but a decrease of 50% and 70% was observed when exposed to 1250 and 2500 µM, respectively. Exposure to 250, 500, 1000, 2000 and 3000 µM MA on rat cerebellum neural (R2) cells resulted in a concentration-dependent cell death at 48 hrs (Zhou *et al*., 2004) and treatment with 1000 µM MA on human neuroblastoma carcinoma (SH-SY5Y) cells at 24 hrs resulted in a significant decrease in cell viability compared to control values (Parameyong *et al*., 2013). Ajjimaporn *et al*. (2005) and Ayadi and Zigmond (2011) investigated MA effects on dopaminergic cells (SK-N-SH and MN9D cells, respectively). Ajjimaporn *et al*. (2005) observed a dose dependent decrease in cell viability after exposure to 10, 100, 500 and 1000 µM with 1000 µM reaching 47% at 24 hrs. When the time period was extended, exposure to 1000 µM at 72 hrs resulted in a 32% viability status. Ayadi and Zigmond (2011) observed no effect on the MN9D cells when exposed to 500 and 1000 µM however they reported higher MA concentration (e.g. 3000 µM) to be toxic. The above-mentioned studies support the findings that for most cell types (endothelial, epithelial, neuronal and fibroblast-like), higher MA concentrations above physiological ranges have a greater suppressive effect on viability *in vitro*.

In contrast to MA effects, 24 hr R_f exposure resulted in fluctuated viability (%) levels at different time intervals. An increase was noted at 24, 48 and 96 hrs, while no difference was observed at 72 hrs when compared to non-exposed cells. Interestingly, the live cell numbers of cells exposed to R_f were suppressed in a dose-dependent manner even though the viability was either increased or unaffected. This could indicate that the suppression is not a result of metabolic activity and may have its mechanism in another cell pathway linked to cell growth. The data illustrated similar effects after both acute and chronic exposure on metabolic activity. The viability increased in a dose-dependent manner followed by either an increase or a metabolic activity similar to their respective controls at the highest R_f concentrations at all time, intervals with the exceptions of 96 hrs which showed a significant decrease in viability at the higher R_f concentrations. To date, this study is the only of its kind to report on the effects of R_f on the viability and cell numbers on bEnd5 endothelial cells.

Moreover, there are no studies that have reported on any other forms of endothelial cells. There were, however, only a few reports on the effects of R_f on other cell lines. The effects of R_f on chick skeletal muscle primary cells were illustrated by Lamosova *et al.* (1997). Growth and proliferation was affected by concentrations greater than 2%. The authors suggested that rooibos may have inhibited the low levels of ROS required for normal cell division which could be attributed to its potent scavenging activity as a result of its high polyphenol contents. This could explain the decrease in cell numbers observed in this study even though the viability (%) was not affected as much. Could it be that this herbal tea may have initially insulted homeostasis because of its potent ROS scavenging effect? In addition, Beltran-Debon *et al.* (2011) showed that after continuous exposure to the herbal tea, the 3T3-L1 adipocytes' viability was not affected. However, rooibos affected the cell metabolism and regulated cellular energy homeostasis in which they proved the involvement in the cells energy pathways. Moreover, the effects of rooibos on adrenal steroidogenesis using human adrenocortical carcinoma (H295R) cell line, demonstrated its effects on glucocorticoids which play a large role in cell metabolism (including that of the central nervous system). The viability of these cells were unaffected by rooibos, however, the decrease in

glucocorticoids was metabolically related (Scholms *et al*., 2012). The findings in this study in combination with previous literature illustrate the potential of R_f to regulate cellular metabolic activity and energy production in both endothelial cells and on other cell types.

Cells exposed to the combinations of 0.1 and 0.05% R_f, and MA for 24 hr and chronic exposure, resulted in an initial increase in viability at 24 hrs of exposure when compared to controls. A decrease in cell viability was noted at 48 and 72 hrs, while at 96 hrs the experimental cells were similar to that of the controls. Overall, while different trends were observed with viability, it is interesting that the live cell numbers at the same time intervals were not different from the controls. Even more surprisingly, while both single compounds resulted in decreased cell numbers compared to controls, the combinatorial effects of these compounds showed similar cell numbers. To date, no studies have analysed the effects of MA in combination with *A. linearis*, however, other plants and antioxidant agents have been investigated on other cell types and tissues.

A flavonoid derived from milk thistle (*Silybum marianum* also known as silibinin) was co-administration with MA for 7 days in mice. Silibinin had shown to attenuate the memory impairment as well as the decreased DA and serotonin levels of the prefrontal cortex and hippocampus (respectively) induced by MA (Shanmugam *et al*., 2008; Lu *et al*., 2010). Wang and co-workers (2008) reported that treatment with vitamin E (which also acts as an antioxidant) prevented MA-induced Jun-N-terminal kinase (JNK) phosphorylation and inhibited MA-activated caspases-3 in SH-SY5Y cells. JNKs and caspases are known to play a role in the regulation of stress responses including stress adaptation, cell survival and death (McCubrey *et al*., 2006). Another study also concluded that pre-treatment with vitamin E reduced MA-induced ROS formation and prevented cell death (Wu *et al*., 2007). Wu *et al*. (2006) conducted an experiment involving repeated intra-peritoneal MA administration (5 mg/kg, 4 injections at 2 hrs intervals) pre-treated with baicalein (0.3-1.0 mg/kg) which is a flavonoid derived from the root of *Scutelaria baicalensis* Georgi shown to demonstrate free radical scavenging and lipid peroxidation (Hara *et al*., 1992; Gao *et al*., 1999). They observed lowered

MA-induced striatal myeloperoxidase, lipid peroxidation markers and neutrophils. MA-induced striatal DA loss was also improved. Since MA causes increased ROS activity and R_f has potent antioxidant potential both of which demonstrated an imbalance in cellular homeostasis when administered singularly, it is plausible that the combination of MA and R_f may restore the redox state of the cells resulting in the re-established cell numbers and minimal cell death observed at 96 hrs.

The permeability of the endothelial monolayer was assessed in response to daily exposure of the compounds and their combinations from 24 through to 144 hrs. Overall, dose-dependent increases in electrical resistance were observed across all time lines in response to single compound exposure of MA and R_f. The increase was concurrent with an increase in cell viability (%) at 24 hrs, while decreased viability was observed at 48 and 72 hrs with the viability remaining unchanged at 96 hrs. Since permeability and electrical resistance are inversely proportional, exposure to the individual compounds of MA and R_f resulted in the monolayer being less permeable. It is conceivable that the monolayer would respond in this manner to the presence of the herbal tea. However, it is unexpected that the resistance would also increase in the presence of MA. It may be possible that this lipid-soluble compound causes the endothelial cells to "tighten" as a protective response to the presence of MA.

Interestingly, the lower concentrations of MA (0.1 and 1 µM mostly) had the greatest effect by increasing permeability with the highest concentrations resulting in an opposite effect. It is also the higher MA concentrations that resulted in the lowest viability (%). Since viability is linked to changes in metabolic and energy pathways of a cell, it may be possible that the decrease in viability observed reflects the cells' effort to increase the integrity of the monolayer by using its energy resources to change expression of tight junction proteins, which therefore increased TEER.

Zhang *et al*. (2009), Martins *et al*. (2010), Carey *et al*. (2012) and Rosas-Hernandez *et al*. (2013) observed a decrease in TEER readings when the cells were exposed to higher MA concentrations in contrast to the results seen in this study. Martins *et al*. (2010)

illustrated no changes in electrical resistance when GPNT cells were exposed to 1 and 50 µM MA. In addition, Rosas-Hernandez and colleagues (2013) also observed no significant differences when bovine BMVECs were exposed to 100 µM MA. However, electrical resistance dose-dependently decreased when cells were exposed to 250, 500, 1000 and 2500 µM MA. Carey *et al*. (2012) reported a decrease in electrical resistance by 10% as compared to controls when ARPE-9 cells were exposed to 500 µM MA whereas Zhang *et al*. (2009) observed a significant drop by 60% when hBMVECs were exposed to 5000 µM. It should be noted that the latter authors used supraphysiological concentrations of MA. Furthermore, the TEER results of the above mentioned studies were subjected to short durations with the longest time interval reaching only 24 hrs. Thus, since this study exposed the cells to the compounds for up to 144 hrs and also incorporated hydrocortisone (which fortifies the synthesis of blood-brain barrier characteristics in serum-free *in vitro* systems as established by Hoheisel *et al*., 1998) in the growth medium as well as the utilization of a different cell type, it is difficult to compare to previous reports. Moreover, while most authors expose their monolayer with a once-off single exposure, this study replaced the growth medium with fresh MA-containing media every 24 hrs.

Other studies also investigated the effects of MA within less than 24 hr time intervals (Abdul-Muneer *et al*., 2011 and Ramirez *et al*., 2009; Martins *et al*., 2013). 1 and 50 µM MA had no effect on primary BMVECs when exposed for 6 hrs (Martins *et al*., 2013). Abdul-Muneer *et al*. (2011) observed a significant decline in electrical resistance when hBMVECs were exposed to 20 and 200 µM (the highest concentration had the greatest effect) for 10 hrs. Ramirez *et al*. (2009) reported a 20-50% dose-dependent decrease after hBMVECs were exposed to 50 and 250 µM MA for 21 hrs in which they proposed the observation to be as a result of partial loss of monolayer integrity. The decline in electrical resistance observed in these studies may possibly be due to supraphysiological concentrations being more toxic to the cells. It is clear that the effects of MA exposure are both dose- as well as time-dependent.

Mahajan and colleagues (2008) exposed BMVECs to MA concentrations 20-fold less than the lowest concentration used in this study. The time period of exposure was, however, longer than 24 hrs (10, 25 and 50 nM). They reported that for 24, 48 and 72 hrs a dose-dependent decrease in TEER was observed. The maximum effect was observed when the endothelial cells were exposed to 50 nM at 48 hrs post-MA treatment. Since the cells in this study were constantly exposed to the same concentration of MA in fresh growth medium daily, it could explain the direct relationship observed between the dose and permeability, since most waste products are removed and the cells are supplied with fresh nutrients. The reason for replacing the medium on a daily basis is founded on the logic that MA abusers seldom skip 24 hrs of not administering MA. Thus, the *in vitro* is always exposed to the same concentration of MA for 144 hrs unlike the once-off exposed cells that metabolize the MA over the time period. It should be highlighted at this point that there are as yet no reports on the metabolism or bioavailability of MA in mouse brain endothelial cells both, *in vitro* or *in vivo*.

Exposure to R_f initially resulted in increases in TEER (correlating with an increased viability). At 72 hrs, TEER was still elevated; however, viability (%) was unaffected. While at 96 hrs only higher concentrations of R_f, resulted in similar TEER readings compared to controls but viability had decreased. Electrical resistance remained higher than controls for 120 and 144 hrs, however, this study did not investigate the effect of R_f on viability at these time intervals. Overall, as the R_f concentrations increased for all time intervals, the permeability decreased. Chronic exposure to R_f may, thus, have resulted in an increase in the integrity of the monolayer. Since there are currently no reports on the effect of R_f on TEER, the author is left with only the current results of this study. Thus, further analysis specifically at the biochemical and molecular level are required in order to explain the possible mechanisms involved in the decrease in permeability observed.

While there are no reports on R_f, studies have, however, investigated the effect of polyphenols on endothelial cells. Youdim *et al*. (2003) reported on the uptake of citrus

flavonoids by rat brain endothelial and bEnd5 cells. These results demonstrated the ability of flavonoids and other metabolites to traverse the BBB. However, the authors could not explain how the flavonoids impacted the endothelial cells, directly. These studies do give insight into the potential of flavonoids as a treatment for neuroprotection. Youdim *et al.* (2004) also assessed the ability of flavonoids to traverse the *in vitro* ECV304/rat-C6 co-culture and *in situ* (rat) BBB models. The study concluded that flavonoids from certain families are able to penetrate the BBB and convey protection in a neuronal setting.

The studies conducted by Youdim *et al*. (2003 and 2004) implicated the possible involvement of the drug efflux transporters as a means by which flavonoids could potentially traverse the BBB and exert their neuroprotective effect. Although the precise efflux transporters have not yet been fully elucidated, they suggested the involvement of P-glycoprotein (P-gp). P-gp operates as an adenosine triphosphate (ATP)-driven efflux pump by controlling the movement of structurally diverse compounds across the BBB. Interestingly, Beltran-Debon and co-workers (2011) reported that viability (%) of adipocytes was not affected by continuous R_f exposure and that these effects were proven to be energy-related. It may be that the energy-affiliated role of P-gp strongly links to the findings of this study. Previous literature also illustrated the energy regulatory effects of rooibos on other cells types (as discussed with viability). This is also supported by the possible interactions between P-gp, epicatechin (Youdim *et al*., 2003) and quercetin (Youdim *et al*., 2004), the latter also known to be a potent antioxidant of rooibos herbal tea (Ferreira *et al.*, 1995; Joubert and Ferreira, 1996; Nijveldt *et al.*, 2001). This further supports the possibility that energy pathways play a role in the modulatory effects of daily R_f on the viability of the endothelial cells coupled with a decrease in barrier permeability. A more detailed investigation of R_f flavonoid P-gp interaction is required, which focuses on the efflux proteins as well as pathways linked to the actions of these transporters.

Exposure to combinations of MA and R_f resulted in increased TEER readings as well as viability (%). These readings were the highest recorded when compared to the effects of

the single compounds. Similar relationships were observed for the viability, in which the single compounds resulted in decreased viability up until 96 hrs while their combinations resulted in an increase. It is therefore highlighted that the increased viability occurred simultaneously with the increased resistance. Thongsaard and Marsden (2002) reported that *Thunbergia laurifolia* (TH) Linn an herbal plant which also possesses flavonoids (Rice-Evans *et al*., 1996; Chanawirat, 2000) stimulated DA release in the same manner as AMPH. Since MA and some polyphenolic as well as non-polyphenol compounds in R_f are lipophilic it can be suggested based on the above-mentioned study, that they are agonistic and result in the increased effects in permeability observed. This section of the study demonstrated that R_f reversed the permeability caused by physiological concentrations of MA.

The effects on the bEnd5 cell cycles were also investigated in response to once-off exposure to the compounds. This section of the study made use of only physiological concentrations of MA (0.1, 1 and 10 µM) and selected R_f concentrations (0.05 and 0.1%) as well as their combinations. Exposure to MA between 24 and 96 hrs increased cell populations in the G1-phase with a decreased cellular fraction in the S- and more specifically in the G2-M-phases. This suggested that the cells accumulated in the G1-phase where preparation for DNA replication occurs. Comparably, an increase in viability (%) and a decrease in cell numbers were observed at 96 hrs. The arrest at the G1-phase may have been as a result of the interference observed at the G2-M phase where cell division should occur. In other words, MA may have blocked the G1-to-S phase transition resulting in the retardation of the cell cycle and thus a decrease in the G2-M population. The decreased cell numbers observed at 96 hrs potentially reflects the inability of cells to proliferate while the increased viability may indicate compensatory mechanisms activated in order to provide more energy for cell division.

To date, few studies have investigated the effects of MA on cell cycles. Shao *et al*. (2012) demonstrated that supraphysiological concentrations of 1000 µM MA resulted in apoptosis and cell cycle arrest in human embryonic endothelial (EA.hy926) cells at 24 and 48 hrs. The authors, however, did not elaborate nor allocate which specific phase of

the cycle was affected. Their results were not unexpected since their cells were exposed to supra MA concentrations. For the same time intervals, Capélôa *et al*. (2014) observed no differences in cell cycle phases when exposing human glioblastoma (U-118) cell lines to 1 µM MA. This is consistent with the effect of 1 µM MA on the cell cycle phases observed at 24 and 48 hrs in this study. Yuan and colleagues (2011) observed modified cell cycle dynamics and altered stages of development in response to chronic *in vivo* administration of MA on rat hippocampus progenitor cells. Without influencing phase length, MA had resulted in decreased cell populations in the S-phase which displayed association with G1-phase arrest. The observations made by Yuan *et al*. (2011) mirrored the altered cell numbers observed in the S-phase in this study.

The rate of cell proliferation and growth is largely influenced by the ability of cells to enter and undergo cell division and thereby completing an entire cell cycle. Studies have demonstrated that alterations in endothelial proliferation and S-phases have been linked to glutathione (GSH)-deficient states (Maxine *et al*., 2008) and *in vitro* ROS (Buşu *et al*., 2013), which both play major roles in the regulation of cell redox states. In this study, it is evident that MA has influenced both cell growth and cell cycles. Since the adverse effects of MA have been attributed to mechanisms which involved increased ROS production (Fleckenstein *et al.*, 1997; Lin *et al.*, 1999; Cervinski *et al.*, 2005; Ramirez *et al.*, 2009), the change in redox state in the endothelial cells may have modulated the S-phase and resulted in the adverse effects on the BBB.

By 96 hrs, bEnd5 cells exposure to once-off R_f showed an increase in relative cell numbers in the G1-phase across all time intervals (as was also noted with MA exposure). This was accompanied by cell population suppression in the S-phase, however R_f resulted in a greater decrease when compared to the MA exposed cells. No differences were observed in the G2-M phase for all time intervals when compared to controls but the cell population was notably higher than the MA group. The viability (%) increased and cell numbers had decreased by 96 hrs to the once-off exposure to R_f. The decreased cell numbers did not reflect the cellular fractions observed in the G2-M phase. The effect on the G1-phase and the two latter parameters were similar to that

observed with MA exposure. It should be noted that decreased S-phase cellular fractions are accompanied by reduced numbers in the G2-M phase since the synthesis of DNA components are required prior to mitosis.

The findings in this study could have been more specific if the exposure groups and controls were synchronized. Unsynchronized whole cultures do not properly distinguish between closely spaced phases e.g. the late G1- form the early S-phase (Schorl and Sedivy, 2007), and therefore synchronization offers a method for a more critical study of molecular and biochemical events (Davis *et al*., 2001, Lee *et al*., 2011; Vecsler *et al*., 2013). It allows for specific expression of critical cell cycle components such as tumour suppressor proteins at the restriction point in the late G1-phase (Lee *et al*., 1988; Chen *et al*., 1989), cyclin A expression at late G1 to S-phase transition (Solomon, 1993; Sherr and Roberts, 1995) and cyclin B/cdc2 activity onset at the G2 to M-phase transition (Draetta *et al*., 1988; Ducommun *et al*., 1991). Thus, the unsynchronized phases of the cells in this study could have influenced the results observed at the S- and G2-M- phase after exposure to R_f when compared to MA, since these single compounds had mirroring effects with respect to viability, permeability and the G1-phases.

To date, no studies have investigated the effects of R_f on cell cycle phases in brain endothelial cells. It has been reported that human microvascular endothelial cells exposed to the plant flavonoid, apigenin for 48 hrs resulted in inhibition of cell proliferation by blockage in the G2-M phase (Trochon *et al*., 2000). However, it resulted in arrest at the G2-M and/or G1-phase of keratinocytes, human diploid fibroblasts and neuronal cells (Sato *et al.*, 1994; Lepley *et al.*, 1996; Lepley and Pelling, 1997; Casagrande and Darbon, 2001). Martin *et al*. (2003) observed an accumulation of cells in the G1-phase with suppressed cell numbers in the S-phase after an 18 hr treatment of delphinidin (DP), a class of potent antioxidants *viz*. anthocyanins, on bovine aortic endothelial cells. When normal human embryonic fibroblasts (NHF) were exposed to DP, a decrease in cellular fraction in G1-phase and an increase in S-phase were observed after 24 hr treatment (Lazzé *et al*., 2004). Moreover, using human umbilical vascular endothelial cells, Arakaki *et al*. (2004) observed arrested progression

in the G1-phase after exposure to selected flavones (the “parent” compound of flavonoids). Lazzé and colleagues (2004) also exposed NHFs to cyanidin (an aglycone anthocyanin) and trans-resveratol (polyphenol found in grapes and red wine) for 24 hrs. Both antioxidants resulted in growth inhibition characterized by decreased cells in S-phase and cell accumulation in G1-phase.

Studies have also reported on the effects of flavonoids found in *A. linearis* on cancer cell lines. Luteolin exposure resulted in G1-phase arrest in human gastric-and human melanoma cancer cells (Matsukawa *et al*., 1993) whereas G2-M phase arrest was observed in human prostate cancer cells (Haddad *et al*., 2006). Exposure to quercetin resulted in G1 arrest in colon- (Ranelletti *et al*., 1992), gastric- (Yoshida *et al*., 1990), leukemic cancer cells (Yoshida *et al*., 1992) and human melanoma (OCM-1) cells (Casagrande and Darbon, 2011). It, however, resulted in G2-M phase arrest when breast- (Avila *et al*., 1994) and laryngeal cancer cells (Ferrandina *et al*., 1998) were exposed to the compound. Furthermore, arrested G1- and/or G2-M-phases of numerous cancer cells have also been observed when exposed to other polyphenolic agents such as daidzein (Matsukawa *et al*., 1993; Casagrande and Darbon, 2001), genistein (Matsukawa *et al*., 1993; Kuzumaki *et al*., 1998; Casagrande and Darbon, 2001; Kobayashi *et al*., 2002), silibinin, baicalin and its metabolite baicalein (Chen *et al*., 2001; Hogan *et al*., 2007). All the above-mentioned reports highlight the challenges of the cell specific effects of individual polyphenols when analysing their cell cycles. Moreover, the effect of the whole herbal tea extract would undoubtedly also display varying effects.

Endothelial and epithelial cells share similar markers (Hoyer *et al*., 1973; Gimbrone *et al*., 1978; Folkman *et al*., 1979; Hial *et al*., 1979; Cines *et al*., 1998; Hur *et al*., 2004) and even characteristics with cancer cells. These include TJ involvement associated with cell motility (Kojima and Sawada, 2012; Webb *et al*., 2014), the presence of tumour suppressor protein (p53) involved in cell death (Rivlen *et al*., 2014), endothelial cell surface markers (Carson-Walter *et al*., 2001; Hilda *et al*., 2004), *Thoc1* protein expression involved in cell proliferation (Li *et al*., 2007), and various other gene

expressions (Zhang *et al*., 1997). These common characteristics amongst the various cell types and even cancer cells could support the similarities observed in the current study pertaining to cell growth and cycle. It is, however, pertinent to acknowledge that these cells also contain their own distinct levels of expression of specific proteins which present themselves as different phenotypic characteristics.

Exposure on cell cycles to the combinations of MA and R_f resulted in a significant decrease in G1-phase cell populations across all time intervals when compared to controls. While the effects of the single compound exposure of MA and R_f resulted in relative cell numbers greater than controls. In the G2-M phase, combinatorial effects displayed a decreased cellular fraction at 96 hrs which interestingly was comparable to that of single compound MA and R_f exposure. The S-phase populations were greater than controls and that of the cell numbers of the single compounds' exposure. Since it becomes difficult to properly distinguish between closely spaced phases between the late G1- form and the early S-phase (Schorl and Sedivy, 2007) in unsynchronized whole cultures, increased population numbers observed in the S-phase may not be indicative of the combinatorial effects of the compounds but as a result of non-synchronicity. Additional biochemical pathways, their biomarkers and a synchronized state is required in order to properly elucidate whether these effects are indeed as a result of the exposure to the combinations. However, these findings are seen significant albeit exploratory.

To date, the effects of MA and R_f's combinations on endothelial cell cycles have not been investigated. Studies performed by Zaragoza *et al*. (2000 and 2001) do, however, report on the effects of cocaine in combination with different antioxidant reagents and rat hepatocytes. The cells were exposed to cocaine *in vitro* in the presence of deferoxamine (DO) and *N*-acetylcysteine (NAC) for 24 hrs. In the absence of antioxidants, cocaine exposure resulted in the activation of apoptotic pathways using flow cytometry and DNA fragmentation analysis. In the presence of NAC and DO, these effects were abrogated. This study did not however look at specific cell cycles. They concluded that NAC and DO, when incubated in the presence of cocaine, exerted a protective effect against cocaine toxicity. MA and cocaine have been shown to exert

similar effects on the dopaminergic system (Schechter and Glennon, 1985; Washton and Zweben, 2009) and since antioxidants could reduce the effects of cocaine, it is plausible that the antioxidant potential of R_f could protect against the effects of MA. However, it is acknowledged that the cell-specific nature of the BBB endothelial cells, may give rise to varying results. The improved cell viability and cell numbers at 96 hrs as a result of R_f's addition to MA suggests that the herbal tea may be conveying protection against MA. This potential protective effect was also demonstrated with the increased electrical resistance to the bEnd5 cell monolayer and the alleviated G1-phase cell numbers when compared to the effects of the single MA exposure. The synergistic effect may have potentially modulated the synthesis of DNA and ultimately replication resulting in the redistribution of the cell cycle phases' populations.

In conclusion, while the effects of once-off exposure to R_f on bEnd5 cell viability was similar to that of MA, MA resulted in lower cell numbers when compared to R_f. Interestingly, while chronic exposure to R_f did not affect viability, the exposure to MA suppressed it. Moreover, both compounds decreased permeability and saw the arrest of the G1-phase in the cell cycle. The cells exposed once-off to the combination of MA and R_f, resulted in similar viability compared to controls, however, exhibited increased levels when exposed chronically. Once-off exposure also resulted in similar cell numbers to that of controls. The increase in electrical resistance was more profound with exposure to the combinations than the single compounds and a reversal of cell cycle arrest at G1-phase accompanied by an increase in S-phase cell population was observed. The findings of this study suggest that R_f may act antagonistically to MA by restoring cell numbers, viability and cell cycle phases. The agonistic effects of R_f and MA on permeability may be seen as a protective mechanism by the endothelial cells in response to the presence of exogenous compounds. Thus, the protective potential of R_f on the central component of the BBB *viz.* the endothelial cells is illustrated using the above-mentioned parameters. Although in its infancy, this study gives insight into the possible mechanisms by which MA affects the BBB and the potential of R_f as a protective agent, and allowing for a possible non-invasive treatment with which to reduce the rate of MA relapse and addiction.

CHAPTER 5

5. Future Perspectives

This study gave broad insight into the ability of MA and R_f to alter the bEnd5 cell monolayer profile. However in order to validate these observations, it is necessary to identify specific markers that correspond to the activation or inhibition of certain cellular pathways. Since viability and proliferation may be linked to energy related pathways, studies ranging from ATP analysis to observing specific mitochondrial enzyme activity should be elucidated. These observations may be fundamental in explaining the effects on BBB integrity and cell cycle phases when exposed to these lipophilic compounds. It would not be unexpected if MA affects the energy production pathways since it is reported to a stimulant of exothermic reactions.

It is imperative for the BBB to maintain a low permeability status which has been demonstrated in this study to be altered by MA and R_f in a similar manner. Since the current study is novel, mechanisms of these alterations on BBB integrity are vastly unclear and future studies should attempt to investigate post- translational and -transcriptional tight junction expression to fully determine their effects. Furthermore, since only whole cell cultures were used, studies should incorporate synchronized cells and specific cell cycle checkpoints addressing phase length in order to fully understand the effects on the endothelial cell cycle phases. In addition, since the BBB does not only consist of endothelial cells, co-cultures (either bi- or tri-cultures) should be used in order to closely mimic an *in vivo* model.

Incorporating the above mentioned approaches would allow for a more accurate method in which to assess MA, R_f and their combinations' ability to modulate the cellular activity.

APPENDIX A

Table 2.1 Preparation of gallic acid stock standard concentrations with respective contents per tube for the measurement of polyphenols

Tubes	Gallic acid stock solution (µl)	10% EtOH (µl)	Final gallic acid Concentration (mg/l)	Well no.
A	0	1000	0	A1-A3
B	25	975	20	A4-A6
C	62.5	937.5	50	A7-A9
D	125	875	100	A10-A12
E	312	688	250	B1-3
F	625	375	500	B4-6

Table 2.2 Preparation of quercetin stock standard concentrations with respective contents per tube for the measurement of flavonols

Tubes	Quercetin stock (µl)	95 % EtOH (µl)	Final quercetin concentration (mg/l)	Wells no.
A	0	1000	0	A1-A3
B	75	925	5	A4-A6
C	125	875	10	A7-A9
D	250	750	20	A10-A12
E	500	500	40	B1-B3
F	1000	0	80	B4-B6

Table 2.3 Preparation of catechin stock standard concentrations with respective contents per tube for the measurement of flavanols

Tubes	Catechin stock (µl)	Methanol (µl)	Final catechin concentration (µM)	Final catechin concentration (mg/l)	Well no.
A	0	1000	0	0	A1-A3
B	5	995	5	1.36	A4-A6
C	10	990	10	2.72	A7-A9
D	25	975	25	6.8	A10-A12
E	50	950	50	13.6	B1-B3
F	100	900	100	27.2	B4-B6

Table 2.4 Preparation of Trolox stock standard concentrations with respective contents per tube for the Oxygen Radical Absorbance Capacity (ORAC) assay

Tubes	Trolox stock solution (µl)	Phosphate Buffer (µl)	Final Trolox concentration (µM)	Well no.
A	0	750	0	A1-A3
B	125	625	83	A4-A6
C	250	500	167	A7-A9
D	375	375	250	A10-A12
E	500	250	333	B1-3
F	625	125	417	B4-6

Table 2.5 Preparation of Trolox stock standard concentrations with respective contents per tube for the ABTS (2,2'-azino-di-3-ethylbenzthialozine sulphonate) (TEAC) radical cation scavenging assay

Tubes	Trolox standard (µl)	Ethanol (µl)	Final Trolox concentration (µM)	Well no.
A	0	1000	0	A1-A3
B	50	950	50	A4-A6
C	100	900	100	A7-A9
D	150	850	150	A10-A12
E	250	750	250	B1-3
F	500	500	500	B4-6

Table 2.6 Preparation of ascorbic acid stock standard concentrations with respective contents per tube for the Ferric Reducing Antioxidant Power (FRAP) assay

Tubes	Ascorbic acid stock solution (µl)	Distilled water (µl)	Final ascorbic acid concentration (µM)	Well no.
A	0	1000	0	A1-A3
B	50	950	50	A4-A6
C	100	900	100	A7-A9
D	200	800	200	A10-A12
E	500	500	500	B1-3
F	1000	0	1000	B4-6

APPENDIX B

Table 3.2 Effects on bEnd5 live cell numbers after 24 hr exposure to selected MA concentrations using trypan blue over various time intervals (Mean ± SEM, n=5)

Time/ Compound	Pure Methamphetamine			
	24 hrs	48 hrs	72 hrs	96 hrs
Ctrl	0.50±0.10	9.55±0.88	26.88±0.88	119.22±5.35
0.1 µM	1.96±0.49	6.55±0.88	29.88±6.8	77.19±6.96
1 µM	2.07±0.44	8.88±1.43	36.85±8.89	59.90±4.06
10 µM	1.82±0.38	15.52±2.11	46.66±5.00	80.67±3.56
100 µM	0.70±0.12	11.90±273	40.36±6.40	94.15±5.03
1000 µM	0.73±0.14	9.32±1.51	22.25±2.46	63.13±5.16

Table 3.3 Effects on bEnd5 % viability after 24 hr exposure to selected MA concentrations using trypan blue viability assay over various time intervals (Mean ± SEM, n=5)

Time/ Compound	Pure Methamphetamine			
	24 hrs	48 hrs	72 hrs	96 hrs
Ctrl	98.47±0.52	99.87±0.39	100.00±0.00	99.42±0.89
0.1 µM	100.00±0.00	97.92±0.61	99.51±0.13	96.10±0.69
1 µM	100.00±0.00	100.00±0.00	99.78±0.11	98.97±0.24
10 µM	100.00±0.00	100.00±0.00	94.78±1.41	99.58±0.16
100 µM	100.00±0.00	97.49±0.69	99.70±0.15	96.54±0.97
1000 µM	97.62±1.71	94.67±1.71	99.42±0.29	99.43±0.22

Table 3.4 Effects on bEnd5 % viability after 24 hr exposure to selected MA concentrations using XTT viability assay over various time intervals (Mean ± SEM, n=5)

Time/ Compound	Pure Methamphetamine			
	24 hrs	48 hrs	72 hrs	96 hrs
Ctrl	100.00±0.00	100.00±0.00	100.00±0.00	100.00±0.00
0.1 µM	92.43±6.07	97.23±16.45	119.34±11.44	76.05±6.06
1 µM	98.20±9.42	89.76±9.40	132.31±13.44	93.97±9.12
10 µM	107.24±6.38	88.06±19.38	150.51±1.09	108.93±7.93
100 µM	102.34±10.17	79.15±9.23	101.65±3.10	102.43±4.82
1000 µM	93.47±12.99	84.83±3.31	115.73±3.72	84.03±2.40
2000 µM	98.90±1.39	89.11±6.35	126.10±9.06	81.92±2.80
3000 µM	79.27±9.99	55.07±0.96	73.17±3.25	38.60±10.97

Table 3.5 Effects on bEnd5 % viability after daily exposure to selected MA concentrations using XTT viability assay over various time intervals (Mean ± SEM, n=5)

Time/ Compound	Pure Methamphetamine			
	24 hrs	48 hrs	72 hrs	96 hrs
Ctrl	100.00±0.00	100.00±0.00	100.00±0.00	100.00±0.00
0.1 µM	92.43±6.07	116.33±16.28	72.30±0.90	83.43±4.26
1 µM	98.20±9.42	108.80±20.53	90.38±1.57	76.38±3.51
10 µM	107.24±6.38	113.65±8.74	88.05±3.62	74.50±4.13
100 µM	102.34±10.17	112.76±3.65	74.63±6.11	87.54±2.24
1000 µM	93.47±12.99	72.58±14.74	74.05±8.22	47.47±0.24

Table 3.6 Effects on bEnd5 monolayer electrical resistance after daily exposure to selected MA concentrations using transendothelial electrical resistance (TEER) assay over various time intervals (Mean ± SEM, n=4)

Time/ Compound	Pure Methamphetamine					
	24 hrs	48 hrs	72 hrs	96 hrs	120 hrs	144 hrs
Ctrl	16.84±0.68	18.35±0.67	21.35±0.51	19.30±0.65	18.98±0.61	14.55±0.51
0.1 µM	18.22±0.62	14.23±0.30	16.73±0.40	16.78±0.23	16.90±0.36	14.63±0.46
1 µM	18.49±0.64	15.75±0.30	18.98±0.32	20.00±0.37	20.28±0.18	16.60±0.69
10 µM	19.05±0.58	18.03±0.56	20.68±0.37	21.78±0.36	21.23±0.37	18.43±0.71
100 µM	18.28±0.68	21.78±0.99	18.42±1.02	24.96±0.56	22.38±0.83	21.35±0.96

Table 3.7 Effects on bEnd5 cell cycle phases after 24 hr exposure to selected MA concentrations using flow cytometry at 24 hrs (Mean ± SEM, n=3, ≥ 10 000 events analysed)

Phases/ Concentration	Flow Cytometry Analysis		
	G1	S	G1-M2
Ctrl	55.79±3.29	37.07±5.34	7.15±3.76
0.1µM	45.19±2.40	44.81±2.75	9.99±5.00
1 µM	63.38±0.00	34.43±0.00	2.19±0.00
10 µM	67.05±1.15	32.37±1.18	0.57±0.49

Table 3.8 Effects on bEnd5 cell cycle phases after 24 hr exposure to selected MA concentrations using flow cytometry at 48 hrs (Mean ± SEM, n=3, ≥ 10 000 events analysed)

Phases/ Concentration	Flow Cytometry Analysis		
	G1	S	G1-M2
Ctrl	50.31±5.10	38.94±6.30	10.75±3.13
0.1µM	67.56±3.76	24.01±12.06	8.43±8.43
1 µM	64.36±7.23	35.65±2.40	0.22±0.01
10 µM	70.19±7.15	29.53±7.01	0.28±0.28

Table 3.9 Effects on bEnd5 cell cycle phases after 24 hr exposure to selected MA concentrations using flow cytometry at 72 hrs (Mean ± SEM, n=3, ≥ 10 000 events analysed)

Phases/ Concentration	Flow Cytometry Analysis		
	G1	S	G1-M2
Ctrl	52.71±3.06	35.40±5.33	11.90±2.75
0.1µM	74.92±1.81	16.84±2.61	8.24±4.16
1 µM	54.04±7.23	44.24±8.67	1.72±1.72
10 µM	58.88±7.66	28.90±0.72	12.22±8.34

Table 3.10 Effects on bEnd5 cell cycle phases after 24 hr exposure to selected MA concentrations using flow cytometry at 96 hrs (Mean ± SEM, n=3, ≥ 10 000 events analysed)

Phases/ Concentration	Flow Cytometry Analysis		
	G1	S	G1-M2
Ctrl	60.66±6.65	33.04±7.34	7.70±2.00
0.1µM	80.70±0.00	18.77±0.00	1.53±0.00
1 µM	85.34±0.44	13.89±0.77	1.77±0.34
10 µM	79.27±2.72	15.08±7.74	5.65±1.73

APPENDIX C

Table 3.11 Effects on bEnd5 live cell numbers after 24 hr exposure to selected R_f concentrations using trypan blue over various time intervals (Mean ± SEM, n=5)

Time/ Compound	Fermented Rooibos			
	24 hrs	48 hrs	72 hrs	96 hrs
Ctrl	5.20±0.73	18.00±0.81	28.83±2.10	38.59±1.65
0.0625%	5.64±0.25	28.95±1.07	33.25±0.97	27.13±1.37
0.125%	7.50±0.49	28.88±0.76	26.20±1.17	31.63±2.11
0.25%	7.30±0.68	22.10±2.66	21.30±1.07	25.83±1.36
0.5%	7.08±0.96	18.83±2.16	16.35±1.86	23.00±1.88
1%	4.30±0.18	9.10±2.06	9.25±2.37	15.75±2.27

Table 3.12 Effects on bEnd5 % viability after 24 hr exposure to selected Rf concentrations using trypan blue viability assay over various time intervals (Mean ± SEM, n=5)

Time/ Compound	Fermented Rooibos			
	24 hrs	48 hrs	72 hrs	96 hrs
Ctrl	100.00±0.00	100.00±0.00	100.00±0.00	99.93±0.07
0.05%	98.06±1.25	100.00±0.00	100.00±0.00	99.21±0.45
0.0625%	100.00±0.00	100.00±0.00	100.00±.0.00	99.70±0.22
0.125%	100.00±0.00	100.00±0.00	99.41±0.41	100.00±0.00
0.25%	100.00±0.00	100.00±0.00	100.00±0.00	97.53±1.13
0.5%	99.41±0.40	100.00±0.00	100.00±0.00	99.81±0.13
1%	98.27±0.88	100.00±0.00	100.00±0.00	100.00±0.00

Table 3.13 Effects on bEnd5 % viability after 24 hr exposure to selected Rf concentrations using XTT viability assay over various time intervals (Mean ± SEM, n=5)

Time/ Compound	Fermented Rooibos			
	24 hrs	48 hrs	72 hrs	96 hrs
Ctrl	100.00±0.00	100.00±0.00	100.00±0.00	100.00±0.00
0.003125%	63.51±3.51	119.19±1.69	105.96±1.63	113.81±1.79
0.0625%	70.58±6.87	114.13±3.85	96.89±2.63	119.88±3.99
0.0125%	74.36±8.04	112.19±4.97	95.51±2.73	112.32±6.26
0.025%	92.60±6.47	109.95±8.72	103.81±2.49	108.90±4.74
0.05%	96.88±9.63	115.21±2.77	100.69±2.18	115.47±6.48
0.1%	93.53±4.36	94.55±9.11	94.83±11.86	83.15±7.99

Table 3.14 Effects on bEnd5 % viability after daily exposure to selected R_f concentrations using XTT viability assay over various time intervals (Mean ± SEM, n=5)

Time/ Compound	Fermented Rooibos			
	24 hrs	48 hrs	72 hrs	96 hrs
Ctrl	100.00±0.00	100.00±0.00	100.00±0.00	100.00±0.00
0.003125%	63.51±3.51	81.97±4.52	101.51±3.86	97.95±8.66
0.0625%	70.58±6.87	86.94±2.56	105.61±8.46	95.34±1.22
0.0125%	74.36±8.04	109.27±10.95	112.36±7.81	100.10±2.30
0.025%	92.60±6.47	110.02±8.24	116.63±12.78	91.73±2.87
0.05%	96.88±9.63	129.43±10.88	109.13±11.04	80.95±5.08
0.1%	93.53±4.36	100.05±11.36	108.23±7.25	61.19±7.58

Table 3.15 Effects on bEnd5 electrical resistance after daily exposure to selected Rf concentrations using transendothelial electrical resistance (TEER) assay over various time intervals (Mean ± SEM, n=4)

Time/ Compound	Fermented Rooibos					
	24 hrs	48 hrs	72 hrs	96 hrs	120 hrs	144 hrs
Ctrl	15.03±0.90	13.46±0.77	17.74±0.57	17.73±0.54	12.67±0.37	13.07±0.47
0.0625%	18.83±0.57	18.81±0.70	19.99±0.60	18.04±0.71	16.14±0.71	17.53±0.82
0.0125%	17.90±0.75	18.34±0.41	21.21±0.48	18.85±0.34	19.50±0.26	20.25±0.76
0.025%	21.81±0.67	19.44±0.56	22.76±0.45	17.11±0.71	20.24±0.37	16.95±0.86
0.05%	22.29±0.44	18.18±0.66	23.13±0.38	16.12±0.41	21.48±0.35	18.60±1.23
0.1%	20.36±0.73	20.22±0.40	25.22±0.36	16.20±0.40	23.44±0.33	15.10±0.68

Table 3.16 Effects on bEnd5 cell cycle phases after 24 hr exposure to selected R_f concentrations using flow cytometry at 24 hrs (Mean ± SEM, n=3, ≥ 10 000 events analysed)

Phases/ Concentration	Flow Cytometry Analysis		
	G1	S	G1-M2
Ctrl	55.79±3.29	37.07±5.34	7.15±3.76
0.05%	63.21±2.70	29.32±4.217	7.47±4.20
0.1%	63.40±2.94	17.02±7.82	19.57±4.89

Table 3.17 Effects on bEnd5 cell cycle phases after 24 hr exposure to selected R_f concentrations using flow cytometry at 48 hrs (Mean ± SEM, n=3, ≥ 10 000 events analysed)

Phases/ Concentration	Flow Cytometry Analysis		
	G1	S	G1-M2
Ctrl	50.31±5.10	38.94±6.30	10.75±3.13
0.05%	66.28±0.63	26.11±1.31	7.62±1.87
0.1%	73.18±2.26	22.46±6.62	4.36±4.36

Table 3.18 Effects on bEnd5 cell cycle phases after 24 hr exposure to selected R_f concentrations using flow cytometry at 72 hrs (Mean ± SEM, n=3, ≥ 10 000 events analysed)

Phases/ Concentration	Flow Cytometry Analysis		
	G1	S	G1-M2
Ctrl	52.71±3.06	35.40±5.33	11.90±2.75
0.05%	71.61±2.69	24.57±1.11	3.82±1.59
0.1%	64.25±1.49	33.04±1.94	2.46±1.01

Table 3.19 Effects on bEnd5 cell cycle phases after 24 hr exposure to selected R_f concentrations using flow cytometry at 96 hrs (Mean ± SEM, n=3, ≥ 10 000 events analysed)

Phases/ Concentration	Flow Cytometry Analysis		
	G1	S	G1-M2
Ctrl	60.66±6.65	33.04±7.34	7.70±2.00
0.05%	83.66±0.70	3.27±0.84	13.05±1.59
0.1%	86.41±0.13	3.13±0.36	10.46±0.46

APPENDIX D

Table 3.20 Effects on bEnd5 live cell numbers after 24 hr exposure to 0.05% R_f and selected MA concentrations using trypan blue over various time intervals (Mean ± SEM, n=5)

Time/ Concentration	Fermented Rooibos and Pure Methamphetamine			
	24 hrs	48 hrs	72 hrs	96 hrs
Ctrl	3.78±0.56	19.00±1.15	31.35±1.41	45.13±3.53
0.05%+0.1 µM	3.53±0.27	21.81±0.64	22.00±1.67	37.78±6.65
0.05%+1 µM	4.10±0.50	16.33±1.69	21.83±1.24	43.10±4.57
0.05%+10 µM	2.63±0.39	18.53±0.70	32.75±1.14	37.15±2.37
0.05%+100µM	1.88±0.28	20.68±1.97	24.88±1.31	41.85±2.44

Table 3.21 Effects on bEnd5 % viability after 24 hr exposure to 0.05% R_f and selected MA concentrations using trypan blue viability assay over various time intervals (Mean ± SEM, n=5)

Time/ Concentration	Fermented Rooibos and Pure Methamphetamine			
	24 hrs	48 hrs	72 hrs	96 hrs
Ctrl	100.00±0.00	100.00±0.00	100.00±0.00	100.00±0.00
0.05%+0.1 µM	100.00±0.00	100.00±0.00	100.00±0.00	99.34±0.48
0.05%+1 µM	100.00±0.00	100.00±0.00	100.00±0.00	97.56±0.62
0.05%+10 µM	100.00±0.00	100.00±0.00	99.73±0.20	95.18±1.30
0.05%+100µM	100.00±0.00	100.00±0.00	99.67±0.24	95.76±0.99

Table 3.22 Effects on bEnd5 % viability after 24 hr exposure to 0.05% R_f and selected MA concentrations using XTT viability assay over various time intervals (Mean ± SEM, n=5)

Time/ Concentration	Fermented Rooibos and Pure Methamphetamine			
	24 hrs	48 hrs	72 hrs	96 hrs
Ctrl	100.00±0.00	100.00±0.00	100.00±0.00	100.00±0.00
0.05%+0.1 µM	172.28±14.32	111.34±9.84	78.67±3.77	100.89±1.04
0.05%+1 µM	136.79±10.36	94.75±13.61	76.79±4.23	103.43±2.67
0.05%+10 µM	127.52±9.16	65.37±10.63	91.13±7.62	106.42±1.17

Table 3.23 Effects on bEnd5 % viability after daily exposure to 0.05% R_f and selected MA concentrations using XTT viability assay over various time intervals (Mean ± SEM, n=5)

Time/ Concentration	Fermented Rooibos and Pure Methamphetamine			
	24 hrs	48 hrs	72 hrs	96 hrs
Ctrl	100.00±0.00	100.00±0.00	100.00±0.00	100.00±0.00
0.05%+0.1 µM	172.28±14.32	81.44±9.26	109.05±5.96	114.43±3.61
0.05%+1 µM	136.79±34.75	65.82±3.40	98.06±6.40	113.99±5.69
0.05%+10 µM	127.52±9.16	70.17±4.26	84.91±9.44	110.78±2.27

Table 3.24 Effects on bEnd5 electrical resistance after daily exposure to 0.05% R_f and selected MA concentrations using transendothelial electrical resistance (TEER) assay over various time intervals (Mean ± SEM, n=4)

Time/ Compound	Fermented Rooibos and Pure Methamphetamine					
	24 hrs	48 hrs	72 hrs	96 hrs	120 hrs	144 hrs
Ctrl	13.18±0.29	16.46±0.70	19.38±0.25	15.62±0.41	14.98±0.24	11.76±084
0.05% + 0.1µM	13.05±0.33	15.28±0.31	17.51±0.68	18.20±0.56	20.38±0.88	22.91±0.58
0.05% + 1 µM	13.83±0.29	18.00±0.39	18.76±0.38	19.13±0.50	23.04±0.52	24.58±0.58
0.05% + 10 µM	16.15±0.35	20.23±0.35	17.94±0.23	18.10±0.69	22.86±0.62	25.16±0.83

Table 3.25 Effects on bEnd5 cell cycle phases after 24 hr exposure to 0.05% fermented rooibos and selected MA concentrations using flow cytometry at 24 hrs (Mean ± SEM, n=3, ≥ 10 000 events analysed)

Phases/ Concentration	Flow Cytometry Analysis		
	G1	S	G1-M2
Ctrl	55.79±3.29	37.07±5.34	7.15±3.76
0.05%+0.1 µM	43.21±0.26	38.04±0.35	18.75±0.41
0.05%+1 µM	41.56±2.47	40.01±0.89	18.43±2.62
0.05%+10 µM	44.08±1.10	38.27±1.15	17.64±0.90

Table 3.26 Effects on bEnd5 cell cycle phases after 24 hr exposure to 0.05% fermented rooibos and selected MA concentrations using flow cytometry at 48 hrs (Mean ± SEM, n=3, ≥ 10 000 events analysed)

Phases/ Concentration	Flow Cytometry Analysis		
	G1	S	G1-M2
Ctrl	50.31±5.10	38.94±6.30	10.75±3.13
0.05%+0.1 µM	48.92±2.35	24.56±6.27	26.52±0.50
0.05%+1 µM	44.97±6.41	52.03±5.31	3.00±0.57
0.05%+10 µM	41.74±4.52	56.87±0.96	1.39±0.57

Table 3.27 Effects on bEnd5 cell cycle phases after 24 hr exposure to 0.05% fermented rooibos and selected MA concentrations using flow cytometry at 72 hrs (Mean ± SEM, n=3, ≥ 10 000 events analysed)

Phases/ Concentration	Flow Cytometry Analysis		
	G1	S	G1-M2
Ctrl	52.71±3.06	35.40±5.33	11.90±2.75
0.05%+0.1 µM	46.81±2.86	49.58±2.36	5.43±3.14
0.05%+1 µM	36.15±1.24	59.81±3.46	2.15±2.63
0.05%+10 µM	44.51±5.43	20.32±1.01	35.16±1.34

Table 3.28 Effects on bEnd5 cell cycle phases after 24 hr exposure to 0.05% fermented rooibos and selected MA concentrations using flow cytometry at 96 hrs (Mean ± SEM, n=3, ≥ 10 000 events analysed)

Phases/ Concentration	Flow Cytometry Analysis		
	G1	S	G1-M2
Ctrl	60.66±6.65	33.04±7.34	7.70±2.00
0.05%+0.1 µM	48.77±2.55	50.02±3.84	1.21±1.30
0.05%+1 µM	50.72±2.91	48.07±3.60	1.21±3.15
0.05%+10 µM	45.50±0.39	51.22±1.21	3.18±3.28

APPENDIX E

Table 3.29 Effects on bEnd5 live cell numbers after 24 hr exposure to 0.1% R_f and selected MA concentrations using trypan blue over various time intervals (Mean ± SEM, n=5)

Time/ Concentration	Fermented Rooibos and Pure Methamphetamine			
	24 hrs	48 hrs	72 hrs	96 hrs
Ctrl	13.38±1.79	23.43±1.89	34.40±3.25	68.80±5.55
0.1%+0.1 µM	7.30±0.86	21.53±1.33	32.08±2.84	65.98±3.32
0.1%+1 µM	8.43±0.49	25.96±0.31	30.25±2.25	57.18±3.32
0.1%+10 µM	10.80±0.69	17.78±0.55	35.75±4.12	51.08±1.60
0.1%+100 µM	12.85±1.13	22.89±1.20	24.53±3.04	50.20±2.71

Table 3.30 Effects on bEnd5 % viability after 24 hr exposure to 0.1% R_f and selected MA concentrations using trypan blue viability assay over various time intervals (Mean ± SEM, n=5)

Time/ Concentration	Fermented Rooibos and Pure Methamphetamine			
	24 hrs	48 hrs	72 hrs	96 hrs
Ctrl	100.00±0.00	100.00±0.00	100.00±0.00	99.81±0.10
0.1%+0.1 µM	100.00±0.00	100.00±0.00	99.63±0.20	99.36±0.27
0.1%+1 µM	100.00±0.00	100.00±0.00	97.81±0.66	98.84±0.28
0.1%+10 µM	100.00±0.00	100.00±0.00	95.03±1.16	96.11±1.08
0.1%+100 µM	100.00±0.00	100.00±0.00	99.29±0.39	94.23±0.86

Table 3.31 Effects on bEnd5 % viability after 24 hr exposure to 0.1% R_f and selected MA concentrations using XTT viability assay over various time intervals (Mean ± SEM, n=5)

Time/ Concentration	Fermented Rooibos and Pure Methamphetamine			
	24 hrs	48 hrs	72 hrs	96 hrs
Ctrl	100.00±0.00	100.00±0.00	100.00±0.00	100.00±0.00
0.1%+0.1 µM	135.43±9.26	80.63±13.88	63.02±9.66	102.61±3.56
0.1%+1 µM	157.94±10.19	80.30±6.89	74.53±6.96	95.26±3.89
0.1%+10 µM	125.72±11.65	63.75±16.24	70.38±5.44	99.89±0.41

Table 3.32 Effects on bEnd5 % viability after daily exposure to 0.1% R_f and selected MA concentrations using XTT viability assay over various time intervals (Mean ± SEM, n=5)

Time/ Concentration	Fermented Rooibos and Pure Methamphetamine			
	24 hrs	48 hrs	72 hrs	96 hrs
Ctrl	100.00±0.00	100.00±0.00	100.00±0.00	100.00±0.00
0.1%+0.1 µM	135.43±9.26	59.09±2.79	102.80±3.40	112.46±3.48
0.1%+1 µM	157.94±10.19	62.50±9.29	98.06±6.20	114.56±12.25
0.1%+10 µM	125.72±11.65	58.05±6.25	109.05±6.76	113.74±8.77

Table 3.33 Effects on bEnd5 electrical resistance after daily exposure to 0.1% R_f and selected MA concentrations using transendothelial electrical resistance (TEER) assay over various time intervals (Mean ± SEM, n=4)

Time/ Compound	Fermented Rooibos and Pure Methamphetamine					
	24 hrs	48 hrs	72 hrs	96 hrs	120 hrs	144 hrs
Ctrl	13.18±0.29	16.46±0.70	19.39±0.25	15.63±0.41	14.98±0.24	11.76±0.84
0.1% + 0.1µM	14.23±0.30	16.62±0.39	20.84±0.30	18.15±0.90	24.76±0.58	27.33±0.85
0.1% + 1 µM	15.45±0.37	18.35±0.65	17.21±0.54	18.97±0.52	25.23±0.58	25.68±0.48
0.1% + 10 µM	16.32±0.25	20.58±0.46	21.38±0.47	19.45±0.81	25.78±0.38	24.38±0.55

Table 3.34 Effects on bEnd5 cell cycle phases after 24 hr exposure to 0.1% fermented Rooibos and selected MA concentrations using flow cytometry at 24 hrs (Mean ± SEM, n=3, ≥ 10 000 events analysed)

Phases/ Concentration	Flow Cytometry Analysis		
	G1	S	G1-M2
Ctrl	55.79±3.29	37.07±5.34	7.15±3.76
0.1%+0.1 µM	41.93±2.19	57.11±2.98	0.92±0.79
0.1%+1 µM	44.38±0.55	37.06±0.56	8.55±0.43
0.1%+10 µM	41.77±0.95	57.76±0.77	0.46±0.33

Table 3.35 Effects on bEnd5 cell cycle phases after 24 hr exposure to 0.1% fermented Rooibos and selected MA concentrations using flow cytometry at 48 hrs (Mean ± SEM, n=3, ≥ 10 000 events analysed)

Phases/ Concentration	Flow Cytometry Analysis		
	G1	S	G1-M2
Ctrl	50.31±5.10	38.94±6.30	10.75±3.13
0.1%+0.1 µM	43.57±1.09	46.29±0.78	10.15±0.33
0.1%+1 µM	51.82±8.02	47.08±7.51	0.07±0.07
0.1%+10 µM	53.25±1.77	46.05±2.32	0.71±0.71

Table 3.36 Effects on bEnd5 cell cycle phases after 24 hr exposure to 0.1% fermented Rooibos and selected MA concentrations using flow cytometry at 72 hrs (Mean ± SEM, n=3, ≥ 10 000 events analysed)

Phases/ Concentration	Flow Cytometry Analysis		
	G1	S	G1-M2
Ctrl	52.71±3.06	35.40±5.33	11.90±2.75
0.1%+0.1 µM	44.36±1.16	37.52±1.74	18.12±0.90
0.1%+1 µM	48.20±1.43	36.59±1.44	15.21±0.88
0.1%+10 µM	46.90±1.97	47.84±1.60	5.25±2.97

Table 3.37 Effects on bEnd5 cell cycle phases after 24 hr exposure to 0.1% fermented Rooibos and selected MA concentrations using flow cytometry at 96 hrs (Mean ± SEM, n=3, ≥ 10 000 events analysed)

Phases/ Concentration	Flow Cytometry Analysis		
	G1	S	G1-M2
Ctrl	60.66±6.65	33.04±7.34	7.70±2.00
0.1%+0.1 µM	45.47±3.67	47.51±6.11	7.03±2.44
0.1%+1 µM	47.96±3.83	50.89±4.91	1.14±1.14
0.1%+10 µM	46.32±0.65	53.14±1.20	0.55±0.55

APPENDIX F

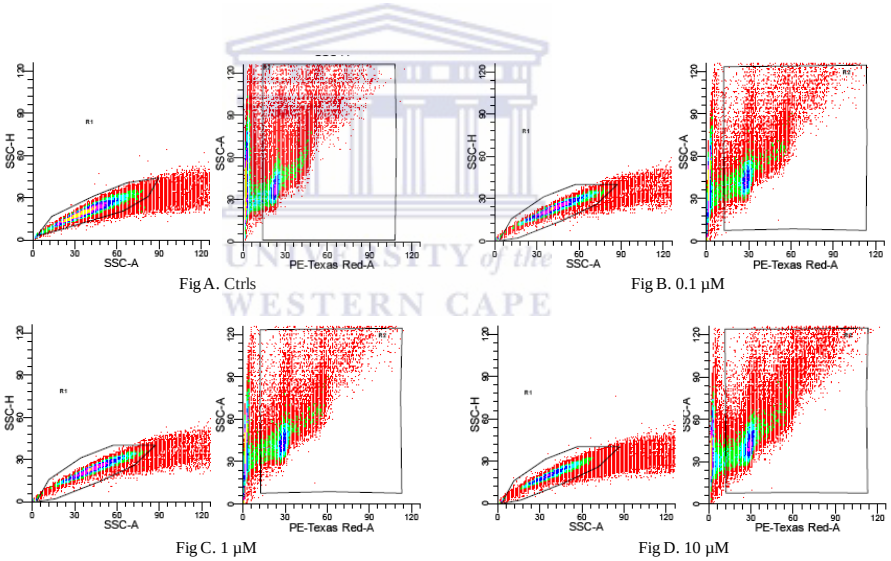

Fig A. Ctrls Fig B. 0.1 µM

Fig C. 1 µM Fig D. 10 µM

Appendix F These Scatter plots display results obtained at 24 hrs using flow cytometry when exposed to **B** 0.1µM. **C** 1 µM. **D** 10 µM methamphetamine and control cells represented by **A** (≥ 10 000 events analysed). Scatter plots were used to generate histogram and the data was tabled and represented as bar graph.

APPENDIX G

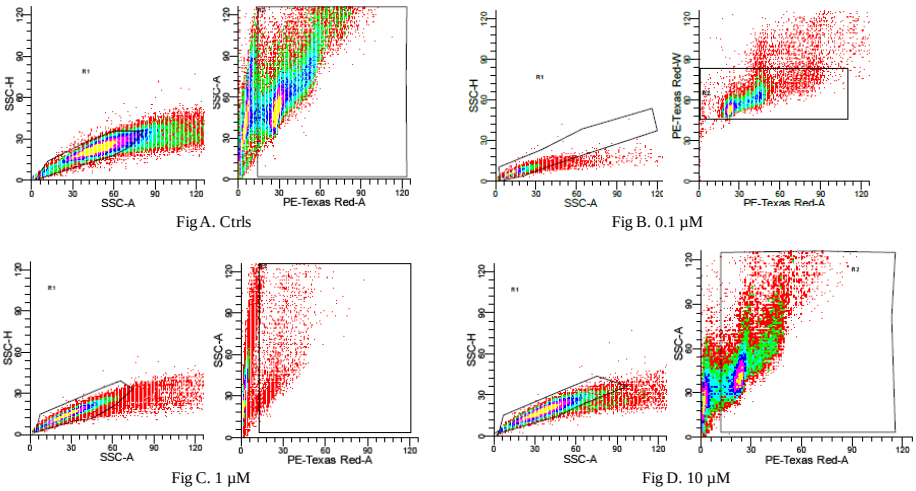

Fig A. Ctrls Fig B. 0.1 µM

Fig C. 1 µM Fig D. 10 µM

Appendix G These Scatter plots display results obtained at 48 hrs using flow cytometry when exposed to **B** 0.1µM. **C** 1 µM. **D** 10 µM methamphetamine and control cells represented by **A** (≥ 10 000 events analysed). Scatter plots were used to generate histogram and the data was tabled and represented as bar graph.

APPENDIX H

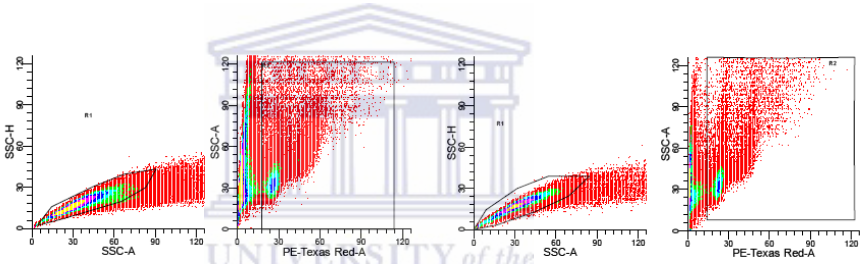

Fig A. Ctrls

Fig B. 0.1 µM

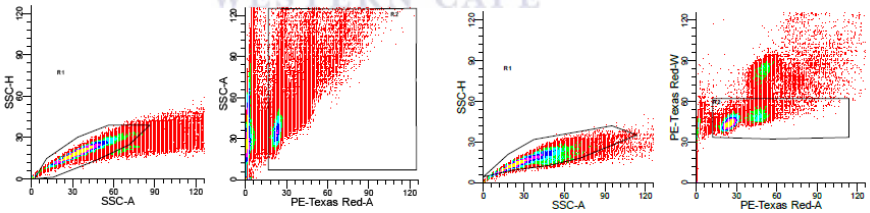

Fig C. 1 µM

Fig D. 10 µM

Appendix H These Scatter plots display results obtained at 72 hrs using flow cytometry when exposed to **B** 0.1µM. **C** 1 µM. **D** 10 µM methamphetamine and control cells represented by **A** (≥ 10 000 events analysed). Scatter plots were used to generate histogram and the data was tabled and represented as bar graph.

APPENDIX I

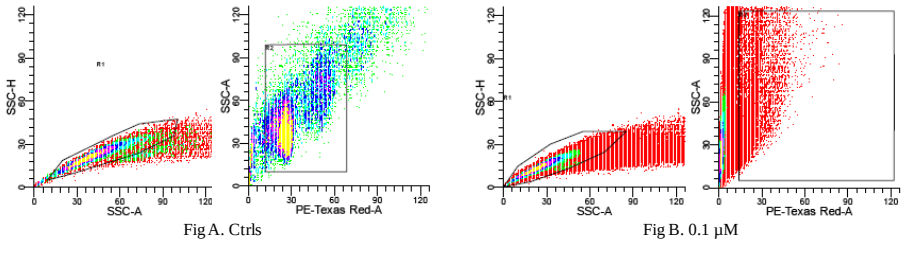

Fig A. Ctrls

Fig B. 0.1 µM

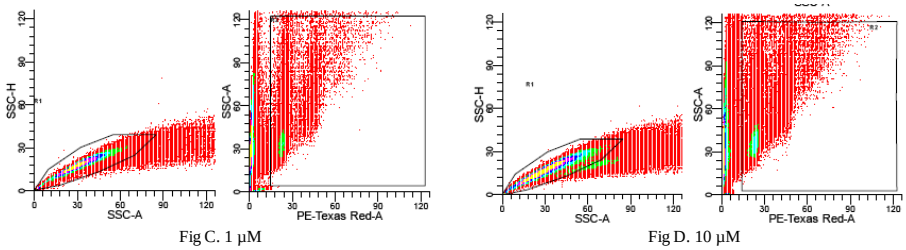

Fig C. 1 µM

Fig D. 10 µM

Appendix I These Scatter plots display results obtained at 96 hrs using flow cytometry when exposed to **B** 0.1µM. **C** 1 µM. **D** 10 µM methamphetamine and control cells represented by **A** (≥ 10 000 events analysed). Scatter plots were used to generate histogram and the data was tabled and represented as bar graph.

APPENDIX J

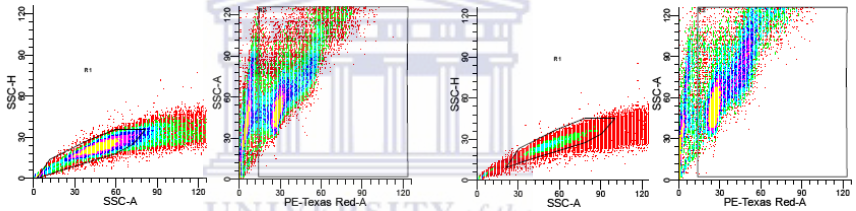

Fig A. Ctrls

Fig B. 0.05%

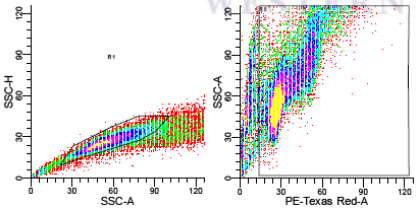

Fig C. 0.1%

Appendix J These Scatter plots display results obtained at 24 hrs using flow cytometry when exposed to **B** 0.05%. **C** 0.1% fermented rooibos and control cells represented by **A** (≥ 10 000 events analysed). Scatter plots were used to generate histogram and the data was tabled and represented as bar graph.

APPENDIX K

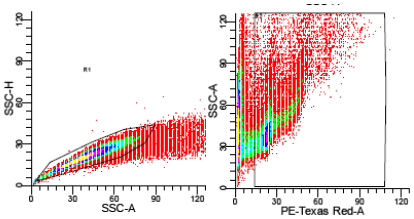

Fig A. Ctrls

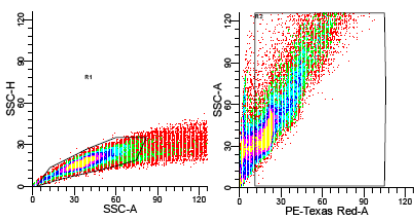

Fig B. 0.05%

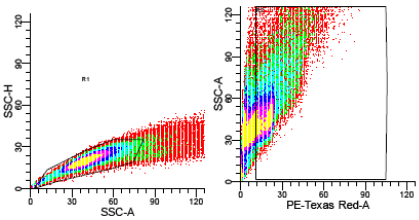

Fig C. 0.1%

Appendix K These Scatter plots display results obtained at 48 hrs using flow cytometry when exposed to **B** 0.05%. **C** 0.1% fermented rooibos and control cells represented by **A** (≥ 10 000 events analysed). Scatter plots were used to generate histogram and the data was tabled and represented as bar graph.

APPENDIX L

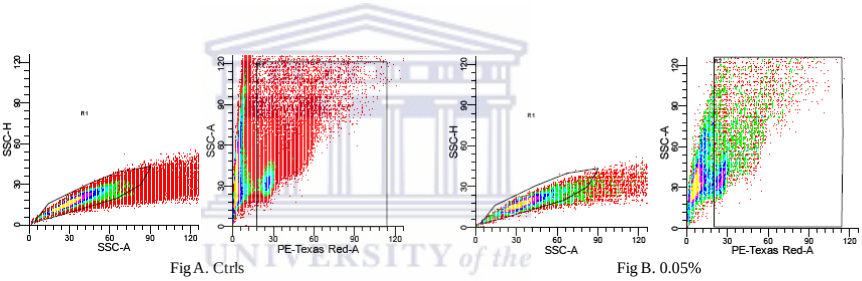

Fig A. Ctrls

Fig B. 0.05%

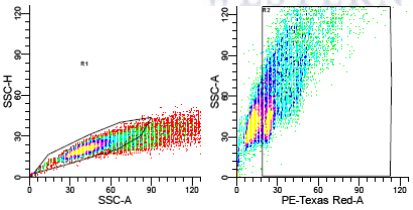

Fig C. 0.1%

Appendix L These Scatter plots display results obtained at 72 hrs using flow cytometry when exposed to **B** 0.05%. **C** 0.1% fermented rooibos and control cells represented by **A** (≥ 10 000 events analysed). Scatter plots were used to generate histogram and the data was tabled and represented as bar graph.

APPENDIX M

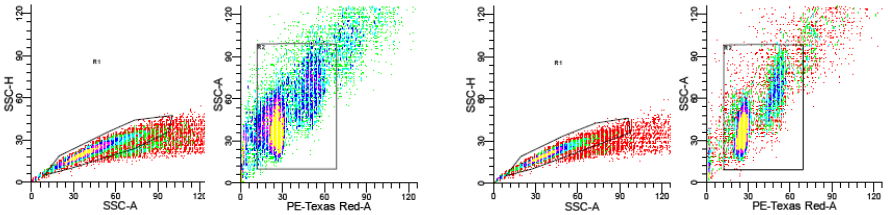

Fig A. Ctrls

Fig B. 0.05%

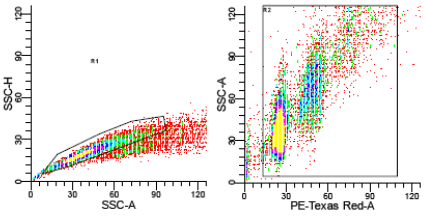

Fig C. 0.1%

Appendix M These Scatter plots display results obtained at 96 hrs using flow cytometry when exposed to **B** 0.05%. **C** 0.1% fermented rooibos and control cells represented by **A** (≥ 10 000 events analysed). Scatter plots were used to generate histogram and the data was tabled and represented as bar graph.

APPENDIX N

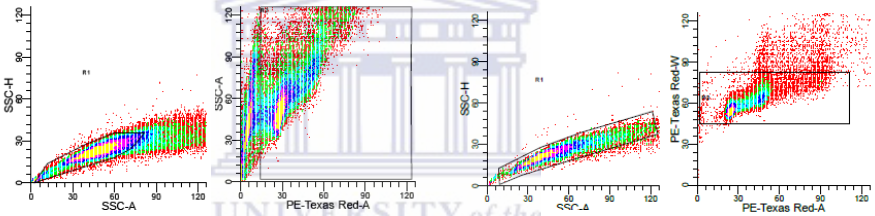

Fig A. Ctrls

Fig B. 0.05% R_f + 0.1 µM MA

Fig C. 0.05% R_f + 1 µM MA

Fig D. 0.05% R_f + 10 µM MA

Appendix N These Scatter plots display results obtained at 24 hrs using flow cytometry when exposed to 0.05% fermented rooibos in combination with **B** 0.1 µM. **C** 1 µM. **D** 10 µM methamphetamine and control cells represented by **A** (≥ 10 000 events analysed). Scatter plots were used to generate histogram and the data was tabled and represented as bar graph.

APPENDIX O

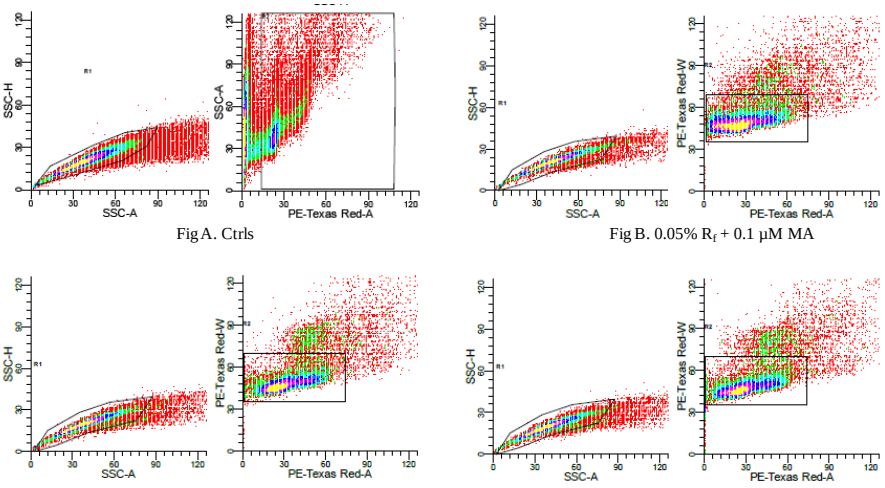

Fig A. Ctrls

Fig B. 0.05% R_f + 0.1 µM MA

Fig C. 0.05% R_f + 1 µM MA

Fig D. 0.05% R_f + 10 µM MA

Appendix O These Scatter plots display results obtained at 48 hrs using flow cytometry when exposed to 0.05% fermented rooibos in combination with **B** 0.1 µM. **C** 1 µM. **D** 10 µM methamphetamine and control cells represented by **A** (≥ 10 000 events analysed). Scatter plots were used to generate histogram and the data was tabled and represented as bar graph.

APPENDIX P

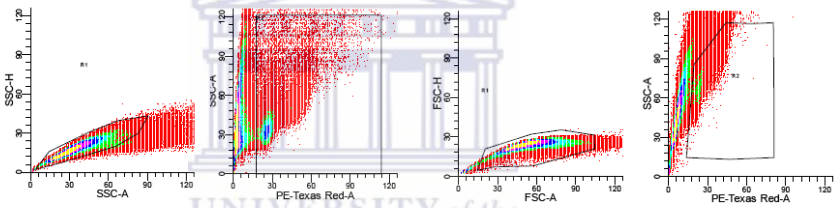

Fig A. Ctrls

Fig B. 0.05% R_f + 0.1 µM MA

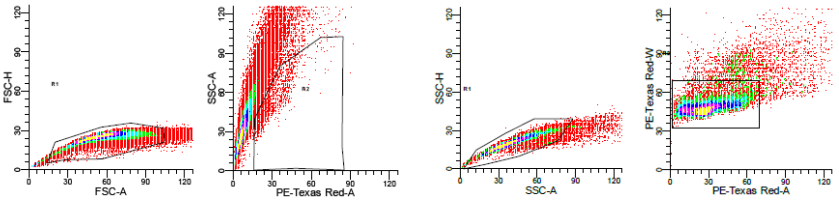

Fig C. 0.05% R_f + 1 µM MA

Fig D. 0.05% R_f + 10 µM MA

Appendix P These Scatter plots display results obtained at 72 hrs using flow cytometry when exposed to 0.05% fermented rooibos in combination with **B** 0.1 µM. **C** 1 µM. **D** 10 µM methamphetamine and control cells represented by **A** (≥ 10 000 events analysed). Scatter plots were used to generate histogram and the data was tabled and represented as bar graph.

APPENDIX Q

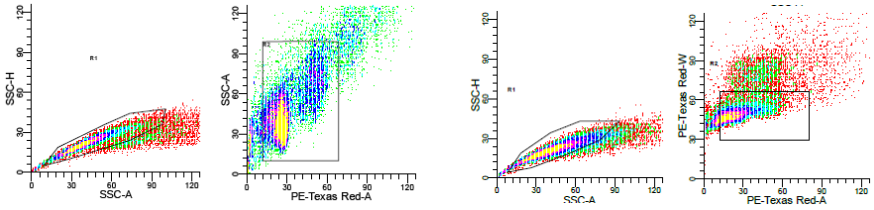

Fig A. Ctrls

Fig B. 0.05% R_f + 0.1 µM MA

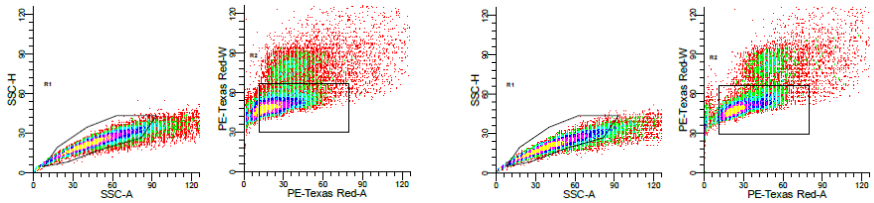

Fig C. 0.05% R_f + 1 µM MA

Fig D. 0.05% R_f + 10 µM MA

Appendix Q These Scatter plots display results obtained at 96 hrs using flow cytometry when exposed to 0.05% fermented rooibos in combination with **B** 0.1 µM. **C** 1 µM. **D** 10 µM methamphetamine and control cells represented by **A** (≥ 10 000 events analysed). Scatter plots were used to generate histogram and the data was tabled and represented as bar graph.

APPENDIX R

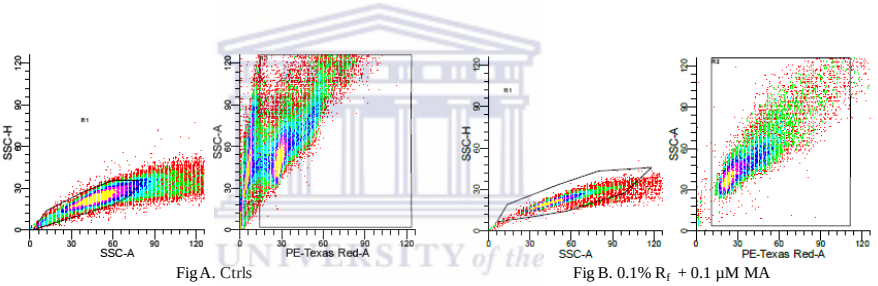

Fig A. Ctrls

Fig B. 0.1% R_f + 0.1 µM MA

Fig C. 0.1% R_f + 1 µM

Fig D. 0.1% R_f + 10 µM MA

Appendix R These Scatter plots display results obtained at 24 hrs using flow cytometry when exposed to 0.1% fermented rooibos in combination with **B** 0.1 µM. **C** 1 µM. **D** 10 µM methamphetamine and control cells represented by **A** (≥ 10 000 events analysed). Scatter plots were used to generate histogram and the data was tabled and represented as bar graph.

APPENDIX S

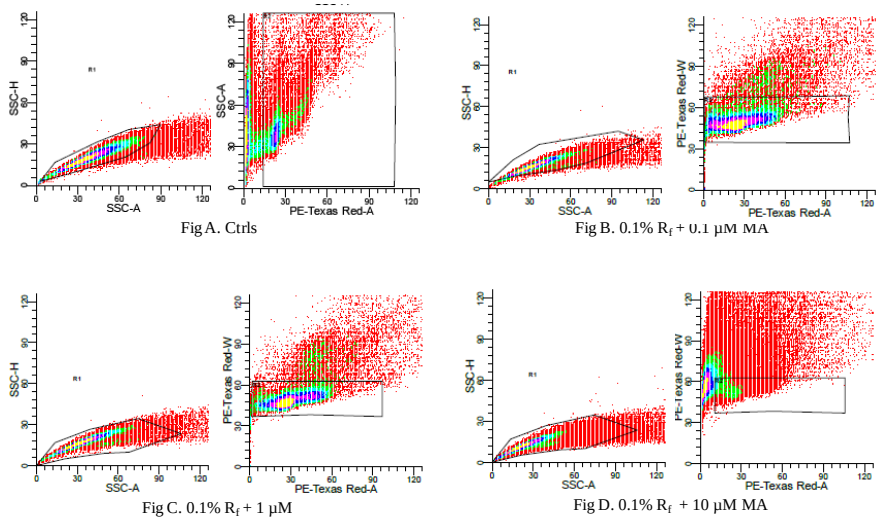

Fig A. Ctrls

Fig B. 0.1% R_f + 0.1 µM MA

Fig C. 0.1% R_f + 1 µM

Fig D. 0.1% R_f + 10 µM MA

Appendix S These Scatter plots display results obtained at 48 hrs using flow cytometry when exposed to 0.1% fermented rooibos in combination with **B** 0.1 µM. **C** 1 µM. **D** 10 µM methamphetamine and control cells represented by **A** (≥ 10 000 events analysed). Scatter plots were used to generate histogram and the data was tabled and represented as bar graph.

APPENDIX T

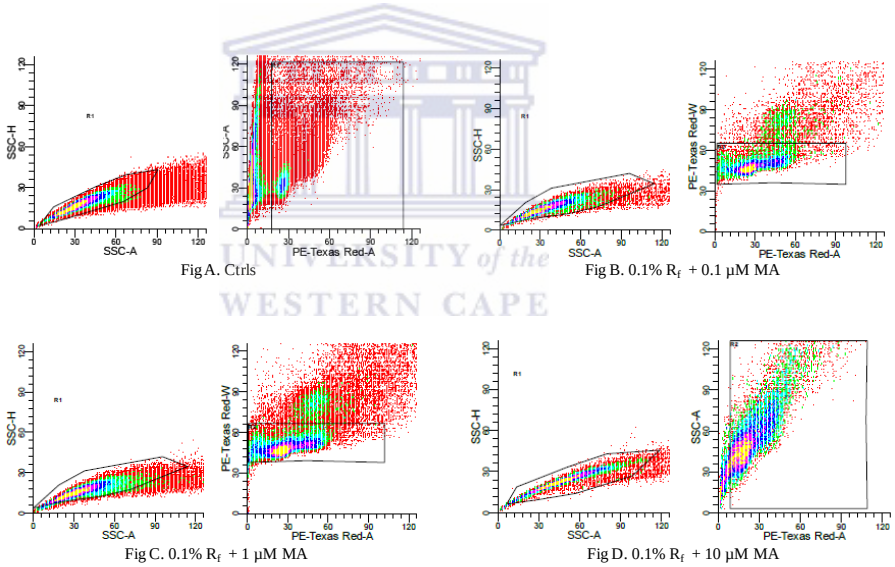

Fig A. Ctrls

Fig B. 0.1% R_f + 0.1 µM MA

Fig C. 0.1% R_f + 1 µM MA

Fig D. 0.1% R_f + 10 µM MA

Appendix T These Scatter plots display results obtained at 72 hrs using flow cytometry when exposed to 0.1% fermented rooibos in combination with **B** 0.1 µM. **C** 1 µM. **D** 10 µM methamphetamine and control cells represented by **A** (≥ 10 000 events analysed). Scatter plots were used to generate histogram and the data was tabled and represented as bar graph.

APPENDIX U

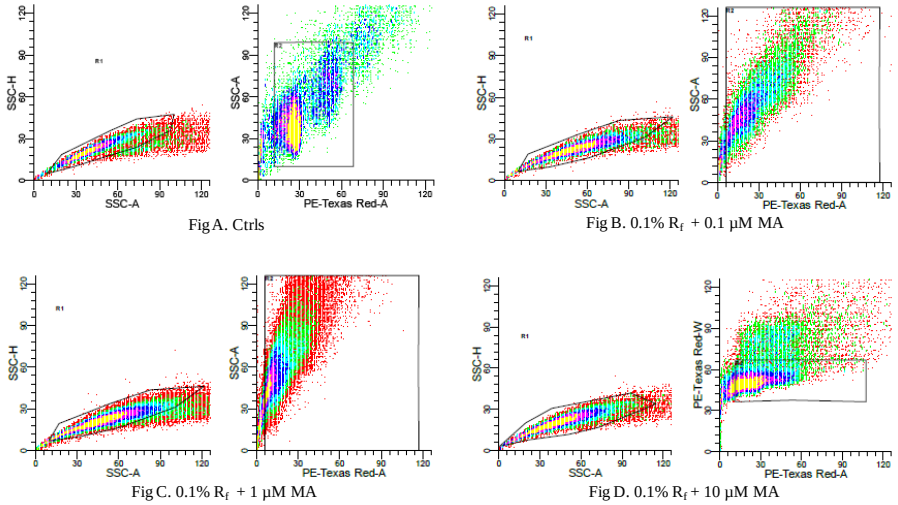

Fig A. Ctrls

Fig B. 0.1% R_f + 0.1 µM MA

Fig C. 0.1% R_f + 1 µM MA

Fig D. 0.1% R_f + 10 µM MA

Appendix U These Scatter plots display results obtained at 96 hrs using flow cytometry when exposed to 0.1% fermented rooibos in combination with **B** 0.1 µM. **C** 1 µM. **D** 10 µM methamphetamine and control cells represented by **A** (≥ 10 000 events analysed). Scatter plots were used to generate histogram and the data was tabled and represented as bar graph.